
26th RAAU

ANNUAL USERS MEETING LNLS/CNPEM

August 24th and 25th, 2016

cnpem.br/rau



MINISTÉRIO DA
CIÊNCIA, TECNOLOGIA,
INOVAÇÕES E COMUNICAÇÕES



Support:



Sponsors:



Agilent Technologies



DECTRIS®

Organizers:

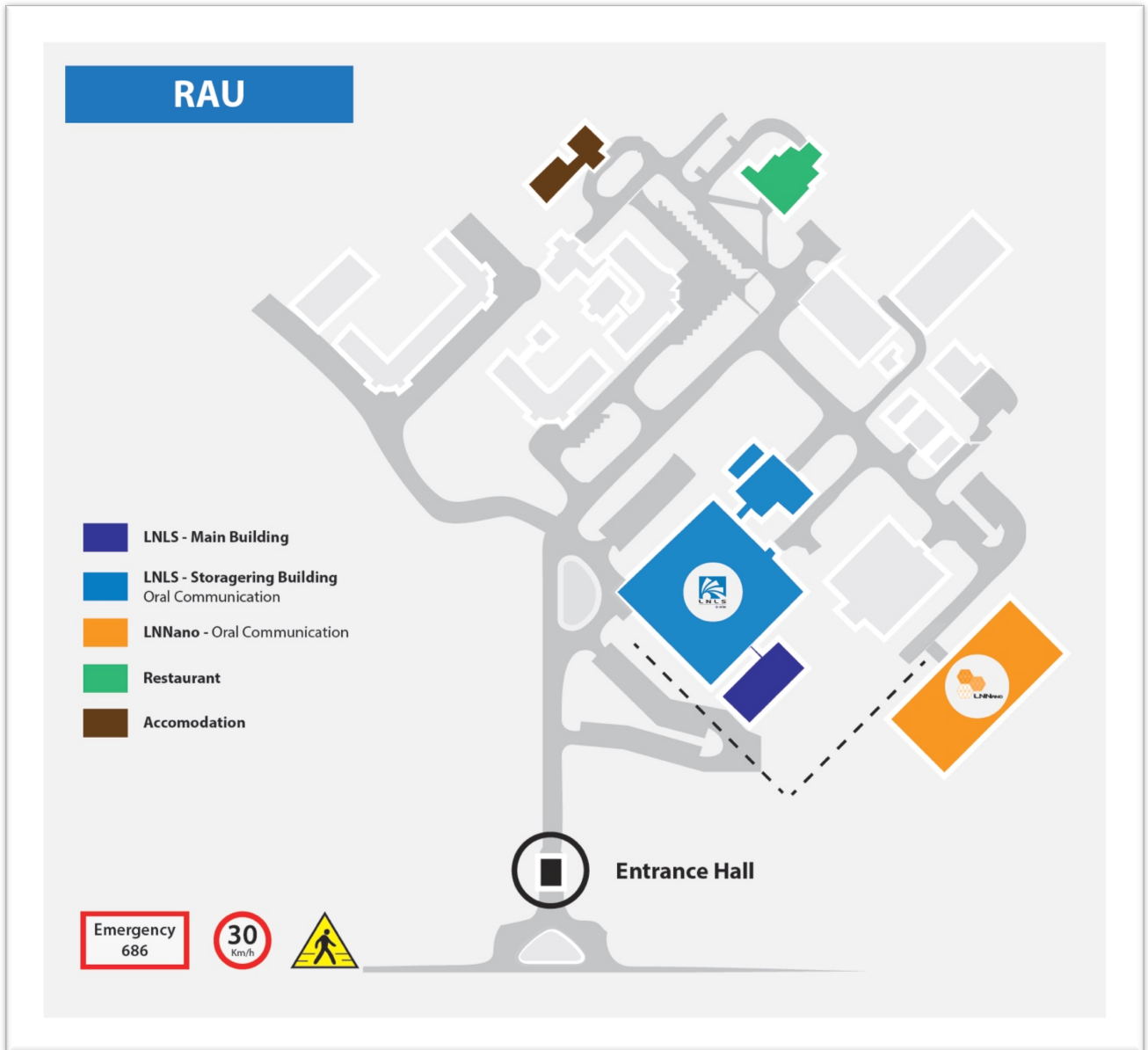


CNPq

MINISTÉRIO DA
CIÊNCIA, TECNOLOGIA,
INOVAÇÕES E COMUNICAÇÕES



CNPEM – Campus Map



■ SUMMARY

- 11 **Presentation**
- 12 **Organizers | Scientific Committee**
- 15 **Program**
- 17 **Abstracts**
-
- 18 **Role of particle size, composition and structure of Co-Ni nanoparticles in the catalytic properties for steam reforming of ethanol addressed by X-ray spectroscopies**
Adriano H. Braga¹, Daniela C. Oliveira², D. Galante², F. Rodrigues³, Frederico A. Lima², Tulio R. Rocha², R. J. O. Mossaneck⁴, João B. O. Santos¹ and José M. C. Bueno¹
- 19 **Electro-oxidation of biomass derived molecules on Pt_xSn_y/C carbon supported nanoparticles**
A. S. Picco³, C. R. Zanata¹, G. C. da Silva², M. E. Martins⁴, C. A. Martins⁵, G. A. Camara¹ and P. S. Fernández^{6,*}
- 20 **3D Studies of Magnetic Stripe Domains in CoPd Multilayer Thin Films**
Alexandra Ovalle¹, L. Nuñez¹, S. Flewett¹, J. Denardin², J. Escrig², S. Oyarzún², T. Mori³, J. Criginski³, T. Rocha³, D. Mishra⁴, M. Fohler⁴, D. Engel⁴, C. Guenther⁵, B. Pfau⁵ and S. Eisebitt⁶.
- 21 **Insight into the activity of Au/Ti-KIT-6 catalysts studied by in situ spectroscopy during the epoxidation of propene reaction**
A. Talavera-López^{*}, S.A. Gómez-Torres and G. Fuentes-Zurita
- 22 **Nanosystems for nasal isoniazid delivery: small-angle x-ray scattering (saxs) and rheology proprieties**
A. D. Lima¹, K. R. B. Nascimento¹, V. H. V. Sarmiento² and R. S. Nunes¹
- 23 **Assembly of Janus Gold Nanoparticles Investigated by Scattering Techniques**
Ana M. Percebom^{1,2,3}, Juan J. Giner-Casares¹, Watson Loh² and Luis M. Liz-Marzán¹
- 24 **Study of the morphology exhibited by carbon nanotube from synchrotron small angle X-ray scattering**
Ana Pacheli Heitmann¹, Iaci M. Pereira², Elisa Castro¹ and Rodrigo L. Lavall¹
- 25 **The support influence on Pt_xPd_{1-x}/SiO₂ (x = 1, 0.7 or 0.3) nanoparticles reactivity**
Gorgeski, M. V. Castegnaró, F. Bernardi, M. C. M. Alves and J. Morais
- 26 **XANES Evaluation of a New Method for the Synthesis of Palladium Nanoparticles**
Brunno Lange Albuquerque¹, E. Latocheski¹, T. R. Silva¹, A. M. Signori¹, D. C. Oliveira² and J. B. Domingos¹
- 27 **Understanding PEO-Lithium Triflate interaction in thin films at nanoscale using IR-SNOM**
Bruno B. M. Torres¹, Francisco C. B. Maia², Raul O. Freitas² and Debora T. Balogh¹
- 28 **Evaluating Chitosan Interaction with Cell Membrane Models using X-Ray Scattering at the Air-Water Interface**
B. B. M. Torres², A. A. M. Gasperini¹, F. J. Pavinatto², T. M. N. Pavinatto², E. N. Lorenzón², E. R. Spada² and O. N. Oliveira Jr.²

- 29 **Inner shell electronic study of $\text{CF}_3\text{C}(\text{O})\text{OC}(\text{O})\text{CF}_3$**
Carlos O. Della Védova^a, Y. B. Martínez^a, Y. B. Bava^a, M. F. Erben^a,
R. L. Cavasso Filho^b and R. M. Romano^a
- 30 **The invar effect studied by time resolved x-ray diffraction**
Carlos William Galdino¹, C. Giles¹, G. N. Kontogiorgos¹, K. Tasca¹ and L. Coelho²
- 31 **Partial substitution of Ni by Co in Ni-type perovskites and evaluation in steam reforming of Liquid Petroleum Gas**
C. N. Ávila-Neto, A. M. M. Arouca, K. F. Oliveira and C. E. Hori
- 32 **X-ray powder diffraction with synchrotron radiation and scanning electron microscopy on NiO/NiMn₂O₄ composite**
C. M. R. Remédios¹, A. J. Freitas Cabral^{1,2}, C. A. Ospina³,
A. Magnus G. Carvalho⁴ and S. L. Morelhão⁵,
- 33 **Advanced Methods for modeling Small Angle Scattering Data**
Cristiano L. P. Oliveira¹
- 34 **Structural Characterization of Ultra Low-k Carbon Doped Silicon Dioxide Films by X-ray Reflectometry and GISAXS**
D. R. Huanca¹, P. Verdonck² and S. G. dos Santos Filho³
- 35 ***In situ* Synchrotron 2D-XRD evaluation of formation and reversion of strain-induced martensite in AISI 201 austenitic stainless steel**
D. R. Almeida Junior¹, I. R. Souza Filho¹, C. Gauss¹, M. J. R. Sandim¹, P. A. Suzuki¹ and H. R. Z. Sandim¹
- 36 **EXAFS study of the local atomic structure in $A\text{Fe}_2\text{As}_2$ ($A = \text{Eu}, \text{Sr}, \text{Ba}$)**
D. Tobia¹, M. E. Saleta², M. Radaeli¹, M. M. Piva¹, S. J. A. Figueroa², G. G. Lesseux¹, C. B. R. de Jesus¹, R. R. Urbano¹, E. Granado¹ and P. G. Pagliuso¹
- 37 **Residual X-ray back-diffraction: Can we further increase the energy resolution at angles above 90°?**
Edson M. Kakuno¹, Marcelo G. Hönnicke², Raymond Conley³, Cesar Cusatis⁴, Elina Kasman³, João B. Marques⁵ and Flávio C. Vicentin⁶.
- 38 **Ga doped ZnO nanowires growth on ZnO thin films prepared by the two stages hydrothermal method**
E. Heredia, C. Bojorge, H. Cánepa and N.E. Walsõe de Reca
- 39 **Effect of coating on $\gamma\text{-Fe}_2\text{O}_3$ nanoparticles studied using XAS**
E. Lede¹, S. J. Stewart¹, M. P. Morales² and P. de la Presa^{3,4}
- 40 **About a New Synthetic Method of Palladium Nanoparticles: An *In Situ* SAXS Kinetic Analysis**
Eloah Latocheski¹, B. L. Albuquerque¹, D. Faggion Jr.¹, A. M. Signori¹ and J. B. Domingos¹
- 41 **Delayed light emission of TetraPhenyl Butadiene excited by liquid argon scintillation light. Current status and future plans.**
Ettero Secreto
- 42 **XANES spectroscopy for electronic characterization of manganese (II) coordination complexes**
Eugenia A. Orosco Condori, Luciana C. Juncal, Carlos O. Della Védova and Rosana M. Romano

- 43 **Low-resolution structural studies of the splicing regulatory kinase SRPK2**
E. A. A. Barbosa¹, T.V. Seraphim², M.V. Barros, R.R. Teixeira³, J.C. Silva⁴, J.C. Borges² and G.C Bressan¹.
- 44 **Investigation of the valence shell of Ru(II) polypyridil complexes by UV vacuum absorption and XEOL**
Fabio da Silva Miranda¹, Juliana da S. Goulart¹, Alan G. P. Sobrinho¹, Chiraz Belouezzane¹ and Rosa M. Sakae¹
- 45 **Structure stability and electronics of Ag and Cu atomic quantum clusters: EXAFS and XANES studies.**
Félix G. Requejo¹, Lisando J. Giovanetti¹, José M. Ramallo-López¹, Shahana Huseyinova², David Buceta² and Arturo López-Quintela²
- 46 **Reversal Magnetization dependence with oxidation state in YFe_{1-x}Cr_xO₃ Perovskites**
F.A. Fabian¹, P.P. Pedra¹, C.C.S. Barbosa¹, K. O. Moura², J.G.S. Duque¹ and C.T. Meneses²
- 47 **Structural Investigation, Cation Distribution and Oxidation State in Core-Shell Magnetic Nanoparticles**
F. H. Martins¹, J. A. Gomes¹, R. Aquino¹, F. Porcher², J. Mestink-Filho³, R. Perszynski⁴ and J. Depeyrot¹
- 48 **An Infrastructure for X-ray Emission Spectroscopy with High Energy Resolution at LNLS**
F. Alves Lima¹, M. E. Saleta¹, R. P. Santos¹ and M. A. Eleotério¹
- 49 **Application of X-Ray Phase Contrast Microtomography Using Brazilian Synchrotron Light Laboratory to Improve the Visualization of External and Internal Structures of *Rhodnius prolixus* head**
G. Sena¹, A. Almeida², L. Nogueira³, D. Braz¹, M. Gonzalez⁴, P. Azambuja⁵ and R. Barroso³
- 50 **Table top femtosecond x-ray source for time resolved x-ray diffraction experiments**
George Nicolas Kontogiorgos¹, Carlos Manuel Giles¹, Carlos William Galdino¹
- 51 **Fe speciation in mine tailings using X-ray absorption spectroscopy**
G. Bia, E. Nieva, M. G. García and L. Borgnino
- 52 **Saxs/waxs study of the kinetics of formation of metal organic frameworks**
Gustavo M. Segovia¹, Agustin S. Picco², Jimena S. Tuninetti¹, Marcelo Ceolín¹, Omar Azzaroni¹ y Matias Rafti¹.
- 53 **Study of melting and cristalization of Bi nanoparticles in glass 72B2O3-28Na2O**
Hermann F. Degenhardt^{1,2} and Guinther Kellermann²
- 54 **Synthesis and optical characterization of Y2O3:Eu and Y2O3:EuTi nanoparticles for use in bioimaging**
Ísis F. Manali¹, Lucas C. V. Rodrigues², Douglas Galante¹ and Verônica C. Teixeira¹

- 55 **Influence of Protic Ionic Liquid on Structure of Proton-conducting SPEEK-Zirconia Membranes for Anhydrous Fuel Cell Application**
João Arthur Batalha¹, K. Dahmouche² and A. Gomes¹
- 56 **Compact X-ray Spectrometer for the Nanofocus Beamline at SIRIUS**
J. I. Robledo^{1,2}, H. J. Sánchez^{1,2}, C. A. Pérez³ and M. Honnicke⁴
- 57 **Identification of lithium compounds in Li-enriched *Pleurotus djamor* mushrooms**
J.M.R. da Luz¹, T.P.M. Machado¹, M.C.S. Da Silva¹, L. Vergutz², D. Galante³ and M.C.M. Kasuya¹
- 58 **“In-situ” XAFS and SAXS study of the kinetics of growth of Au nanowires**
J. M. Ramallo-López¹, F. Schunder¹, C. Hoppe², L. J. Giovanetti¹, C. Huck-Iriart¹, F. G. Requejo¹
- 59 **Manganese Compound Mixtures Determined by Core-level RIXS Spectroscopy**
Juan José Leani¹, J. Robledo¹, C. Pérez² and Héctor Jorge Sánchez^{1,3}
- 60 **RIXS combined with PCA for the Study of the Li₄Ti₅O₁₂ (LTO) Molecule with Different Levels of Charge**
Juan José Leani¹, J. Robledo¹, F. Oliva², C. Pérez³ and H. J. Sánchez^{1,4}
- 61 **Studying the 4f electrons in the Kondo lattice antiferromagnet Ce₂RhIn₈**
K. R. Pakuszewski¹, W. S. Silva², C. Giles¹, F. Rodolakis³, Julio C. Cezar², J. C. Campuzano⁴, P. G. Pagliuso¹, and C. Adriano¹
- 62 **Photofragmentation Study of the Acetaldehyde (CH₃CHO) at the Carbon and Oxygen K Edges.**
L. C. Ribeiro¹, M. S. Arruda², F. V. Prudente¹, L. V. A. Mendes¹, A. C. F. Santos³, M. J. Santos¹, R. R. T. Marinho¹ and A. Medina¹.
- 63 **Evaluation of niobia based catalysts for the esterification reaction: the effect of calcination temperatures**
L.L. Rade¹, C.O.T. Lemos¹, R. M. Ribas², R. S. Monteiro^{2,3} and C. E. Hori¹
- 64 **Effect of the Exposure to Air in the morphology of water soluble Silver Nanoparticles Coated with MUA**
Lisandro J. Giovanetti¹, José M. Ramallo-López, M. Cristina E. Hoppe, Félix G. Requejo
- 65 **Advances in the design of new energy storage materials using the new TGM setup for VUV-luminescence studies**
Lucas C.V. Rodrigues¹, Cassio C.S. Pedroso¹, Leonnam G. Merízio¹, José M. Carvalho², Ian P. Machado¹, Otávio P. Bezzan¹, Maria C.F.C. Felinto³, Hermi F. Brito¹, Verônica C. Teixeira⁴ and Douglas Galante⁴
- 66 **XANES study of nickel(II) coordination complexes: comparison of the electronic structure for different geometries and ligand alkylic chain length**
Luciana C. Juncal and Rosana M. Romano

- 67 **Phase-Retrieval as a Regularization Problem**
Marcelo R. Dos Anjos^{3,5}, Eduardo X. Miqueles*¹, João C. Cerqueira², Elias S. Helou⁴, Nikolay Koshev⁴ and Nathaly Archilla¹
- 68 **Charge transfer effects in the chemical reactivity of Pd_xCu_{1-x} nanoalloys**
M.V. Castegnaro¹, A. Gorgeski¹, B. Balke², M.C.M. Alves¹ and J. Morais¹
- 69 **Heterojuncions of Graphene and Pd and Pd/Pt Alloy Nanoparticles: H₂ Sensing and Potential Catalytic Applications**
Dalfovo, M. C., Huck Iriart, C., Giovanetti, L. J., Requejo, F. G. and Francisco J. Ibañez, F. J.
- 70 **Monitoring the redox process for cerium and aluminum-based catalysts by in situ XANES**
M. C. Rangel¹, J. Fonseca^{1,2}, N. Bion², C. M. Morais², Y. E. L. Fonseca³, D. Duprez² and F. Epron²
- 71 **Application of SR μ XRF to evaluate the efficacy of Pb soil extraction of hyperaccumulator plant species versus fastgrowing plants used for phytoextraction of soil contaminants**
Mera M. F.¹, Rubio, M.^{1,2,3}, Pérez C. A.⁴, Carranza L.¹, Cazón S.¹, Ravera M.¹
- 72 **Adsorption of Alkanethiols on Well Defined and Nanoparticle Pd Surfaces**
M. H. Fonticelli¹, A. A. Rubert¹, J. C. Azcárate¹ and A. de Siervo²
- 73 **Short-term bonding of freshly added cadmium in Brazilian Oxisols**
Marina Colzato^{1,2}, M.Y. Kamogawa¹, H.W.P. Carvalho², L.R.F. Alleoni¹ and D.L. Hesterberg³
- 74 **Characterization and low-resolution structure of an extremely-thermostable esterase of potential biotechnological interest from *Pyrococcus furiosus***
Mario de Oliveira Neto¹, César Augusto Gandin¹, Fernanda Mandelli², Thiago A. Gonçalves^{2,3} and Fabio Marcio Squina².
- 75 **Photoluminescence studies under UV and VUV excitation of undoped and rare-earth doped CaYAl₃O₇**
Mário E. G. Valerio¹, Giordano F. C. Bispo¹, Adriano B. Andrade¹ and Verônica C. Teixeira²
- 76 **Study of the profile of layer formed in plasma nitrided ASTM F138 stainless steel**
D.Olzon-Dionysio^(1,a), S. D. de Souza⁽¹⁾, L. G. Martinez⁽²⁾, E. H. da Silva⁽³⁾ and M. Olzon-Dionysio⁽¹⁾
- Selenium distribution and speciation in biofortified mushroom**
- 77 M.C.S. Da Silva¹, P.A.Z. Sereño¹, M.D. Nunes¹, L.F.S. Souza Filho², L. Vergutz³, C.A. Perez⁴, D. B. Abdala⁴ and M.C.M. Kasuya¹
- 78 **PDF Studies on Quasi-Amorphous Materials: Magnetic Nanoparticles and Low Z Materials**
M. E. Saleta¹, B. Pianciola², E. Lima Jr.² and F. Alves Lima¹
- 79 **EXAFS characterization of confined gold nanoparticles for the detection of small molecules in label-free impedance aptasensors**
Martín Mizrahi³, Ana Sol Peinetti¹, Helena Ceretti², Graciela González¹, Silvana Ramírez², Félix Requejo³, Javier Montserrat^{2,4} and Fernando Battaglini¹
- 80 **Local structure of Er³⁺ and Yb³⁺ in oxyfluoride borate glasses studied by EXAFS**
M. Rodriguez^{1,2}, R. Keuchkerian², Santiago Figueroa³ and L. Fornaro¹

- 81 **Effect of matrix composition in the kinetic of grow of Pb nanodroplets in lead-borate glass**
Maximilia F. de Souza^{1,2} and Guinther Kellermann²
- 82 **Identification of arsenic solid species in sulfide mine tailings from the Concordia Mine Argentina using X-ray absorption spectroscopy**
N.E Nieva, L. Borgnino and M.G Garcia.
- 83 **Aluminum Titanate (Al₂TiO₅) ceramics: complementary Al and Ti K-XAS studies**
N.M. Rendtorff²³, L. Andriani¹, R. Moreira Toja², M.A. Violini²³, M.R. Gauna², M.S. Conconi² and F. Requejo¹⁴
- 84 **Microstructural characterization of a natural/synthetic hybrid material by means of PALS and SAXS**
Pablo S. Anbinder¹, Carlos Macchi¹, Javier Amalvy² and Alberto Somoza¹
- 85 **Study of structural features and aggregation of S-layer proteins from lactobacilli**
Patricia Bolla¹, P. Peruzzo², M. Casella¹ and M. de los A. Serradell³
- 86 **Hydrogen production by steam reforming of acetic acid using hydrotalcite precursors**
R. P. Borges¹, R. A. R. Ferreira¹, R. C. Rabelo-Neto², F. B. Noronha², C. E. Hori¹
- 87 **Morphology and size study of (Gd,Er,Yb)-doped NaYF₄ nanoparticles through the X-ray Line Profile Analysis.**
R. Lora-Serrano¹, W Iwamoto¹, E. Estevez-Rams², Jeann C. Rodrigues¹, and B. Aragón-Fernandez².
- 88 **Biochemical and structural characterization of 1-Cys Peroxiredoxin from the human opportunistic pathogen *Aspergillus fumigatus***
R. Bannitz-Fernandes¹; K. F. Godoy²; C. A. Tairum³; I. Malavazi²; M. A. Oliveira³ and L. E. S. Netto¹
- 89 **Chromobacterium violaceum OhrA and OhrB: New Considerations on the Enzymatic Mechanism Steps**
Domingos, RM¹; Meireles, DA¹; da Silva Neto, JF²; Alegria, TGP¹; Teixeira, RD³; Netto, LES¹
- 90 **Analysis of the crystal electric field ground state of intermetallic TbRhIn₅ by using soft X-ray absorption spectroscopy**
R. P. Amaral¹, D. J. Garcia², D. Betancourth³, P. G. Pagliuso³, J. G. S. Duque³ and R. Lora-Serrano¹
- 91 **Study of the synthesis method and barium substitution on nickel catalysts for dry reforming of methane using XPD line**
R. S. Gomes¹, C. B. Rodella², R. S. Batista¹, M. S. Santos¹, D. S. Costa¹ and S. T. Brandão¹
- 92 **A reduction behavior study of aluminum and copper-doped iron oxides by XRD**
Sarah Maria Santana Borges¹, Maria do Carmo Rangel¹, Cristiane Barbieri Rodella²
- 93 **Synthesis and characterization for XRD with synchrotron light of a PtNb CO tolerant electrocatalyst for polymeric membrane fuel cells**
Thairo A. Rocha and Ernesto R. Gonzalez¹
- 94 **Structure and Photoluminescence properties of europium-doped hydroxyapatite 3-D scaffolds.**
Thiago A.R.M. Lima¹ and Mário E.G. Valerio²

- 95 **Use of synchrotron radiation on the investigation of Gd₂O₃: Eu³⁺ structural and optical properties**
Valdivânia A. Nascimento¹, Ísis F. Manali², Cristiane B. Rodella², Lucas C. V. Rodrigues³, Douglas Galante² and Verônica C. Teixeira²
- 96 ***In-situ* XAS and XRD study of CuO/SrTiO₃ and NiO/SrTiO₃ catalysts**
Vitor C. Coletta¹, Francielle C. F. Marcos², Francisco G. E. Nogueira³, Maria I. B. Bernardi¹, Elisabete M. Assaf² and Valmor R. Mastelaro¹
- 97 **Simulated entrapment of microorganisms in halites under Martian conditions and interplanetary transfer of life**
X.C. Abrevaya¹, D. Galante^{2,3}, P. Tribelli⁴, F. Nóbrega⁵, G. Araujo^{3,6}, M.E. Varela⁷, F. Rodler^{8,9}, F. Rodrigues¹⁰, T. Gallo³ and J. E. Horvath²
- 98 **Unusual photofragmentation mechanisms of chlorinated species elucidated by a combination of double and triple ionic coincidences spectra**
Yanina B. Bava¹, Y. B. Martinez¹, R. L. Cavasso Filho² and R. M. Romano¹
- 99 **Comparative study of photoionization and photofragmentation mechanisms of sulfur VOCs**
Yanina B. Bava¹, Yanina Berrueta Martinez¹, Reinaldo L. Cavasso Filho², Yeny A. Tobón Correa³, Sophie Sobanska³ and Rosana M. Romano¹

▪ PRESENTATION

Dear Participant,

On behalf of the organizers, I welcome all the participants of the 26th Annual Users Meeting of the Brazilian Synchrotron Light Laboratory (RAU/LNLS).

This is a very exciting moment for the users community represented in this meeting. On the one hand, the construction of the new synchrotron light source (SIRIUS) continues in a steady and solid pace, while the first-phase beamlines are already fully specified with some components already under construction. On the other hand, the earlier efforts to modernize the current LNLS facilities, including the construction, commissioning and operation of two high-performance beamlines in the soft (PGM) and hard (XDS) x-ray region, amongst other initiatives, seem to have reached a mature stage. As a consequence, previously unattainable conditions of beam intensity, energy resolution, and sample environments are now possible at LNLS, bridging the gap between the capabilities of the earlier facilities and what will be possible to perform in SIRIUS.

It is hoped that this meeting helps in the communication of the science and instrumentation being done in the present and for the future, fertilizing new ideas and creating new links.

The scientific and local committees are acknowledged for their decisive contributions to the organization of this meeting.

Eduardo Granado

Chair of the 26th RAU
On behalf of the LNLS Users Committee

▪ **ORGANIZERS | SCIENTIFIC COMMITTEE**

1. Antonio Gomes (UFC)
2. Eduardo Granado (Chair) - (Unicamp)
3. Elias Salomão Neto (USP)
4. Elisabete Assaf (USP)
5. Maria Luiza Rocco (UFRJ)
6. Mariano H. Fonticelli (UNLP)
7. Mônica Alonso Cotta (Unicamp)
8. Yraima Cordeiro (UFRJ)

▪ **LOCAL COMMITTEE**

1. Dora Marques (Communication – CNPEM)
2. Fábio Reis Fonseca (Communication – CNPEM)
3. Gabriela Campeão (SAU – CNPEM)
4. Graziela Esteves (LNLS – CNPEM)
5. Helio Tolentino (LNLS – CNPEM)
6. Ildéria Maíra dos Santos (Communication – CNPEM)
7. Luciana Noronha (Communication – CNPEM)
8. Pamela Machado (Communication – CNPEM)
9. Priscila Cassiano Alves (LNLS – CNPEM)
10. Renan Picoreti (LNLS – CNPEM)
11. Renata Mioshi (SAU – CNPEM)

- **GENERAL PROGRAM**

August 24th	
08:00 - 08:30	Reception/Registrations
08:30 - 08:45	Opening
08:45 - 09:30	Sirius: Status and Perspectives Antonio José Roque da Silva
09:30 - 10:30	Plenary 1 - Storage Ring Auditorium High Resolution Resonant Inelastic Soft X-ray Scattering - Jan-Erik Rubensson
10:30 - 11:00	Coffee Break
11:00 - 12:30	Oral Communication 1 - Storage Ring and LNNano Auditorium
13:00 - 14:30	Lunch (at CNPEM Restaurant)
14:30 - 16:00	Oral Communication 2 - Storage Ring and LNNano Auditorium
16:00 - 16:30	Coffee Break
16:30 - 19:00	Posters Session

August 25th	
08:15 - 09:15	Plenary 2 - Storage Ring Auditorium Synchrotron Serial Crystallography Meitian Wang
09:15 - 11:00	Thematic Session
11:00 - 11:30	Coffee Break
11:30 - 12:45	Panel discussion: Committee & LNLS with the users
12:45 - 13:00	Closing
13:00 - 14:00	Lunch (at Exhibition Area)
14:00 - 16:00	Visit to Sirius Construction Works

- **THEMATIC SESSIONS**

August 25th, 2016; 9h15 – 11h00 (1h45 in total)		
09h15	Overview of the Sirius/LNLS first-phase beamlines	Harry Westfahl Jr.
09h45	CARNAUBA beamline (Coherent X-ray Nanoprobe)	Hélio Tolentino
10h00	CATERETE beamline (Coherent X-ray Scattering)	Florian Meneau
10h15	EMA beamline (Absorption and Diffraction at extreme conditions)	Narcizo Souza Neto
10h30	MANACA beamline (Macromolecular crystallography)	Ana Zeri
10h45	IPE beamline (Soft X-ray Spectroscopy)	Túlio Rocha

▪ **ORAL COMMUNICATIONS**

Oral Communication 1 | Storage Ring Auditorium

11:00	Davison Ramos de Almeida Junior	Application of SR μ XRF to evaluate the efficacy of Pb soil extraction of hyperaccumulator plant species versus fastgrowing plants used for phytoextraction of soil contaminants
11:15	Éverton de Almeida Alves Barbosa	Low-Resolution Structural Studies of the splicing regulatory Kinase SRPK2
11:30	Cristiano L. P. Oliveira	Advanced Methods for modeling Small Angle Scattering Data
11:45	Fernando Henrique Martins da Silva	Structural Investigation, Cation Distribution and Oxidation State in Core-Shell Magnetic Nanoparticles
12:00	Jose Martin Ramallo Lopez	"In-situ" XAFS and SAXS study of the kinetics of growth of Au nanowires

Oral Communication 1 | LNNano Auditorium

11:00	Frederico Alves Lima	An Infrastructure for X-ray Emission Spectroscopy with High Energy Resolution at LNLS
11:15	Juan José Leani	Manganese Compound Mixtures Determined by Core-level RIXS Spectroscopy
11:30	Ettore Segreto	Delayed light emission of TetraPhenyl Butadiene excited by liquid argon scintillation light. Current status and future plans.
11:45	Mário Ernesto Giroldo Valerio	Study about luminescence in doped and undoped CaYAl ₃ O ₇ using VUV
12:00	Fabio da Silva Miranda	Investigation of the valence shell of Ru(II) polypyridil complexes by UV vacuum absorption and XEOL
12:15	Maria Fernanda Mera	In situ Synchrotron 2D-XRD evaluation of formation and reversion of strain-induced martensite in AISI 201 austenitic stainless steel

Oral Communication 2 | Storage Ring Auditorium

14:30	Lucas Carvalho Veloso Rodrigues	Advances in the design of new energy storage materials using the new TGM setup for VUV-luminescence studies
14:45	Rosana Mariel Romano	Unusual photofragmentation mechanisms of chlorinated species elucidated by a combination of double and triple ionic coincidences spectra
15:00	Yanina Belén Bava	Comparative study of photoionization and photofragmentation mechanisms of sulfur VOCs
15:15	Ximena C. Abrevaya	Simulated entrapment of microorganisms in halites under Martian conditions and interplanetary transfer of life
15:30	Carlos O. Della Védova	Inner shell electronic study of CF ₃ C(O)OC(O)CF ₃

Oral Communication 2 | LNNano Auditorium

14:30	Ana Maria Percebom	Assembly of Janus Gold Nanoparticles Investigated by Scattering Techniques
14:45	Adriano Henrique Braga	Role of particle size, composition and structure of Co-Ni nanoparticles in the catalytic properties for steam reforming of ethanol addressed by X-ray spectroscopies
15:00	Mariano H. Fonticelli	Adsorption of Alkanethiols on Well Defined and Nanoparticle Pd Surfaces
15:15	Brunno Lange Albuquerque	XANES Evaluation of a New Method for the Synthesis of Palladium Nanoparticles
15:30	Verônica de Carvalho Teixeira	Use of synchrotron radiation on the investigation of Gd ₂ O ₃ : Eu ³⁺ properties
15:45	Felix G. Requejo	Structure stability and electronics of Ag and Cu atomic quantum clusters: EXAFS and XANES studies.

- **ABSTRACTS PLANARY I AND II**

High-Resolution Resonant Inelastic Soft X-ray Scattering

Jan-Erik Rubensson

Department of Physics and Astronomy, Uppsala University, Uppsala, Sweden

E-mail: jan-erik.rubensson@fysik.uu.se

Resonant inelastic X-ray scattering (RIXS) reflects fine details in electronic structure and dynamics. The process is site specific on the atomic length scale (sub-nanometer) and time specific on the timescale for nuclear and electronic rearrangements (femto- to attoseconds). Consequently, RIXS spectroscopy has a tremendous potential in atomic and molecular, chemical and condensed matter physics. RIXS techniques have, however, suffered from the lack of adequate radiation sources. In practice this has limited the spectral quality and only a fraction of the inherent advantages have been exploited.

The performance of the SAXES set-up at the ADDRESS beamline of SLS has demonstrated that an energy resolution well above $E/\Delta E \sim 10000$ is feasible, and allowing for separation of fundamental excitations in complex materials including vibrational excitations. This directly provides detailed information about ultrafast dynamics, and facilitates accurate mapping of ground and excited state potential surfaces. In addition, the phenomenology in simple systems gives new information about the scattering process itself.

Measurements on free molecules and liquids will be presented, and discussed in terms of *ab-initio* multimode scattering calculations. Implications for RIXS studies for molecular materials and processes will be discussed.

The development has inspired ambitious RIXS projects at the new and upcoming synchrotron radiation facilities, including the VERITAS beamline at MAX IV, which will be briefly presented.

Serial Crystallography at Synchrotrons and XFELs

Meitian Wang

Swiss Light Source, Paul Scherrer Institute, Switzerland

E-mail: meitian.wang@psi.ch

Third-generation synchrotron sources have made great impacts on modern X-ray based structural biology, and more than 80,000 structures have been determined at macromolecular crystallography (MX) beamlines worldwide since then. Until very recently, most MX structures were determined with diffraction data collected by the rotation method from a single crystal.

Advances in MX beamline optics enabled micron-sized beams, capable of collecting data from microcrystals that individually would not be sufficient for a complete data set. Therefore, in order to obtain a complete dataset, partial datasets from many randomly orientated microcrystals would need to be collected and properly assembled.

This new method is termed serial crystallography (SX), originally developed for X-ray free electron lasers (XFEL), a relatively new X-ray source with such high photon flux that only one still diffraction pattern can be obtained per crystal prior to its destruction. SX is well suited to specimens for which macro-sized crystals for conventional MX are unobtainable, and data can be collected at both room and cryogenic temperatures.

I will present new techniques for measuring, processing, and merging SX data with focus on in meso in situ methods for membrane proteins. The application of SX at current and upcoming fourth-generation synchrotron sources and XFELs will be discussed.

26th RAU

ANNUAL USERS

MEETING LNLS/CNPEM

August 24th and 25th, 2016

ABSTRACTS

cnpem.br/rau



MINISTÉRIO DA
CIÊNCIA, TECNOLOGIA,
INOVAÇÕES E COMUNICAÇÕES



Role of particle size, composition and structure of Co-Ni nanoparticles in the catalytic properties for steam reforming of ethanol addressed by X-ray spectroscopies

Adriano H. Braga¹, Daniela C. Oliveira², D. Galante², F. Rodrigues³, Frederico A. Lima², Tulio R. Rocha², R. J. O. Mossaneck⁴, João B. O. Santos¹ and José M. C. Bueno¹

Federal University of São Carlos, Department of Chemical Engineering, 13565-905, São Carlos, Brazil; 2 Brazilian Center for Research on Energy and Materials, Brazilian Laboratory of Light Synchrotron, 13083-970, Campinas, Brazil; 3University of São Paulo, Institute of Chemistry, 05508-000, São Paulo, Brazil; 4 Federal University of Paraná, Department of Physics, Curitiba, 81531-990, Brazil jmcb@ufscar.br

The Steam Reforming of Ethanol (SRE) is one of promising process to produce H₂ in a renewable way. Ethanol reacts with water at temperatures around 500°C, giving H₂, CO and CO₂ as main products. Active catalysts for this reaction are based on supported nickel nanoparticles [1]. Nevertheless, the lack of stability is one major drawback for this reaction, because of extensive carbon accumulation [1,2]. In order to avoid this problem, improvement of the catalyst by tuning electronic and structural properties is a good attempt. Bimetallic nanoparticles are particularly interesting because of the different structures and catalytic properties they show, compared to parent metal components. The addition of Co has shown interesting results for SRE, such as the enhancement of carbon oxidation reaction rates [3]. In this work, a series of Co, Ni, and CoNi catalysts were prepared. The metallic composition Co/Ni was studied by both surface and bulk techniques. Also, nanoparticle size played a role in the overall activity, redox properties, and carbon accumulation. X-ray characterization showed that the precursors are composed of NiO for the Ni catalysts, Co₃O₄ for Co catalysts, and mixed NiO/NiCo₂O₄ oxides are present in the bimetallic catalysts. After reduction with hydrogen, the bimetallic catalysts presented a surface enrichment by Ni, with Co mostly in the core of nanoparticle, as shown by XPS. The lattice parameter of cubic structures changed with Co addition, confirming that an alloy is formed. By heating the catalysts in SRE atmosphere, XAS spectra showed that oxidation of the nanoparticles surface occurred initially, and as the reaction proceeded and the atmosphere became more reduced, a re-reduction took place. Also, when the oxidation level of the SRE stream was higher, Co migrates to surface of the bimetallic nanoparticle. A complex relation between surface structure of the nanoparticles and the products of SRE reaction is presented. The carbon accumulation measured after SRE reaction at 550°C decreased as the Co concentration increases. By decreasing the nanoparticles size, from around 15 nm to 5 nm, as proved by TEM images, the amount of carbon deposited suffered a greater decrease, especially on Co containing small nanoparticles. These properties may attempt to important features that lead to more stable low-cost materials for biomass-based reforming reactions.

D. Zanchet, J. B. O. Santos, S. Damyanova, J. M. R. Gallo, J. M. C. Bueno. ACS Catal 5, 3841 (2015)
C. N. Ávila-Neto, D. Zanchet, C. E. Hori, R. U. Ribeiro, J. M. C. Bueno. J Catal 307, 222 (2013)
G. P. Szijjártó, Z. Pászti, I. Sajó, A. Erdőhelyi, G. Radnóczy, A. Tompos. J Catal 305, 290 (2013)

Acknowledgements: This work was supported by FAPESP (process 2011/52177-4 and 2013/10858-2). We acknowledge the LNLS staff for helping in XAS experiments and also the LNNano staff for helping in the TEM measurements

Electro-oxidation of biomass derived molecules on Pt_xSn_y/C carbon supported nanoparticles

A. S. Picco,³ C. R. Zanata,¹ G. C. da Silva,² M. E. Martins⁴, C. A. Martins⁵, G. A. Camara¹ and P. S. Fernández^{6,*}

¹ Institute of Chemistry, Universidade Federal de Mato Grosso do Sul, Campo Grande/MS, Brazil. ² São Carlos Institute of Chemistry, University of São Paulo, São Carlos/SP, Brazil. ³ LNLS - Brazilian Synchrotron Light Laboratory, Campinas/SP, Brazil. ⁴ Physical Chemistry Research Institute (INIFTA), Exact Sciences Faculty, CCT La Plata-CONICET, La Plata, Argentina. ⁵ Faculty of Exact Sciences and Technology, Universidade Federal da Grande Dourados, Dourados/MS, Brazil. ⁶ Institute of Chemistry, State University of Campinas. Cidade Universitária "Zeferino Vaz", Campinas/SP, Brazil

*pablo.fernandez@iqm.unicamp.br

Glycerol (GIOH) and ethanol (EtOH) world production have increased exponentially in the last decade. However, the electrooxidation of EtOH (EOE) have been intensely studied due to the huge availability of this fuel. On the other hand, the interest in GIOH is more recent, growing markedly in the last decade with the increasing in the biodiesel production.

In a paper recently published by our group [1], we compared the oxidation of both molecules on Pt/C nanoparticles (NPs). We found that GIOH is more effectively oxidized to CO₂, however, the EOE is able to produce higher currents due to a faster oxidation to acetic acid, compared to the slow complex electrooxidation of glycerol (EOG) to CO₂.

It is well-known that PtSn alloys are excellent materials towards the EOE [2]. In this work, we have comparatively studied the electrocatalytic behavior of PtSn/C NPs on the oxidation of both alcohols by preparing PtSn/C NPs of several compositions. We observed different electrochemical behavior for both molecules on all the catalyst by using cyclic voltammetry and the products/intermediates production/consumption is being monitored by *in situ* FTIR. and long-term chronoamperometry. The products of the reaction during the chronoamperometry are being analysed by HPLC.

All the different behaviors must be a consequence of the structural and compositional differences of the catalyst. Thus, we characterized all the materials by using XRD, TEM, EDX and XAFS measurements *in operando* conditions (XAFS 2 and XDS beamlines at LNLS were used to perform these experiments) to obtain electronic and structural information.

The EXAFS analysis of the PtSn/C NPs under study confirms the alloyed nature of these systems, with Sn contents ranging from 0 to less than 25%. These results are also supported by XRD experiments on which there is no evidence of the formation of alloyed phases with higher content of Sn. In addition, since Sn is able to donate electrons to Pt (diminishing d-vacancies), the XANES analysis shows a clear trend in the white line, which decreases with increasing amounts of Sn. As the adsorption of GIOH and reaction intermediates occurs mainly over Pt atoms, the electronic density of Pt directly affect the binding energy of these species and so the catalytic behavior of each material. The most important result until now is the huge difference on the oxidation currents between both fuels for most of the electrodes. The detection and quantification of products and intermediates will permit us to understand these differences.

[1] C. A. Martins, P. S. Fernández, H. E. Troiani, M. E. Martins, G. A. Camara. J. of Electroanal. Chem. 717–718 , 231 (2014).

[2] A. Kowal, M. Li, M. Shao, K. Sasaki, M. B. Vukmirovic, J. Zhang, N. S. Marinkovic, P. Liu, A. I. Frenkel, R. R. Adzic. Nature Materials 8, 325 (2009).

Acknowledgements: The authors deeply acknowledge FAPESP and LNLS for financial support.

3D Studies of Magnetic Stripe Domains in CoPd Multilayer Thin Films

Alexandra Ovalle¹, L. Nuñez¹, S. Flewett¹, J. Denardin², J. Escrig², S. Oyarzún², T. Mori³, J. Criginski³, T. Rocha³, D. Mishra⁴, M. Fohler⁴, D. Engel⁴, C. Guenther⁵, B. Pfau⁵ and S. Eisebitt⁶.

¹*Pontificia Universidad Católica de Valparaíso, Instituto de Física, Avenida Universidad 330, Curauma, Valparaíso, Chile;* ²*Universidad de Santiago de Chile, Departamento de Física, Avenida Ecuador, 3493, Estación Central, Santiago, Chile;* ³*Brazilian Synchrotron Light Laboratory, Rua Giuseppe Máximo Scolfaro, 10.000 Polo II de Alta Tecnologia de Campinas, Campinas, Sao Paulo, Brazil;* ⁴*Helmholtz Zentrum Berlin, Albert Einstein Strasse 15, 12489, Berlin, Germany;* ⁵*Technische Universität Berlin, Strasse des 17 Juni 135, 10623, Berlin, Germany;* ⁶*Max Born Institut, Max Born Strasse 2a, 12489, Berlin, Germany.*
ale.ovallef@gmail.com

The study of perpendicular anisotropy multilayer samples in two dimensions is now a well established field. Their experimental study in 3D however remains largely unexplored, with only the work of Durr [1] and micromagnetic simulations providing an insight into their predicted structure. New extreme brightness synchrotron sources will hopefully however allow tomographic studies of such samples to become a reality.

With existing sources, whilst holographic studies are commonplace when working with perpendicular illumination, the strong absorption prevents such work at the high incidence angles necessary to study the in-plane closure domains which form on the surface between the principal out-of plane domains. Consequently, we used resonant X-ray scattering at differing incident angles as a tool to obtain statistical information about the spatial domain properties. Using partially-coherent X-rays at the soft x-ray beamline of LNLS and UE 49 SGM at BESSY in Berlin, we collected scattering patterns for different samples with both aligned and non-aligned magnetic domains.

For the thinner samples with 50 repeats of the CoPd unit, the scattering due to the out of plane domains was dominant at all incident angles, and it was not possible to identify any part of the scatter as being due to the small in plane closure domains. However with the thicker sample with 100 repeats of the CoPd unit, the contribution of the in-plane domains was significant for both the aligned (stripe) domain case and non-aligned (worm) domain case. With the stripe domains, at a critical angle where the incident radiation passes on average through 2 adjacent domains, each of opposite orientation, the signal from the out of planes is suppressed allowing scattering from the in-plane component to be observed. In the case of non-aligned domains, the disorder in the domain pattern caused the suppression of the out of plane diffraction signal at high (ca. 70°) incidence angles, allowing an interference pattern to be observed between the in-plane domains on each surface of the sample. Both experimentally observed phenomena have been confirmed by numerical simulations.

[1] H. A. Durr, E. Dudzik, S. S. Dhesi, J. B. Goedkoop, G. van der Laan, M. Belakhovsky, et al., "Chiral magnetic domain structures in ultrathin FePd films," *Science*, vol. 284, pp. 2166-2168, Jun 25 1999.

Insight into the activity of Au/Ti-KIT-6 catalysts studied by in situ spectroscopy during the epoxidation of propene reaction

A. Talavera-López*, S.A. Gómez-Torres and G. Fuentes-Zurita

Departamento de Procesos e Hidráulica, División de Ciencias Básicas e Ingeniería, Universidad Autónoma Metropolitana-Iztapalapa, México D. F.
*talaram20@hotmail.com

This work describes the synthesis and characterization of gold nanoparticles deposited mesoporous titanosilicates designated as Au / Ti-KIT-6. With two different routes impregnation Ti, by direct synthesis (AS) and post-synthesis (PR), with molar ratio of Ti/Si 13% [1]. The solids obtained in the synthesis were evaluated as heterogeneous catalysts in the epoxidation propene reaction. The activity of Au/Ti-KIT-6 catalysts in the reaction were measured by experiments in situ DRS-UV-vis and XANES spectroscopy. During the reaction, the support showed a decrease in band gap energy. The activity and selectivity to propene oxide were closely linked to the reduction of Au^{III} species and to changes in the tetrahedral/octahedral titanium ratio [2]. Also, almost all of the Au³⁺ species initially present in the catalysts were reduced to Au⁺ and Au⁰. Results suggest that the activity loss is connected to the fast reduction of Au species and is also linked to changes in the properties of titanium.

[1] B. Nohair, S. MacQuarrie, C. M. Crudden and Serge Kaliaguine, "Functionalized Mesostructured Silicates as Supports for Palladium Complexes: Synthesis and Catalytic Activity for the Suzuki-Miyaura Coupling Reaction" *J. Phys. Chem. C*, *112*, 6065-6072 (2008)

[2] T. A. Nijhuis, E. Sacaliuc, A. M. Beale and B. M. Weckhuysen, "Propene epoxidation over Au/Ti-SBA-15 catalysts", *Journal of Catalysis*, *248*, 235-248 (2007)

Acknowledgements: the financial support of the Laboratorio Nacional of Luz Sincrotron, Campinas, Brasil for Proposta XAFS2 2015279

Nanosystems for nasal isoniazid delivery: small-angle x-ray scattering (saxs) and rheology proprieties

A. D. Lima¹, K. R. B. Nascimento¹ V. H. V. Sarmento² and R. S. Nunes¹

¹ *Universidade Federal de Sergipe, Departamento de Farmácia, Aracaju, SE Brazil.*

² *Chemistry Department, Federal University of Sergipe, Itabaiana/ SE, Brazil*

Email_corresponding_Lyne_farma@hotmail.com

The isoniazid (ISO) is the first choice drug for tuberculosis treatment [1]. However, due to its low bioavailability after oral administration it has been suggested the development of a stimuli-sensitive drug delivery system for ISO nasal administration. Stimuli-sensitive systems undergo a phase transition in response to external physical or chemical stimuli. In aqueous environments, surfactant systems form monolayers with the polar group facing the water and, after reaching a critical micellar concentration, aggregates called micelles are formed. Systems composed by surfactant, oil and water can form a range of aggregates, as microemulsions (MEs) and liquid crystals (LCs). Depending on the relative amount of the nasal mucus and the surfactant characteristics, these systems can undergo various phase transformations and structured modifications, producing a rigid mucoadhesive drug release matrix that can be used to control drug delivery justifying the use of this system. Therefore, the purpose of this study was to develop and evaluate the LC phase behavior of ISO formulations. The systems were composed of procetyl AWS® (surfactant), oleic acid (oil phase) and phosphate buffer (aqueous phase - AP), The MEs were able to incorporate about 30 mg.g-1 of ISO and were characterized by Polarized light microscopy (PLM), Small Angle X-ray Scattering (SAXS) at beam line 1 of Brazilian Synchrontron Light Laboratory (LNLS) and rheology proprieties. The results showed that the systems are isotropic and with the increase of water content, they exhibited transition to anisotropic systems. There were observed wide peaks typical of micellar structures for isotropic systems. Samples with higher AP content exhibited the appearance of new peaks, indicating the beginning of phase transition to lamellar structures, the thixotropic systems showed recovery of the structure after the removal of shear or tension. For pseudoplastic systems, the viscosity decreased upon application of a shear stress, their structure was gradually recovered when it is removed. In the flow curve, a downslope did not overlap the upward, showing a hysteresis area, which defines the magnitude of thixotropy. These results suggest that the systems in hand have great potential for nasal AZT administration.

[1] C.M. Yuen, A.W. Tolman, T. Cohen, J.B. Parr, S. Keshavjee, M.C. Becerra, **Isoniazid-resistant tuberculosis in children: a systematic review**, *Pediatr Infect Dis J*, 32 (5) (2013), p. e217

Acknowledgements: : CNPq, CAPES, FAPITEC-SE, and LNLS.

Assembly of Janus Gold Nanoparticles Investigated by Scattering Techniques

Ana M. Percebom^{1,2,3}, Juan J. Giner-Casares¹, Watson Loh² and Luis M. Liz-Marzán¹

¹ CIC BiomaGUNE, Paseo de Miramón 182, 20009, Donostia-San Sebastián, Spain; ² Institute of Chemistry, University of Campinas, 6154, Campinas, Brazil; ³ Department of Chemistry, Pontifical Catholic University of Rio de Janeiro, Rio de Janeiro, Brazil.
apercebom@puc-rio.br

Janus or double-faced nanoparticles may behave similarly to surfactants because the interparticle interactions can lead to their assembly. This behaviour can be especially important for systems formed by noble metal nanoparticles due to the possibility of controlling properties related to localized surface plasmon resonances (LSPR).

In this study, we selectively coated each hemisphere of gold nanospheres with polymers of antagonistic chemical nature creating plasmonic Janus nanoparticles. For that, we combined a pair of thiol-terminated polymers, polyethylene glycol (PEG) and either poly(N-isopropylacrylamide) (PNIPAM) or polystyrene (PS) and. The one-pot coating promotes spontaneous segregation of the two polymers at nanoparticles surface. [1]

The segregation of polymer chains was confirmed by 2D NMR. The absence of Nuclear Overhauser Effect between the signals of PEG and PNIPAM or PS indicates that the two different polymers are not in close contact. In addition, we promoted selective staining and growth of a silica semi-shell in the gold hemisphere coated by PEG. It allowed us to observe the formation of Janus gold nanoparticles by TEM.

The nanoparticles coated by PEG+PS assemble in different ways in solvents of different polarities, whereas the ones coated by PEG+PNIPAM are thermosensitive. The assembly phenomenon was investigated by UV-Vis spectroscopy, dynamic light scattering (DLS) and Small-Angle X-ray Scattering (SAXS at LNLS facilities). Results evidenced that the assembly properties can be controlled by changing either the molecular weight of each polymer or the nanoparticle size. The achieved control of nanoparticles assembly might be useful to tune plasmonic properties.

[1] A.M. Percebom, J.J. Giner-Casares, N. Claes, S. Bals, W. Loh, L.M. Liz-Marzán, *Chem. Commun.* 52, 23 (2016).

Acknowledgements: This work was supported by FAPESP (Process 2014/01807-8)

Study of the morphology exhibited by carbon nanotube from synchrotron small angle X-ray scattering

Ana Pacheli Heitmann¹, Iaci M. Pereira², Elisa Castro¹ and Rodrigo L. Lavall¹

¹ Universidade Federal de Minas Gerais, Departamento de Química, Av. Antônio Carlos, 6627, Pampulha, Belo Horizonte, MG CEP 31270-901, Brazil; ² Centro Tecnológico do Exército, Rio de Janeiro, RJ, Brazil
Email: anapacheli@gmail.com

Multiwall carbon nanotubes (MWCNTs) consist of layers of hexagonal graphene sheets of carbon atoms rolled into a seamless cylinder forming concentric layers with many different radii [1]. The incorporation of these carbon nanotubes in other materials e.g. polymer matrix can be facilitated through the noncovalent or covalent modification of the CNT surface. Covalent modification (functionalization) also enables the formation of a strong nanotube/matrix interface [2]. The structural information about nanotube morphology can be obtained by means of X-ray scattering at different length scales. In the present work, SAXS experiments were employed to investigate the nanostructure of five different carbon nanotubes, i.e.: MWCNT (as-grown MWCNTs), MWCNT/Func-5% (5% functionalized MWCNTs), MWCNT/Func-8% (8% functionalized MWCNTs), MWCNT/Func-9% (9% functionalized MWCNTs) and MWCNT/Func-8%-NF (8% functionalized MWCNTs without oxidized fragment). The experiments were performed on the beam line at the National Synchrotron Light Laboratory (LNLS, Campinas, Brazil). To investigate the MWCNT morphology, a thin layer of material was applied onto the surface of a single Kapton tape. SAXS measurements were performed using the MAR-165 detector and two different sample-detector distances, covering a q-range from 0.071 nm⁻¹ to 3.59 nm⁻¹. SAXS 2D isotropic patterns were obtained for all MWCNT specimens. For MWCNT/NF and MWCNT/Func-8%-NF, the scattering curves, derived from the integration of 2-D patterns, presented a broad scattering peak, shoulder, at 0.369 nm⁻¹. The peak position could be correlated to the MWCNT external diameter [3]. However, the shoulder was not observed for functionalized MWCNTs with oxidized fragment. The Guinier and Porod analysis were obtained by a power law of scattering, α , calculated from curve edges. At high angles, Porod's Law reflects the particle surface and, at low angles, Guinier's Law reflects the particle radius of gyration, R_g [4]. The R_g approximation indicated that the functionalization decreased the nanotubes radius, and, at Porod region, $\alpha \approx -4$ indicated a very smooth surface for all specimens yet MWCNT surface is rougher than the other specimens. Porod's plots presented a small positive deviation for all specimen, indicating the presence of either thermal electronic movement or compositional heterogeneity within nanotubes surfaces. Moreover, it was observed that the functionalization controlled the positive deviation. Nevertheless, MWCNT/Func-8%-NF samples presented almost zero deviation, suggesting that the oxidized fragment removal eliminates the surface heterogeneity. It was concluded that the change in surface properties of the carbon nanotubes by functionalization has the advantage in rendering the system less hydrophobic and improved interaction with the polymer matrix. However, extensive acid oxidation resulted in a weaker structure and the characteristic cylindrical arrangements of carbon nanotubes might be degraded. Though, the oxidized fragment removal produced a less active surface.

[1] R. K Challa et al., IEEE Microw. Compon. Lett. 18, 3 (2008)

[2] Z. Spitalsky et al., Prog. Polym. Sci. 35, 3 (2010)

[3] M. Bedewy et al., ACS Nano. 11, 5 (2011)

[4] I. M. Pereira and R. L. Oréfice, Polym. 51, 8 (2010)

Acknowledgements: The authors acknowledge the financial support from the following institutions: National Council for Scientific and Technological Development (CNPq) and the National Synchrotron Light Laboratory (LNLS-Brazil).

The support influence on Pt_xPd_{1-x}/SiO₂ (x = 1, 0.7 or 0.3) nanoparticles reactivity

A. Gorgeski, M. V. Castegnaro, F. Bernardi, M. C. M. Alves and J. Morais

*Instituto de Física - Universidade Federal do Rio Grande do Sul - Porto Alegre, Brasil
deiaorgeski@gmail.com*

Metal nanoparticles (NPs) have attracted a great deal of attention and have been extensively exploited for their unique optical, electric, magnetic and catalytic properties, which are different from those of bulk materials [1, 2]. In the case of bimetallic nanoparticles, which are particularly important in catalysis, the introduction of a second element allows greater flexibility in the variation of structural parameters by varying the distribution of atoms in the particle. The addition of a second metal facilitates the reduction process, which is typically employed in order to bring the catalyst to the active form [3].

Recent studies of our group have shown that isolated Pt-Pd bimetallic nanoparticles present interesting electronic and structural properties, which implies on distinct catalytic activities during reduction and sulfidation processes [4, 5]. In those experiments, the isolated nanoparticles were submitted to the reduction process in an H₂ atmosphere and subsequent sulfidation in H₂S atmosphere at different temperatures. It was observed that the amount of metal-S bonds in the nanoparticles increases with the quantity of Pd.

In this work, we have studied Pt-Pd bimetallic nanoparticles supported in SiO₂, aiming to investigate the structural/chemical changes of real supported heterogeneous catalysts that were induced by reduction and sulfidation processes. Therefore, we attempted to study the influence of the support in the nanoparticles reactivity. The nanoparticles were produced by chemical synthesis and, then, supported on SiO₂. Their long range order and composition were probed by X-Ray Diffraction (XRD) and Rutherford backscattering spectrometry (RBS), respectively. The Pt_xPd_{x-1}/SiO₂ (x = 1, 0.7 or 0.3) systems were studied by in situ x-ray absorption spectroscopy (XAS) during the reduction by H₂ and posterior sulfidation under H₂S atmosphere, both at 300 °C. The measurements were performed in transmission mode at the Pt L₃-edge at XAFS1 and DXAS beamlines of the LNLS. The evolution of the in-situ XAS spectra of the Pt L₃-edge allowed comparing the different bimetallic catalysts, and it was observed that as higher the Pd amount, higher the samples reactivity with sulfur.

This work was funded by CAPES, CNPq, FAPERGS and LNLS.

[1] G. Schmid, *Chem. Rev.* 1992, 92, 1709.

[2] C. Guozhong. and Y. Wang, *Nanostructures and Nanomaterials Synthesis, Properties, and Applications*. 2 Edition, Volume 2, Word Scientific.

[3] J.H. Sinfelt, *J.Catal.* 1973, 29, 308.

[4] J. Boita, F. Bernardi, M.V. Castegnaro, L. Nicolao, M.C.M. Alves, and J. Morais, *J. Phys. Chem. C*, 2014, 118, 5538.

[5] F. Bernardi, M. Alves, A. Traverse, D. Silva, C. Scheeren, J. Dupont, and J. Morais, *J. Phys. Chem. C*, 2009. 113, 3909.

XANES Evaluation of a New Method for the Synthesis of Palladium Nanoparticles

Brunno Lange Albuquerque¹, E. Latocheski¹, T. R. Silva¹, A. M. Signori¹, D. C. Oliveira² and J. B. Domingos¹

¹ Universidade Federal de Santa Catarina, Departamento de Química, Laboratório de Catálise Biomimética – LaCBio, 88040-900, Florianópolis, Brazil

² Laboratório Nacional de Luz Síncrotron, 13083-970, Campinas, SP, Brazil
brunno.la@posgrad.ufsc.br

Metal nanoparticles have been vastly investigated for its distinct catalytic, optical, physico-chemical properties, amongst others. [1] In this context, numerous methods have been described for the synthesis of the nanoparticles. Wet chemical methods show advantages since it's possible to fine-tune its size, shape, dispersion and surface composition. [2] In this work, a new redox method for the reduction of Pd²⁺ in water media by I⁻ is described. Based on previous results that a Pyridinium iodide molecule could act as both stabilizer and reducing agent for the synthesis of Palladium nanocatalysts, the role of I⁻ was investigated. [3] In a straightforward manner, simple mixing of aqueous palladium acetate and KI in the presence of a water-soluble polymer could afford small nanoparticles in the order of 2 nm. To get more information of the process, palladium K-edge XANES were obtained after 30 min and after 24 h of addition of an amount of KI in water. The spectra were acquired at room temperature in transmission mode using an aluminium tube (1.5 cm diameter and 2.5 cm length) filled with the colloidal dispersion and sealed with kapton tape. The fingerprinting analysis (Fig. 1) and linear combination (Fig. 2) of XANES spectra shows clearly that at 30 min only with 2.0 and 5.0 equivalents of KI it's observed the complete reduction of the Pd²⁺, using palladium acetate and isolated Pd(0) nanoparticles as standards. However, after 24 h only 0.25 equivalent of KI didn't show the complete reduction. In the XANES spectra is also important to note the presence of isobestic points, that shows the transition between the species involved during the redox process, which will finally afford Pd(0) nanoparticles.

Figure 1. K-edge XANES spectra of Pd samples.

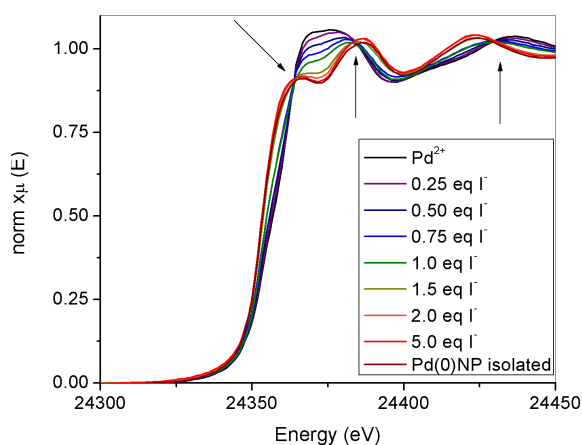
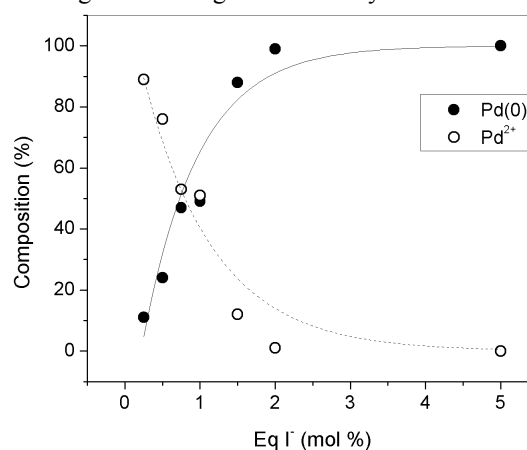


Figure 2. Linear combination of XANES spectra. The connecting lines are a guide for the eyes.



[1] E. Roduner, Chem. Soc. Rev., 35 (2006) 583.

[2] A. Roucoux, J. Schulz, H. Patin, Chem. Rev., 102 (2002) 3757-3778.

[3] A.M. Signori, E. Latocheski, B.L. Albuquerque, D. Faggion, T.B. Bisol, L. Meier, J.B. Domingos, New J. Chem., (2014).

Acknowledgements: This work was supported by CAPES/CNPq and the Brazilian Synchrotron Light Laboratory (LNLS) under proposal XDS-19010 (beam time usage).

Understanding PEO-Lithium Triflate interaction in thin films at nanoscale using IR-SNOM

Bruno B. M. Torres¹, Francisco C. B. Maia², Raul O. Freitas² and Debora T. Balogh¹

¹Universidade de São Paulo, Instituto de Física de São Carlos, São Carlos, Brazil

²Laboratório Nacional de Luz Síncrotron, Campinas, Brazil

brunobassi@ifsc.usp.br

Light emitting electrochemical cells (LEC) are devices similar to light emitting diodes however due to differences in operation mechanism, these cells have some interesting advantages but also poses new challenges, for example, the active layer is more complex being a mixture of a solid electrolyte and an emissive material[1,2]. Polymeric LECs are usually based on polyethylene oxide (PEO) – lithium triflate (TriLi) – conjugated polymer mixture. In order to improve stability and efficiency it is necessary to understand the interactions among these three components. We used in this work traditional FTIR and IR-SNOM to probe such interactions in thin films. Due to the strong crystallization character of PEO, we hoped for some phase separation and IR-SNOM was chosen because of its capability to gather morphological and chemical information allowing us to easily verify the chemical identity of any feature in the films[3]. By FTIR we were able to see that at least three ionic species are present in this films as we vary TriLi concentration. For concentrations higher than 7.5% up to 10% in weight we see the formation of $[\text{Li}_2\text{Triflate}]^+$ that is typical from another crystalline phase PEO_3TriLi and is usually considered less mobile. The question was: Are there any phase separation in these films (10% TriLi)? Despite our expectations, it was possible to probe not only the PEO vibrational modes but also the triflate modes. Along with AFM phase and height maps we can conclude that even with the strong crystallization character of PEO and formation of $[\text{Li}_2\text{Triflate}]^+$ there is no evident phase separation when TriLi is added. It seems that TriLi is homogeneously spread in PEO matrix.

[1] Van Reenen, S. et al. *J. Am. Chem. Soc.* 132, 13776–13781 (2010)

[2] Sun, Q. et al. *J. Disp. Technol.* 3, 211–224 (2007)

[3] Pollard, B. et al. *Nano Letters* 16, 55-61 (2016)

Acknowledgements: We would like to thank FAPESP, CNPq, INCT-INEO for financial support. We also thank LNLS and IR1 Beamline Staff.

Evaluating Chitosan Interaction with Cell Membrane Models using X-Ray Scattering at the Air-Water Interface

B. B. M. Torres², A. A. M. Gasperini¹, F. J. Pavinatto², T. M. N. Pavinatto², E. N. Lorenzón², E. R. Spada² and O. N. Oliveira Jr.²

¹ *Laboratório Nacional de Luz Síncrotron, Campinas, Brazil*

² *Universidade de São Paulo, Instituto de Física de São Carlos, São Carlos, Brazil*
brunobassi@ifsc.usp.br

The polysaccharide Chitosan is used in a variety of biological applications where it interacts with cells and tissues, for instance, as in tissue engineering and as bactericidal agent. The interactions are usually accompanied by some modulation of membrane elasticity and thickness, and can be monitored and characterized with the use of mimetic systems, like floating Langmuir monolayers on top of an aqueous subphase [1]. Many aspects involved in biological actions of chitosan were elucidated by the authors of the present work using models constituted of pure phospholipids, or mixtures of phospholipids, cholesterol and proteins. It was showed that chitosan is able to penetrate into both hydrophilic and hydrophobic regions of the monolayer, and to interact mainly through electrostatic interactions with the lipids (although hydrophobic and polar interactions are also important) [2]. Moreover, a decrease of membrane elasticity and increase in lipid tails alignment is usually observed, and low-molar mass chitosans have more pronounced effect [3]. In this work, GIXOs measurements were taken for Langmuir films formed of six different phospholipids in absence and presence of chitosan (0.2 mg/mL) in the subphase. A first set of phospholipids bearing the same glycerophosphate headgroup (PG), but hydrophobic tails totally saturated (DPPG), with one saturation (POPG), or two saturations (DOPG) was tested. In this group, chitosan was seen to affect strongly the saturated DPPG. In a second group of phospholipids, the same saturated tails were used but the headgroup varied from PG to phosphocholine (PC), and to phosphatidic acid (PA). Here, the negatively charged DPPG and DPPA were more affected, as expected, since chitosan is positively charged. Moreover, DPPA suffered the strongest perturbation, probably because the smaller head moiety imposed less constraints to the approach and action of chitosan. Currently, data treatment and modeling is being conducted in order to extract quantitative and more informative reflectivity results from the measurements. It is highly expected that the placement of chitosan in the monolayer plane (and as a sub-surface layer) could be extrapolated from the electron density profile in the perpendicular direction to the water surface obtained from the reflectivity results.

[1] F.J. Pavinatto, L. Caseli, O.N. Oliveira Jr. *Biomacromolecules*. 11, 1897 (2010).

[2] A. Pavinatto, A.L. Souza, J.A.M. Delezuk, F.J. Pavinatto, S.P. Campana-Filho, O.N. Oliveira Jr. *Coll. Surf. B Bioint.* 114, 53 (2014).

[3] A. Pavinatto, F.J. Pavinatto, J.A.D.M. Delezuk, T.M. Nobre, A. Souza, S.P. Campana-Filho, O.N. Oliveira Jr., *Coll. Surf. B Bioint.* 104, 48 (2013).

Acknowledgements: The authors would like to thank CNPq, FAPESP and LNLS

Inner shell electronic study of CF₃C(O)OC(O)CF₃

Carlos O. Della Védova,^a Y. B. Martínez,^a Y. B. Bava,^a M. F. Erben,^a R. L. Cavasso Filho^b and R. M. Romano^a

^aCEQUINOR (UNLP, CCT-CONICET La Plata). Departamento de Química, Facultad de Ciencias Exactas, Universidad Nacional de La Plata. Blvd. 120 N° 1465, CC 962, La Plata (CP 1900), Argentina.;^bUniversidade Federal do ABC. Av. dos Estados, 5001. CEP 09210-580 Santo André, São Paulo, Brazil

Perfluorinated compounds have been extensively used in industrial applications during the last years. Recently, some perfluorinated species were detected in tissues of animals, in environmental waters, and in the atmosphere.^{1,2} Different processes may be responsible for the presence of these compounds in the environment. For example, the thermolysis of fluoropolymers and the degradation of fluorotelomer alcohols result in the emission of perfluorocarboxylic species to the atmosphere.

In this work, and as part of a general project aimed to the elucidation of the photofragmentation mechanisms of relevant compounds for the atmospheric chemistry, we present the study of trifluoroacetic anhydride using synchrotron radiation with energies between 270 and 715 eV. The photoexcitation and photofragmentation of this species was studied in the SGM beamline at LNLS. The analysis of the Total Ion Yield spectra acquired around the ionization potentials of C 1s, O 1s and F 1s, along with the information obtained from quantum chemical calculations, allowed us to assign different resonant electronic transitions. For instance, we could distinguish contributions from different carbon atoms, being the transition C(C=O) 1s → σ*(C–C) approximately 3.5 eV lower in energy than the C(CF₃) 1s → σ*(C–C). Moreover, the study of the kinetic energy released by the ions detected in different PEPICO spectra, in combination with the interpretation of the double coincidence islands from a PEPIICO spectrum were employed to determine different photofragmentation mechanisms. Double coincidences such as C⁺/CF⁺, O⁺/CF⁺, F⁺/CF⁺, CO⁺/CF⁺, CO⁺/CF₂⁺, CO⁺/CF₃⁺, CF⁺/CF₂⁺, CF⁺/CF₂⁺, CF⁺/CF₃⁺ and CF₂⁺/CF₃⁺ were detected in the PEPIICO spectra. The mechanisms for these coincidences were proposed based on the shape and slope of the corresponding islands.^{3,4}

Acknowledgements: This work has been supported by LNLS under Proposal SGM-17920. We thank Arnaldo Naves de Brito and SGM beamline staff for their assistance throughout the experiments. The authors thank Facultad de Ciencias Exactas, Universidad Nacional de La Plata, CONICET and ANPCyT for financial support.

¹Hurley, M. D.; Ball, J. C.; Wallington, T. J.; Anderson, M. P. S.; Ellis, D. A.; Martin, J. W.; Mabury, S. A. *J. Phys. Chem. A* **2004**, *108*, 5635-5642.

²Shine, K. P.; Gohar, L. K.; Hurley, M. D.; Marston, G.; Martin, D.; Simmonds, P. G.; Wallington, T. J.; Watkins, M. *Atmos. Environ.* **2005**, *39*, 1759-1763.

³Eland, J. H. *Acc. Chem. Res.* **1989**, *22*, 381-387.

⁴Simon, M.; Lebrun, T.; Martins, R.; de Souza, G. G. B.; Nenner, I.; Lavollee, M.; Morin, P. *J. Phys. Chem.* **1993**, *97*, 5228-5237.

The invar effect studied by time resolved x-ray diffraction

Carlos William Galdino¹, C. Giles¹, G. N. Kontogiorgos¹, K. Tasca¹ and L. Coelho²

¹ *Universidade Estadual de Campinas, Departamento de Física da Matéria Condensada, 13083-859, Campinas, Brazil;* ² *Universidade de Brasília, 70910-900, Campus Universitário Darcy Ribeiro, Brasília, Brazil.*
galdino@ifi.unicamp.br

In 1897 Guillaume showed that a Fe 0.64 Ni 0.36 alloy have almost constant thermal expansion in a wide region of temperatures up to the Curie temperature of this ferromagnetic compound [1], quantitatively this would represent values 10 times smaller than the one found for metals. This effect, denominated Invar by its discoverer, is most usually described by a so called 2γ -state proposed by Weiss, thermal excitations of a low volume less probable state would decrease the atomic volume compensating the normal anharmonic expansion, so that those effects compensate each other resulting in the Invar effect.

Pump and probe experiments provide important information on the dynamics of fast phenomena. With the possibility of attaining picosecond X-ray pulses, beamlines at synchrotron sources equipped with choppers are an important tool to study the Invar problem. Our pump and probe experiments were done in a series of measurements, part of which at the ID9 beamline of the European Synchrotron Radiation Facility (ESRF) in Grenoble, France. The laser was adjusted to a high energy density of $800\mu\text{J}/\text{pulse}$ with a frequency of 1kHz, where we studied a bulk sample. The second part of the experiment was done at NW14A beamline of Photon Factory, KEK synchrotron facility in Tsukuba, Japan. The laser also had a frequency of 1kHz but delivered a lower power of 315W, where we studied a thin film deposition. We will also show recent experiments performed at 11-ID-D beamline at the Advanced Photon Source.

[1] Ed Guillaume. Recherches sur les aciers au nickel. dilatations aux temperatures elevees; resistance electrique. CR Acad. Sci, 125(235):18, 1897.

Partial substitution of Ni by Co in Ni-type perovskites and evaluation in steam reforming of Liquid Petroleum Gas

C. N. Ávila-Neto, A. M. M. Arouca, K. F. Oliveira and C. E. Hori

¹ *Universidade Federal de Uberlândia, Faculdade de Engenharia Química, 38400-902, Uberlândia, Brazil
avilaneto@ufu.br*

Reforming of long chain hydrocarbons is an alternative to lighter compounds such as methane. In this context, liquefied petroleum gas (LPG), consisting mainly of butane and propane, is a promising option due to its extensive distribution network in Brazil. LPG reforming may be conducted using perovskite precursors, but a major cause of deactivation is the severe formation of carbon [1]. This work focuses on evaluating the substitution of Ni by Co in $\text{LaNi}_{1-x}\text{Co}_x\text{O}_3$ perovskites in steam reforming of LPG. The perovskites were synthesized using a sol-gel method, characterized by XAS and *in situ* XRD, and finally evaluated in steam reforming of LPG at 873 K. Once reduced, the perovskites lose their identity and are converted into Ni and Co crystallites supported on La_2O_3 with some level of alloying between the two metals. The Ni crystallites of reduced samples augments in size as more Ni is replaced by Co. In reaction conditions, we observed the same phenomenon, but the crystallites are smaller in general. The Co crystallites are smaller than the Ni crystallites in the recently reduced samples, but as the reaction begins, the Co atoms agglomerate and originate larger particles. In addition, Co has a tendency to oxidize as more Ni is substituted by Co. The partial substitution of Ni by Co has affected negatively the perovskite performance in LPG reforming. The presence of Co, which should serve as a carbon oxidation promoter, reduced the selectivity for LPG reforming products and increased the selectivity for carbon and methane.

[1] O. González, J.P. Lujano and M.R. Goldwasser, *Catal. Today*. 107-108, 436-443 (2005).

Acknowledgements: This work was supported by CNPq (grant number 470711 2013-2). The authors would like to thank CNPq for financial support and LNLS for the use of XAFS-1 and XPD beamlines and financial support.

X-ray powder diffraction with synchrotron radiation and scanning electron microscopy on NiO/NiMn₂O₄ composite

C. M. R. Remédios¹, A. J. Freitas Cabral^{1,2}, C. A. Ospina³,
A. Magnus G. Carvalho⁴ and S. L. Morelhão⁵,

¹*Instituto de Ciências Exatas e Naturais, Universidade Federal do Pará, Belém, PA, Brazil.*

²*Universidade Federal do Oeste do Pará, Santarém, PA, Brazil.*

³*Laboratório Nacional de Nanotecnologia, CNPEM, 13083-970, Campinas, SP, Brazil.*

⁴*Laboratório Nacional de Luz Síncrotron, CNPEM, 13083-970, Campinas, SP, Brazil.*

⁵*Instituto de Física, Universidade de São Paulo, São Paulo, SP, Brazil.*

Email_corresponding_rocha@fisica.ufc.br

Sometimes, in the production of materials unwanted crystalline phases are formed besides desired crystalline phase. The presence of these secondary phases, even if in low concentrations, can change the overall physical properties of the sample. Nevertheless, it is worth mentioning that production of materials with two crystalline phases can result in new and interesting effects [1, 2]. Therefore, the development of new methods that facilitate the control of the purity of samples and control of the proportion of components in multiphase samples are very important. Recently, in our earlier work, exchange bias like effect in polycrystalline NiO/NiMn₂O₄ composite produced by a simple sol-gel method was observed, which resulted from the exchange coupling between the spins of NiO and NiMn₂O₄ at interfaces [3]. X-ray powder diffraction with synchrotron radiation, Rietveld method, scanning electron microscopy and energy dispersive X-ray (EDX) analysis are used for characterizing structural features that can be affected by this method of synthesis. It includes strong evidences of interfaces between nickel oxide and nickel manganite particles, shading light on the mechanism of spin exchange coupling between these materials. Rietveld refinement results for NiO/NiMn₂O₄ sample provided with high accuracy the percentages of NiO and NiMn₂O₄ crystalline phases. EDX mapping images showed that NiO particle is fixed to NiMn₂O₄ particle, which leads us to believe in interface between NiO and NiMn₂O₄ materials.

[1] W.J. Gong, W. Liu, D. Li, S. Guo, X.H. Liu, J.N. Feng, B. Li, X.G. Zhao, Z.D. Zhang, J. Appl. Phys. 109, 07D711 (2011).

[2] S.K. Sharma, J.M. Vargas, M. Knobel, K.R. Pirota, C.T. Menses. J. Appl. Phys. 107, 09D725 (2010).

[3] A. J. F. Cabral, J. Peña Serna, B. R. Salles, M. A. Novak, A. L. Pinto, C. M. R. Remédios, J. A. Comp. 630, 74 (2015).

Acknowledgements: LNLS, LNNano and the Brazilian agencies: CNPq and CAPES.

Advanced Methods for modeling Small Angle Scattering Data

Cristiano L. P. Oliveira¹

¹ *Department of Experimental Physics, Institute of Physics, University of São Paulo
crislpo@if.usp.br*

Spectroscopic techniques are widely used for the investigation of several types of systems. These techniques are based on the several types of interaction of the used radiation with matter, which, on the other hand, depends on the intrinsic characteristics of the radiation and its energy. A wide class of spectroscopic methods is the scattering methods: light scattering, X-ray scattering and Neutron scattering. In these cases the experimental data can provide interesting structural information about the studied system as, for example, particle shape and its internal structure, overall structural arrangement of particles, response to the variation of environmental conditions as temperature, pH, ionic strength, etc. However, one of the main difficulties when using scattering methods is the analysis and interpretation of the results. In this work several advanced modeling techniques will be presented [1-6], permitting the simulation, analysis and modeling for small angle scattering experimental data, which can be used in a broad range of applications, providing the correct determination of the structural parameters. Several applications on real systems like proteins, protein complexes and aggregates, micelles, membranes, nanoparticles, etc, will be shown, demonstrating the applicability of the methods.

[1] Oliveira CLP, Behrens MA, Pedersen JS, al. e: A SAXS Study of Glucagon Fibrillation. *Journal of Molecular Biology* 2009, 387(1):147-161.

[2] Oliveira CLP, Gerbelli BB, Silva ERT, Nallet F, Navailles L, Oliveira EA, Pedersen JS: Gaussian deconvolution: a useful method for a form-free modeling of scattering data from mono- and multilayered planar systems. *Journal of Applied Crystallography* 2012, 45:1278-1286.

[3] Alves C, Pedersen JS, Pinto Oliveira CL: Modelling of high-symmetry nanoscale particles by small-angle scattering. *Journal of Applied Crystallography* 2014, 47:84-94.

[4] Oliveira CLP, Santos PR, Monteiro AM, Figueiredo Neto AM: Effect of Oxidation on the Structure of Human Low- and High-Density Lipoproteins. *Biophysical Journal* 2014, 106(12):2595-2605.

[5] Oliveira CLP, Monteiro AM, Figueiredo Neto AM: Structural Modifications and Clustering of Low-Density Lipoproteins in Solution Induced by Heating. *Brazilian Journal of Physics* 2014, 44(6):753-764.

[6] Oliveira, C. L. P. (2016). Modelagem de dados de espalhamento e difração a baixos ângulos Tese de Livre Docência, Universidade de São Paulo, São Paulo, SP, Brazil.

Acknowledgements: This work was supported by FAPESP and CNPq

Structural Characterization of Ultra Low-k Carbon Doped Silicon Dioxide Films by X-ray Reflectometry and GISAXS

D. R. Huanca¹, P. Verdonck² and S. G. dos Santos Filho³

^[1] Universidade Federal de Itajubá, Instituto de Física e Química, 37500-903, Itajubá, Brazil; ² IMEC, B-3001 Heverlee, Leuven, Belgium, ³ Universidade de São Paulo, Laboratório de Sistemas Integráveis, 05508-010, São Paulo, Brazil. droqueh@unifei.edu.br

For scaling the future microelectronic devices, it was identified that one key factor was the substitution of both the high-k dielectrics employed as gates of the modern transistors [1] and the low-k dielectric used for interconnections in modern microelectronic circuits [2, 3]. One example of the advanced low-k dielectrics are carbon-doped silicon dioxide (SiCOH) in which voids were included to achieve $k < 2.0$. However, due to problems associated to materials infiltration into the pores during the CMOS process, which promotes the emergence of a current leakage through the dielectric. In order to overcome this difficulty, it is needed to find a procedure which allows the partial sealing of the porous structure, but avoiding the loss of its dielectric properties. In this sense, we deposited 180 nm of SiCOH film upon silicon substrate by chemical vapor deposition (CVD) method and then they were submitted to plasma treatment composed by a mixture of Ar/N₂ and Ar/H₂ at 100 W and 200 W, respectively. The thickness and refractive index of them were estimated by ellipsometry, while XRR and GISAXS analysis were employed for computing the mass density, porosity, pore shape and size, and also the thickness as a plasma treatment function. These experiments were carried out by using an X-ray beam with wavelength = 0.1549 nm. For GISAXS, the X-ray incident angles were 0.15° and 0.25° that were chosen in order to maximize the scattering intensity. The results show that the total thickness and critical angle (refractive index) of the films are 176.8 nm and 0.120° (1.254), for the pristine sample; 166.5 nm and 0.143° (1.263) for the film treated by Ar/N₂, whereas for the one treated by Ar/H₂ these values were 171.1 nm and 0.136° (1.258), respectively. The fitting procedure of both XRR and GISAXS spectrum shows that plasma treatment produces pore sealing of the films superficial region, so that the total thickness is composed by two layers, being the superficial one thinner with higher mass density. For the sample treated by Ar/N₂-plasma the entire thickness (mass density) was $T = 6.6 \text{ nm} + 159.9 \text{ nm} (= 0.99 \text{ g/cm}^3 + 0.75 \text{ g/cm}^3)$, while for the Ar/H₂-plasma treated sample it was $T = 34.2 \text{ nm} + 137.0 \text{ nm} (= 0.97 \text{ g/cm}^3 + 0.73 \text{ g/cm}^3)$. The SiCOH porous structure can be modeled as composed by three non-interacting types of pores: two spheres with rougher interfaces (radius 1.01 to 1.28 nm) and one cylinder (radius 1.28-1.33 nm and length about 39 nm) which varies slightly after plasma exposition. The porosity was found to be equal to 47% for the pristine sample, while for the samples treated by Ar/N₂- and Ar/H₂-plasma, it was about 42 and 39%, respectively.

In conclusion, pores of the superficial region of SiCOH films were successfully sealed by plasma treatment forming a thin layer which is dependent on the plasma composition, being the Ar/N₂-plasma more suitable for this task. In addition, the GISAXS analysis reveals that the pore structure can be modeled by two spheres and one cylinder with geometrical dimensions that remain almost constant in spite of the plasma exposition.

[1] K. Maex, M. R. Baklanov, D. Shamiyan, F. Iacopi, S. H. Brongersma and Z. S. Yanovitskaya, J. Appl. Phys., 93, 8793 (2003).

[2] H. Treichel, J. Elect. Mat., 30, 290 (2001).

P. Verdonck, A. Maheshwari, J. Swerts, A. Delabie, T. Witters, H. Tielens, S. Dewilde, A. Franquet, J. Meererschaut, T. Conard, J. L. Prado, S. Armini, M. R. Baklanov, S. V. Elshocht, A. Uedono, D. R. Huanca, S. G. dos Santos Filho, and G. Kellerman, ECS J. Sol. Stat. Technol., 2, N103 (2013). *Acknowledgements:* The authors would like to thank to FAPESP for financial supports

***In situ* Synchrotron 2D-XRD evaluation of formation and reversion of strain-induced martensite in AISI 201 austenitic stainless steel**

D. R. Almeida Junior¹, I. R. Souza Filho¹, C. Gauss¹, M. J. R. Sandim¹, P. A. Suzuki¹ and H. R. Z. Sandim¹

¹ University of Sao Paulo, Escola de Engenharia de Lorena, 12602-810, Lorena, Brazil
davison.ajr@usp.br

Metastable austenite in austenitic stainless steels is prone to transform into martensite upon either cooling or straining. Hcp (ϵ)- or bcc (α')-type martensites can form. Upon straining, the so-called strain-induced martensite (SIM) is responsible for high strength and good formability of austenitic stainless steels [1]. Reversion annealing of austenitic stainless steels transforms SIM back to austenite and leads to grain refinement in bulk scale [2]. In this work, the formation and reversion of SIM in AISI 201 austenitic stainless steel were tracked by *in situ* 2D X-Ray diffraction (XRD²) during uniaxial straining (tensile test) and further annealing. This experiment was carried out in the X-Ray Diffraction and Thermo-Mechanical Simulation (XTMS) workstation placed at XRD1 line of LabNano (CNPEM). In this experiment, 2D pictures of the diffraction cones were collected using a 2D-detector Raonix® model SX16. The images were taken with the detector centered in $\theta = 40$; 56.75 and 73.5° to cover a space with as much detected cones as possible. During *in situ* analyzes (straining and further annealing), images were taken after each 20 s with the detector placed at $\theta = 40^\circ$. The open source Dracon software, written in Matlab® code by LabNano staff was used to convert the 2D images into usual diffractograms. As the images cover almost 25° of the eta (η) angle, each peak in the converted diffractograms is calculated as the integral intensity at each θ angle. It ensures better accuracy on quantification, even in sheets with strong crystallographic texture. It was noticed a deviation in the peak positions after conversion when compared to theoretical values. Both the geometry and the assembly of the detector as well as the calibration parameters seem to affect peak positions in converted diffractograms. The deviation of the peak position was evaluated for each θ position of detection. We defined a parabolic function to correct the images taken at $\theta = 40^\circ$: The function found was $\theta_{\text{corr}} = 0.00205 \theta^2 + 0,8359 \theta + 3.27642$, where θ_{corr} and θ are the corrected and uncorrected peak positions (in degrees), respectively. After conversion, the diffractograms were fitted with a pseudo-Voigt function using High-ScorePlus© software to obtain the integrated area and peak position. The phase quantification was performed by the comparison method, as reported elsewhere [3]. After an equivalent true strain of 0.34, it was found around 69% and 7% of α' - and ϵ -martensites, respectively. Following, the material was annealed up to 800°C with a heating rate of $3^\circ\text{C}/\text{min}$. It turned out that ϵ reversion is complete at 400°C while α' keeps its volume fraction unchanged. The α' reversion started taking place at 500°C and it was completed at about 800°C .

[1] P. Hilkhuijsen, H.J.M. Geijselaers, T.C. Bor, J. Alloys Comp. 577S (2013) S609.

[2] A. S. Hamada, A. P. Kisko, P. Sahu, L. P. Karjalainen, Mater. Sci. Eng. A 628 (2015) 154.

[3] C. Gauss, I.R. Souza Filho, M.J.R. Sandim, P.A. Suzuki, A. J. Ramires, H.R.Z. Sandim, Mater. Sci. Eng. A 651 (2016) 507.

Acknowledgements: The authors are grateful to Aperam South America for supplying the steel used in this work, to LabNano of National Research Center for Energy and Materials (CNPEM – Campinas – SP) for allowing the use of their facilities and to Mr L. Wu for his help and fruitful discussions. D.R.A Jr and IRSF thanks to CNPq and CG to CAPES for their scholarships. Authors are also deeply acknowledged by the financial support from FAPESP (Grant 2013/26506-8).

EXAFS study of the local atomic structure in $A\text{Fe}_2\text{As}_2$ ($A = \text{Eu}, \text{Sr}, \text{Ba}$)

D. Tobia¹, M. E. Saleta², M. Radaeli¹, M. M. Piva¹, S. J. A. Figueroa², G. G. Lesseux¹, C. B. R. de Jesus¹, R. R. Urbano¹, E. Granado¹ and P. G. Pagliuso¹

¹ Instituto de Física “Gleb Wataghin”, Universidade Estadual de Campinas – UNICAMP, 13083-859, Campinas, SP, Brazil; ² Laboratório Nacional de Luz Síncrotron (LNLS), 13083-970, Campinas, SP, Brazil
ifitobia@ifi.unicamp.br

The recent discovery of superconductivity in new families of Fe-based intermetallics and oxides has opened new fields for the research of the properties of high temperature superconductors. [1,2] From the structural point of view, these Fe-based superconductors share a local structure, based on planar layers of FeAs. The Fe $3d$ electrons form multiple bands at the Fermi level and play an important role in superconductivity. The non-doped $A\text{Fe}_2\text{As}_2$ compounds (named $A122$) are oxygen free iron arsenides (with $A = \text{Ba}, \text{Sr}, \text{Ca}, \text{Eu}$). At room temperature the $A122$ systems are paramagnetic and crystallize in a tetragonal structure. At low temperature they exhibit a spin-density-wave (SDW) ordering transition, connected with a structural phase transition to an orthorhombic structure. This phase is formed at a critical temperature T_{SDW} , observed typically in the $100\text{K} < T_{\text{SDW}} < 200\text{K}$ range and usually is reflected as anomalies in the electric resistivity, magnetic susceptibility and specific heat. Although the pure $A122$ compounds are not superconductors, in these systems it was observed that the SDW phase can be destabilized through chemical substitution or external applied pressure, leading to the emergence of superconductivity. [3,4] On the other hand, the atomic substitution of the alkali atoms with different ionic radii in the A site results in a change of the cell parameters. As a result, these systems also experience a change in the effects of chemical pressure. [5] In this context it is of great interest to investigate the role of the local distortion on the Fe-As bonds for temperatures above and below T_{SDW} , as the Fe-As bond distance controls directly the chemical pressure on Fe. X-ray absorption spectroscopy (XAS) is an ideal local technique to obtain information about the relationship between local structural distortions and the system spin dynamics. [6] In this work we present an extended X-ray absorption fine structure (EXAFS) study of the As local environment in $A\text{Fe}_2\text{As}_2$ (for $A = \text{Eu}, \text{Sr}, \text{Ba}$) as a function of temperature. We have investigated the effects of each particular A -site ion on the Fe-As bond from a local point of view. We employed high quality single crystals grown from In-flux and the measurements were performed in transmission mode in the As K absorption edge, at the XAFS-2 beamline of the Brazilian Synchrotron Light Laboratory (LNLS).

[1] Y. Kamihara et al., J. Am. Chem. Soc. 130 (2008) 3296

[2] X. H. Chen et al., Nature 453 (2008) 761

[3] T. M. Garitezi et al., J. Appl. Phys. 115 (2014) 17D711; Bras. J. Phys. 43 (2013) 223

[4] M. M. Piva et al., J. Phys. : Condens. Matter 27 (2015) 145701

[5] S. R. Saha et al., Phys. Rev. Lett. 103, 037005 (2009)

[6] E. Granado et al., Phys. Rev. B 83 (2011) 184508 ; E. M. Bittar et al., Phys. Rev. Lett. 107 (2011) 267

Acknowledgements: This work was supported by FAPESP. The authors acknowledge LNLS for the beamtime.

Residual X-ray back-diffraction: Can we further increase the energy resolution at angles above 90°?

Edson M. Kakuno¹, Marcelo G. Hönnicke², Raymond Conley³, Cesar Cusatis⁴, Elina Kasman³, João B. Marques⁵ and Flávio C. Vicentin⁶.

¹Universidade Federal do Pampa, Campus Bagé, 96413-170, Brazil; ²Universidade Federal da Integração Latino-Americana, 85866-000, Foz do Iguaçu, Brazil; ³Advanced Photon Source, Argonne National Laboratory, 60439, Argonne, USA; ⁴Universidade Federal do Paraná, DF, 81531-990, Curitiba, Brazil; ⁵Universidade Federal de Mato Grosso, 78060-900, Cuiabá, Brasil; ⁶Laboratório Nacional de Luz Síncrotron, Centro Nacional de Pesquisa em Energia e Materiais, 13083-970, Campinas, Brazil.
edson.kakuno@unipampa.edu.br

Soft residual X-ray back-diffraction (SRXBD), X-ray diffraction at angles exactly equal to 90° and above at low energies (~ 3.2 keV), was carried out at Soft X-rays Spectroscopy (SXS) beamline at Laboratório Nacional de Luz Síncrotron (LNLS). This work is a continuation of a previous experiment [1] where we characterize the forward-diffracted beam (o-beam) profiles, taken at different temperatures, in ultra-thin (5 μm thick) Si 220 crystals in the absence of multiple-beam diffraction (MBD). In the present work we characterize the residual X-ray back-diffracted h-beam in order to investigate its energy resolution. Our goal is to check if the energy resolution, at such condition, can be further increased. For this, a high-quality, artificially grown, α-Quartz single crystal (11-20) ($\Delta d/d = 5 \cdot 10^{-7}$) [2] was used to analyze the h-beam residual X-ray back-diffraction. The use of α-Quartz (11-20) is because it has a higher energy resolution than Si 220 back-diffraction. The measurements were started at the exactly thin-crystal X-ray back-diffraction. This was checked by looking to the forward o-beam back-diffraction profile at different thin crystal temperatures. Then, we further reduce the thin crystal temperature in order to take diffraction at angles above 90 degrees. Our measurements were carried out in thin crystal temperature ranging from the room temperature ~ 300 K until 268 K in steps of 5K, for each temperature, at fixed thin crystal angle, one α-Quartz (11-20) analyzer crystal rocking curve was acquired. The full width of half maximum (FWHM) of the α-Quartz (11-20) analyzer crystal rocking curve will be shown and discussed in order to explore the energy resolution at diffraction angles above 90°. With these results we aim to a future development of a soft inelastic X-ray scattering spectrometer, based on spherical multilayer analyzer, where experiments such as element-specific magnetic imaging tools [3] could be explored.

[1] Hönnicke M.G., Conley, R., Cusatis, C., Kakuno, E. M., Zhou, J., Bouet, N., Marques, J. B., Vicentin, F. C. (2014). J. Appl. Cryst. 47 1658-1665, 2014.

[2] Hönnicke, M. G., Huang, X.-R., Cusatis, C., Koditwaku, C. N., Cai, Y.Q. (2013). J. Appl. Cryst., 46, 939-944.

[3] Mentis, T. O., Sanchez-Hanke, C. & Kao, C. C. (2002). J. Synchrotron Rad. 9, 90–95.

Acknowledgements: Acknowledgements The authors acknowledge LNLS/CNPEM/MCT for the beamtime (under proposal SXS-19050). MGH and CC gratefully acknowledges CNPq/PQ (309109/2013-2 and 309614/2013-9) for their research fellow. RC and EK are supported by the US Department of Energy, Office of Science, Office of Basic Energy Sciences, under contract number DE-AC02-06CH11357.

Ga doped ZnO nanowires growth on ZnO thin films prepared by the two stages hydrothermal method

E.Heredia, C. Bojorge, H.Cánepa and N.E. Walsøe de Reca

UNIDEF (CITEDEF-CONICET-MINDEF), J.B. de La Salle 4397, (1603) Villa Martelli, Pcia. de Buenos Aires, Argentina

Ga:ZnO based films have been actively studied because of their applications as solar cells, gas sensors, piezoelectric transducers, ultrasonic oscillators and for different optoelectronic applications. Besides their interesting optical, electrical and piezoelectrical properties, this material exhibits a high chemical and mechanical stability. Ga:ZnO presents novel properties and potential applications in optoelectronic fields because its non linear optical properties, excitonic emission at room temperature and quantum size effect.

In the present work we studied Ga-doped ZnO nanowires growth on Ga:ZnO thin films obtained by the two stages hydrothermal method. Samples with different number of layers and different percentage of dopant were characterized by grazing incidence small-angle X-ray scattering (GISAXS) and X-ray reflectivity (XR). This experiments were performed at Laboratório Nacional de Luz Síncrotron (LNLS). Structural characterization by Field Emission Scanning Electron Microscopy (FESEM) were carried out at Centro de Microscopias Avanzadas (CEA) of UBA (Buenos Aires-Argentina). Present results were also compared to those obtained for Ga:ZnO films.

Effect of coating on γ -Fe₂O₃ nanoparticles studied using XAS

E. Lede¹, S. J. Stewart¹, M. P. Morales² and P. de la Presa^{3,4}

¹ IFLP, CCT-La Plata, CONICET, Departamento de Física, Facultad de Cs. Exactas, Universidad Nacional de La Plata, CC 67, 1900 La Plata, Argentina; ² Departamento de Biomateriales y Materiales Bioinspirados, Instituto de Ciencia de Materiales de Madrid/CSIC, Sor Juana Ines de la Cruz 3, Campus de Cantoblanco, Madrid 28049, Spain; ³ Instituto de Magnetismo Aplicado, UCM-ADIF-CSIC, P.O. Box 155, 28260 Las Rozas, Spain; ⁴ Departamento de Física de Materiales, Facultad de CC. Físicas, UCM, 28040 Madrid, Spain
lede@fisica.unlp.edu.ar

During the last years there has been an exponential growth in studies devoted to optimize the heating efficiency of magnetic nanoparticles (MNPs) under alternating magnetic fields for tumor hyperthermia applications [1]. To this aim, one of the challenges is to find biocompatible MNPs having a high specific absorption rate, which can be synthesized in large amounts using simple, cheap and reproducible methods. In addition, the surface coating of iron oxide MNPs is also a matter of study due to its influence on the stability of MNPs.

In this work, we present a XANES investigation on iron oxide (maghemite) nanoparticles of 6, 10 y 12 nm sizes with and without organic coating like DMSO and APS [2]. Our results demonstrate that the local structure around Fe atoms is affected by the topological modifications of the MNPs due to the coating characteristics. In particular, the pre-edge region accounts for a superficial rearrangement caused by the coating, which increases the number of iron octahedral sites. On the other hand, the EXAFS results reveal that the coating facilitates more ordered medium-range structures.

[1] P. Guardia, R. Di Corato, L. Lartigue, C. Wilhelm, A. Espinosa, M. Garcia Hernandez, F. Gazeau, L. Manna, T. Pellegrino, ACS Nano 6, 3080 (2012).

[2] P. de la Presa, Y. Luengo, M. Multigner, R. Costo, M. P. Morales, G. Rivero, and A. Hernando. J. Phys. Chem. C 116, 25602 (2012).

Acknowledgements: This work was supported by LNLS (proposal XAFS1-14573) and CONICET, Argentina.

About a New Synthetic Method of Palladium Nanoparticles: An *In Situ* SAXS Kinetic Analysis

Eloah Latocheski¹, B. L. Albuquerque¹, D. Faggion Jr.¹, A. M. Signori¹ and J. B. Domingos¹

¹ Universidade Federal de Santa Catarina, Departamento de Química, 88040-900, Florianópolis, Brazil.
eloahlatocheski@hotmail.com

Nanoparticle research has greatly increased in the last decades, mainly due to its wide range of applications, such as photochemistry, optics and catalysis, that arise from the versatile ability of changing properties according to its size, shape, and chemical composition.[1] For catalytic applications, size control is extremely relevant, once the surface/volume ratio is maximized with nanoparticle's size decreasing.[1] Many synthetic methods have been described for the control of size and shape of Silver, Gold and Palladium nanoparticles.[2] But little attention is devoted to the mechanism of nanoparticles formation or done by improper methods of kinetic processing. Synchrotron based Small Angle X-ray Scattering (SAXS) measurements are the ideal tool for the investigation of the kinetics of the nanoparticle formation.[3] Due to its setup, it allows the fast acquisition of statistically relevant data for size, dispersion and number of particles formed at a desired time.[3] In this work we present a SAXS kinetic study of Palladium nanoparticles formation, using a novel synthetic method. This method relies on the chemical reduction of Pd²⁺ by I⁻ in water medium and at room temperature. The nanoparticles kinetics formation were investigated as a function of KI, Pd²⁺ (from two different precursor salts) concentrations and the influence of the stabilizing agent, in this case polyvinylpyrrolidone (PVP). NPs size (diameter) vs. time kinetics curves were constructed acquiring time-based SAXS spectra (Fig. 1), using exposure of 4s, until its saturation (Fig.2). The scattering curves were corrected by subtraction of the scattering from the pure solvent and then placed on an absolute scale using water as the standard. The fitting procedures and other analysis were performed using the SASfit software. From these SAXS measurements was possible to correlate the nanoparticles formation behavior with the synthetic conditions, as illustrated for example on Figure 3, where the nanoparticles size (final diameter) showed to be exponentially depended on the reducing agent concentration (KI).

Figure 1. Scattering pattern obtained for the nanoparticles in different times.

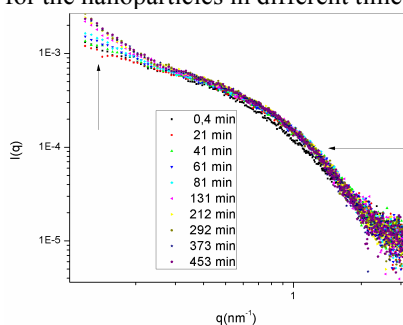


Figure 2. Kinetic of nanoparticle growth.

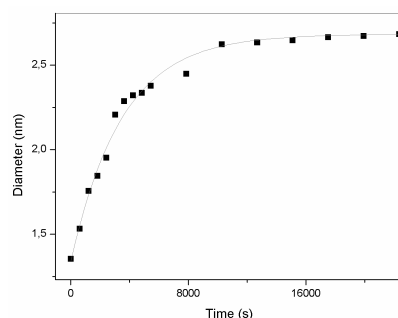
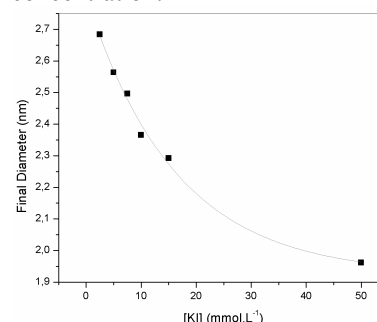


Figure 3. Final NPs diameter as function of the reducing agent (KI) concentration.



- [1] A. Roucoux, J. Schulz, H. Patin, Chem. Rev., 102 (2002) 3757-3778.
[2] Z. S. Pillai and P. V. Kamat, J. Phys. Chem. B, 103 (2004) 945-951.
[3] T. Li, A. J. Senesi, B. Lee, Chem. Rev., (2016) Article ASAP.

Acknowledgements: This work was supported by CAPES/CNPq and the Brazilian Synchrotron Light Laboratory (LNLS) under proposal SAXS1-19004 (beam time usage).

Delayed light emission of TetraPhenyl Butadiene excited by liquid argon scintillation light. Current status and future plans.

Ettore Secretò

Tetraphenyl-butadiene is the wavelength shifter most widely used in combination with liquid argon. The latter emits scintillation photons with a wavelength of 127 nm that need to be downshifted to be detected by photomultipliers with glass or quartz windows. Tetraphenyl-butadiene has been demonstrated to have an extremely high conversion efficiency, possibly higher than 100% for 127 nm photons, while there is no precise information about the time dependence of its emission. It is usually assumed to be exponentially decaying with a characteristic time of the order of one ns, as an extrapolation from measurements with exciting radiation in the near UV. This work shows that tetraphenyl-butadiene, when excited by 127 nm photons, re-emits photons not only with a very short decay time, but also with slower ones due to triplet states de-excitations. This fact can strongly contribute to clarifying the anomalies in liquid-argon scintillation light reported in the literature since the 1970s. Precision measurements of the properties of TPB, when excited by Vacuum Ultra Violet photons are being carried on at the Brazilian Synchrotron Light Laboratory in Campinas.

XANES spectroscopy for electronic characterization of manganese (II) coordination complexes

Eugenia A. Orosco Condori, Luciana C. Juncal, Carlos O. Della Védova and Rosana M. Romano

CEQUINOR (UNLP-CONICET), Departamento de Química, Facultad de Ciencias Exactas, Universidad Nacional de La Plata, La Plata, Argentina
e_orosco@quimica.unlp.edu.ar

Manganese (II) with five unpaired d electrons has been considered in the last years a good candidate for the design of contrast agents for medical Magnetic Resonance Imaging [1,2]. In this way we have prepared and characterized Mn (II) complexes containing xanthates (ROC(S)S-) and N-donor molecules (pyridine, 2,2'-bipyridine, 1,10-phenantroline) as ligands. Their characterization included vibrational (IR and Raman) and UV-visible spectroscopies, together with single-crystal X-ray diffraction analysis and TD-DFT calculations. In order to determine the electronic structure of the complexes the sulfur and manganese K-edge X-ray absorption spectra were measured. Measurements were carried out at the SXS beamline for S K-edge and at the XAFS-1 beamline for Mn K-edge. The XANES spectra in the S K-edge region show two main resonances between 2468 and 2471 eV corresponding to $S1s \rightarrow \pi^*_{C-S}$ and $S1s \rightarrow \sigma^*_{C-S}$ transitions. In the Mn K-edge region spectra there are pre-edge structures in the region of 6535 to 6540 eV, that arise from $Mn1s \rightarrow Mn3d$ transitions while the main edge was observed at 6550 eV. These results are of special interest to obtain information about occupied and unoccupied orbitals, and furthermore, to find a relationship with the stability of these compounds.

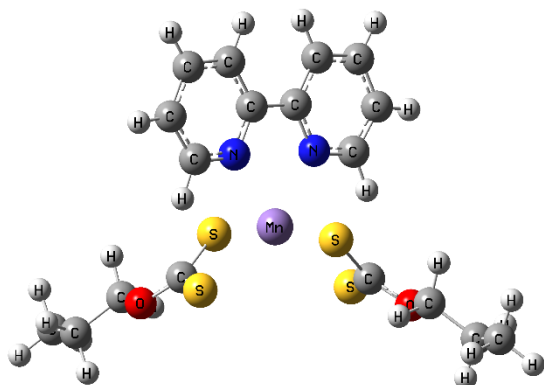


Figure 1. Chemical structure of $Mn(n\text{-propylxanthate})_2\text{bipy}$.

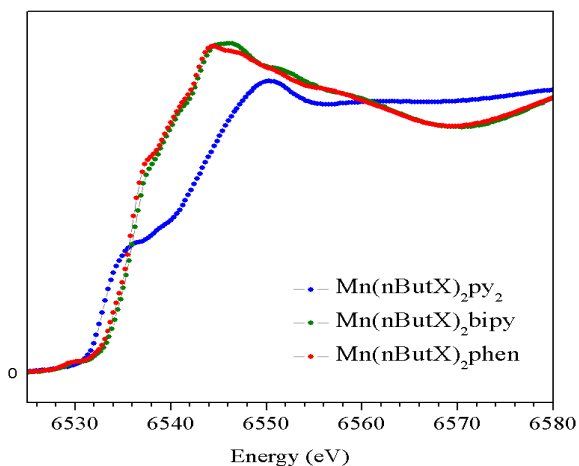


Figure 2. Manganese K-edge X-ray absorption spectra.

- [1] D. Pan, S.D. Caruthers, A. Senpan, A.H. Schmieder, S. a. Wickline, G.M. Lanza, Wiley Interdiscip. Rev. Nanomedicine Nanobiotechnology 3 (2011) 162–173.
[2] B. Drahos, I. Lukes, E. Toth, Eur. J. Inorg. Chem. (2012) 1975–1986.

Acknowledgements: This work was supported by LNLS under proposals SXS-16063 and XAFS1-17950. The authors would like to thank the beamlines staff for their assistance throughout the experiments, and also Facultad de Ciencias Exactas, Universidad Nacional de La Plata, CONICET and ANPCyT for financial support.

Low-resolution structural studies of the splicing regulatory kinase SRPK2

E. A. A. Barbosa¹, T.V. Seraphim², M.V. Barros, R.R. Teixeira³, J.C. Silva⁴, J.C. Borges² and G.C. Bressan¹.

¹ Universidade Federal de Viçosa, Departamento de Bioquímica e Biologia Molecular, 36570-900, Viçosa (MG), Brazil; ² Universidade de São Paulo, Instituto de Química, 13560-970, São Carlos (SP), Brazil; ³ Universidade Federal de Viçosa, Departamento de Química, 36570-900, Viçosa (MG), Brazil; ⁴ Laboratório Nacional de Biociências/CNPEM, 13083-970, Campinas(SP), Brazil.
Corresponding author: gustavo.bressan@ufv.br

The pre-mRNA splicing activity is tightly controlled by various regulatory factors, which act directly on spliceosome assembly and activity. The Serine Arginine-rich proteins (SR proteins) are fundamental splicing factors involved in this process, regulating constitutive and alternative exon selection in a broad number of genes. The activity of SR proteins, in turn, depends on their phosphorylation status, which is mainly controlled by members from the SR-rich Protein Kinases family (SRPKs). These kinases provide a huge potential in target-based drug discovery initiatives, since their activity have been found dysregulated in several human and animal diseases, such as cancer. The two better characterized members of SRPK family are described as monomeric proteins encompassing two kinase lobes bifurcated by an intrinsically unstructured spacer domain (SID), being this SID an exclusive attribute to SRPKs among other kinases [1]. Although the crystallographic structures obtained for heavily truncated SRPK1 and SRPK2 recombinant forms are well accomplished due to their spatial composition similar to others eukaryotic kinases [1], there is a lack of information about the overall shape of their full-length versions in solution. The more than 40% of the SRPK1 and SRPK2 primary sequences that are missed at the available crystallographic data encompass the intrinsically unstructured N-terminal and SID, which have been implicated in important functions such as subcellular distribution control, increasing of substrate phosphorylation rates and substrate binding control [2],[3]. In this study we performed structural studies of a full-length version of recombinant SRPK2, which is functionally related to the proliferative activity of leukemia cells [4]. Hydrodynamic parameters were estimated through analytical size exclusion chromatography and analytical ultracentrifugation experiments. Further structural insights into the SRPK2 overall shape were obtained by small angle X-ray scattering approach. Aiming at rationally develop novel compounds with antitumoral activity, some putative SRPKs inhibitors were synthesized. Our compounds were titrated against SRPK2 *in vitro* and intrinsic tryptophan fluorescent measurements were performed to achieve conformational changes. Subsequent kinase assay were also accomplished and IC₅₀ were estimated. Taken together our results pointed to an elongated molecule in solution with a Stokes radius equal to 50 Å and sedimentation coefficient $s_{20,w}^{\circ} = 7.1S$ to the monomer. The flexibility of the recombinant protein was studied by a kratky Plot which results reinforces the natively unfolded conformation of the spacer domain of recombinant SRPK2.

- [1] S. S. Taylor, M. M. Keshwani, J. M. Steichen, and A. P. Kornev, *Philos. Trans.*, vol. 367, , pp. 2517–28, Sep. 2012.
[2] X.-Y. Zhong, J.-H. Ding, J. a Adams, G. Ghosh, and X.-D. Fu, *Genes Dev.*, vol. 23, , pp. 482–95, Feb. 2009.
[3] R. M. Plocinik, S. Li, T. Liu, K. L. Hailey, J. Whitesides, J. Whitehouse, C.-T. Ma, X.-D. Fu, G. Gosh, V. L. Woods, P. a Jennings, and J. a Adams, *J. Mol. Biol.*, vol. 410, , pp. 131–45, Jul. 2011.
[4] S.-W. Jang, S.-J. Yang, A. Ehlén, S. Dong, H. Khoury, J. Chen, J. L. Persson, and K. Ye, *Cancer Res.*, vol. 68, pp. 4559–4570, Jun. 2008.

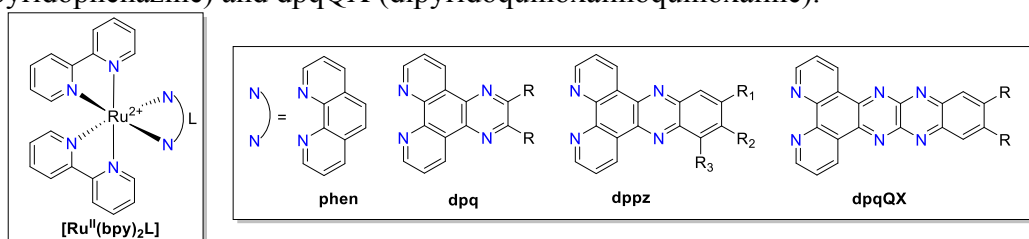
Acknowledgements: This work was supported by CAPES, CNPQ, FAPEMIG, FUNARBE/FUNARPEX. The authors would like to thank to Brazilian Synchrotron National Laboratory (LNLS/CNPEM)

Investigation of the valence shell of Ru(II) polypyridil complexes by UV vacuum absorption and XEOL

Fabio da Silva Miranda¹, Juliana da S. Goulart¹, Alan G. P. Sobrinho¹, Chiraz Belouezzane¹ and Rosa M. Sakae¹

¹Universidade Federal Fluminense, Laboratório de Fotoquímica Molecular, Departamento de Química Inorgânica, 24020-141, Niterói, RJ, Brazil.
miranda@vm.uff.br

There are many interests in ruthenium (II) polypyridil complexes due to their chemical stability, rich electrochemistry, high absorption in the UV-visible region dominated by intense ligand-centered $\pi \rightarrow \pi^*$ bands and metal-to-ligand charge-transfer (MLCT) bands, luminescence characteristics and long lived excited states that make this class of compounds an important target for several applications as dye sensitizer solar cells (DSSC), photocatalysts, bimolecular sensors, artificial photosynthesis and light emitter devices. We are interested in the chemistry of $[\text{Ru}^{\text{II}}(\text{bpy})_2\text{L}]$ class, where bpy = 2,2'-bipyridine, and L are heterocyclic polyconjugate ligands derivate from 1,10-phenanthroline (see scheme 1), these ligands are divided in three different classes in this work: dpq (dipyridoquinoxaline), dppz (dipyridophenazine) and dpqQX (dipyridoquinoxalinoquinoxaline).¹



Scheme 1. General structure of the studied compounds.

The preliminary results correlated well with our previous photophysical and electrochemical results. The Figure shows the absorption spectra of the 3 main compounds studied. The spectra collected with the quartz can be used to determine the HOMO energy of these compounds.

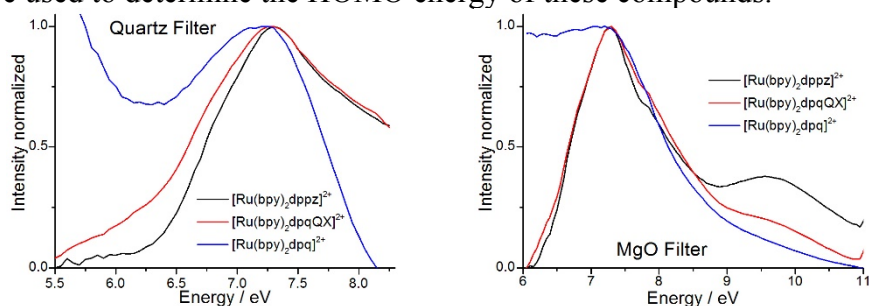


Figure 1. TEY spectra at the valence region of some selected compounds.

DFT calculation were performed at PBE0/def2-TZVP/COSMO level and correlated with the collected TEY spectra. The XEOL spectra were obtained for all compounds and it was observed that the most intense emission occur in the compounds that have large quantum yield in solution. In summary TEY and XEOL are very important techniques to study the electronic structure of ruthenium polypyridil compounds at the valence shell.

[1] F. S. Miranda, et. al., Tetrahedron 64, 5410 (2008).

Acknowledgements: The authors would like to thank to LNLS, FAPERJ, CNPq, CAPES for financial support and to TGM team: Douglas Gallante, Veronica de Carvalho Teixeira and William Roberto de Araujo.

Structure stability and electronics of Ag and Cu atomic quantum clusters: EXAFS and XANES studies.

Félix G. Requejo¹, Lisando J. Giovanetti¹, José M. Ramallo-López¹, Shahana Huseyinova², David Buceta² and Arturo López-Quintela²

¹ *Instituto de Investigaciones Fisicoquímicas Teóricas y Aplicadas – INIFTA (CONICET, UNLP), 1900 La Plata, Argentina.*

² *Physical Chemistry Department, Faculty of Chemistry, and NANOMAG Laboratory, Research Tecnological Institute, University of Santiago de Compostela, E-15782 Santiago de Compostela, Spain.
requejo@fisica.unlp.edu.ar*

Clusters seem to display stabilities that are greater than those of nanoparticles, as can be deduced by the fact that nanoparticles are etched in the presence of strong binding ligands to produce stable nanomaterials. On the other hand, clusters display a chemistry (highly dependent on cluster size) that is different than that of bulk or nanomaterials due to their different geometrical and electronic structure. It is interesting to note that, in general, a particular window of cluster sizes has been found to be the active species for a particular reaction¹⁻⁴ because of the strong dependence of the geometric and electronic structure on cluster size. Some representative examples are, for instance, Ag clusters for the propylene epoxidation by molecular oxygen,⁵ and Cu clusters have also been found to be the active species in some Cu-catalyzed reactions, such as selective hydrogenations.⁶ Thus, stability and structure configuration are key aspects to tune physicochemical properties of atomic quantum clusters (AQC).

In present contribution, Ag₁₃ and Cu₂₀ AQC electrochemically obtained, and protected with metacrilate and cysteine respectively, were characterized by EXAFS and XANES. Ag local-environment in Ag AQC exhibit a drastic change configuration with temperature, revealed by EXAFS, while Cu AQC stability is studied in function of their environment and UV-irradiation.

[1] Buceta, D.; Piñeiro, Y.; Vázquez-Vázquez, C.; Rivas, J.; López-Quintela, M. *Metallic Clusters: Theoretical Background, Properties and Synthesis in Microemulsions*. *Catalysts* 2014, 4 (4), 356-374

[2] Attia, Y. A.; Buceta, D.; Blanco-Varela, C.; Mohamed, M. B. Barone, G.; López-Quintela, M. A. *Structure-Directing and High-Efficiency Photocatalytic Hydrogen Production by Ag Clusters*. *J. Am. Chem. Soc.* 2014, 136 (4), 1182–1185.

[3] Buceta, D.; Blanco, M. C.; López-Quintela, M. A.; Vukmirovic, M. B. *Critical Size Range of Sub-Nanometer Au Clusters for the Catalytic Activity in the Hydrogen Oxidation Reaction*. *J. Electrochem. Soc.* 2014, 161 (7), D3113–D3115.

[4] Huseyinova, S.; Blanco, J.; Requejo, F.G.; Ramallo-López, J.M.; M. Carmen Blanco, Buceta, D; and López-Quintela, M.A. *Synthesis of Highly Stable Surfactant-free Cu₅ Clusters in Water*. *J. Phys. Chem. C*, Article ASAP. DOI: 10.1021/acs.jpcc.5b12227

[5] Lei, Y.; Mehmood, F.; Lee, S.; Greeley, J.; Lee, B.; Seifert, S.; Winans, R. E.; Elam, J. W.; Meyer, R. J.; Redfern, P. C.; et al. *Increased Silver Activity for Direct Propylene Epoxidation via Subnanometer Size Effects*. *Science* 2010, 328 (5975), 224–228.

[6] Maity, P.; Yamazoe, S.; Tsukuda, T. *Dendrimer-Encapsulated Copper Cluster as a Chemoselective and Regenerable Hydrogenation Catalyst*. *ACS Catal.* 2013, 3 (2), 182–185.

Acknowledgements: We thank CONICET (PIP No 1035) and LNLS (Proposals SXS-20150180 and XAFS1-17190) for the partially financial support of this research.

Reversal Magnetization dependence with oxidation state in $\text{YFe}_{1-x}\text{Cr}_x\text{O}_3$ Perovskites

F.A. Fabian¹, P.P. Pedra¹, C.C.S. Barbosa¹, K. O. Moura², J.G.S. Duque¹ and C.T. Meneses²

¹ *University of Federal Sergipe, Nucleo de Pós Graduação em Física, 49100-000, São Cristóvão, SE, Brazil;*

² *Universidade Estadual de Campinas, Instituto de Física, 13083-859, Campinas, SP, Brazil.*

fernandafabianro@gmail.com

The mixed rare earth and transition metal oxides have been extensively investigated due to the intriguing physical and chemical properties in structure, magnetism and transport behavior [1]. Perovskite-type oxides with the general formula REBO_3 (where RE is a rare earth or yttrium and B is a transition metal) have been extensively studied not only due to the high potential for technological applications but also by the exotic physical properties [2,3]. In particular, the rare-earth orthochromites and orthoferrites compounds stand out because their very peculiar ground states. In this work, we have carried out a detailed study of the magnetic and structural properties of $\text{YFe}_{1-x}\text{Cr}_x\text{O}_3$ ($0 < x < 1$) samples with orthorhombic structure obtained by co-precipitation method. Analysis of X-ray diffraction data using Rietveld refinement show that all samples present an orthorhombic crystal system with space group Pnma. $\text{YFe}_{1-x}\text{Cr}_x\text{O}_3$ ($0 < x < 1$) samples were successfully obtained via co-precipitation method. The XRD data showed very narrow diffraction peaks indicating that samples have good crystallinity. The Rietveld refinement reveals that all samples belong to the orthorhombic structure with space group Pnma. Besides, these analyses also showed a reduction in cell volume with the increase in concentration of Cr which was attributed to the difference between the ionic radii of Fe and Cr. The XANES data carried out at the Cr and Fe K-edge point out to the existence of +2 and +3 oxidation states to Cr and Fe ions. The magnetization versus temperature shows a shift in the transition temperature and decreasing of magnetization with the Cr concentration. At $x = 0.5$ we observe the reverse magnetization phenomenon which is ascribed to the Dzyaloshinsky–Moriya interaction. Besides, the M vs H curves show a small saturation effect and the magnetic susceptibility does not follow the Curie–Weiss law above the transition temperature. We have assigned this fact to stronger magnetic interaction among the mixed valence of the Cr and Fe ions.

[1] Y.W. Long et al, *J. Magn. Magn. Mater.* 322, 1912–1916 (2010).

[2] A. Dahmani, et al, *Mat. Chem. Phys.* 77, 912 (2002).

[3] H. Shen et al, *Ceram. Int.* 38, 1473 (2012).

Acknowledgements: This work was supported by Capes, CNPq and FAPITEC-SE. The authors would like to thank for access to the facilities of National Synchrotron Light Laboratory (LNLS).

Structural Investigation, Cation Distribution and Oxidation State in Core-Shell Magnetic Nanoparticles

F. H. Martins¹, J. A. Gomes¹, R. Aquino¹, F. Porcher², J. Mestink-Filho³, R. Perszynski⁴ and J. Depeyrot¹

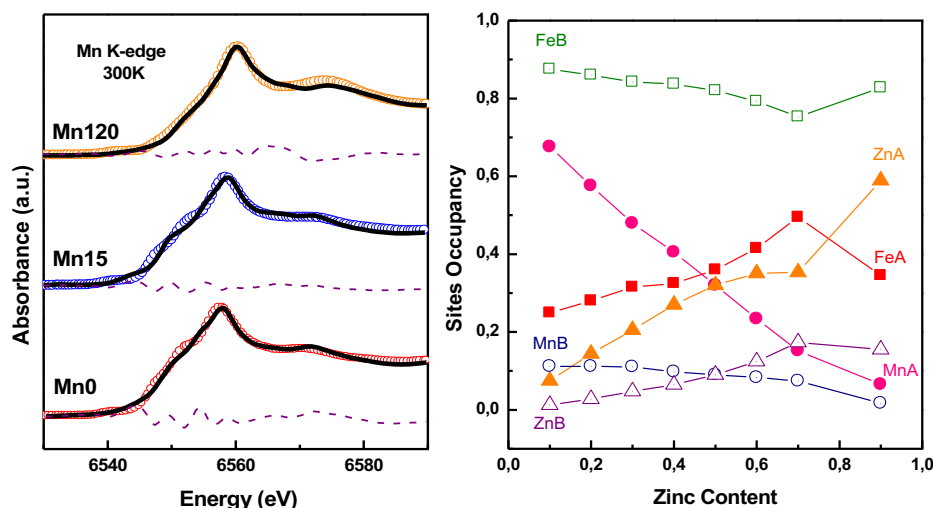
¹ Complex Fluids Group, Universidade de Brasilia-UnB, Brasilia (DF), Brazil

² Laboratoire Léon Brillouin - LLB, Gif sur Yvette, France

³ Instituto de Pesquisas Energéticas e Nucleares, USP, São Paulo (SP), Brazil

⁴ Sorbonne Universités, UPMC Univ. Paris 06, Laboratoire PHENIX, F-75005 Paris, France
nandofisunb@gmail.com

CS-NPs elaborated to make ferrofluids present increased core-shell coupling when the core anisotropy is harder than that of the shell [1], a result which could improve the efficiency of the conversion of electromagnetic energy into heat for magnetic hyperthermia treatment. As the magnetic anisotropy and the NPs magnetization are structure dependent for both the core and the shell, an insight on the local structure of these nanocrystals is of primary interest. The aim of the present work is to investigate $\text{MnFe}_2\text{O}_4@ \gamma\text{-Fe}_2\text{O}_3$ and $\text{ZnMnFe}_2\text{O}_4@ \gamma\text{-Fe}_2\text{O}_3$ CS-NPs using Neutron Powder Diffraction, in field Mossbauer spectroscopy, X-ray Absorption Spectroscopy (XAS) and X-ray Powder Diffraction. These NPs are obtained by coprecipitation in alkaline media and a hydrothermal surface treatment is performed to obtain the core-shell structure. Our results indicate that contrarily to zinc ferrite based CS-NPs [2], in Mn-ferrite based ones, the cation distribution is strongly related with the mixed valence states of Mn cations. The increase of the oxidation degree deduced from the Linear Combination Fit of XANES data is due to both the synthesis in highly basic solution and the surface treatment. It affects the interatomic distances and the size of the cubic cell, which are found to be smaller than expected. A high degree of inversion is then measured for the NPs core, with about 65% of octahedral sites occupied by manganese cations. In NPs based on Zn-Mn mixed ferrite cores, NPD spectra show modifications of the magnetic structure as the zinc content increases. Rietveld refinements allow the extraction of the site occupancy and indicate the strong affinity of both Mn and Fe cations for B-sites and of Zn cations for A-sites. LCF of XANES spectra indicate that 2/3 of Mn ions present a +3 oxidation state. Such mixed valence states seems to be promising for catalytic activity.



[1] R. Cabreira-Gomes, F. G. Silva, R. Aquino, P. Bonville, F. A. Tourinho, R. Perzynski and J. Depeyrot. J. Magn. Magn. Mater. 368, 409 (2014).

[2] J. A. Gomes, G. M. Azevedo, J. Depeyrot, J. Mestnik-Filho, F. L. O Paula, F. A. Tourinho and R. Perzynski. J. Phys. Chem C, 116, 24281 (2012).

We acknowledge the Brazilian agencies CNPq, CAPES, FAP/DF and the LNLS and LLB facilities.

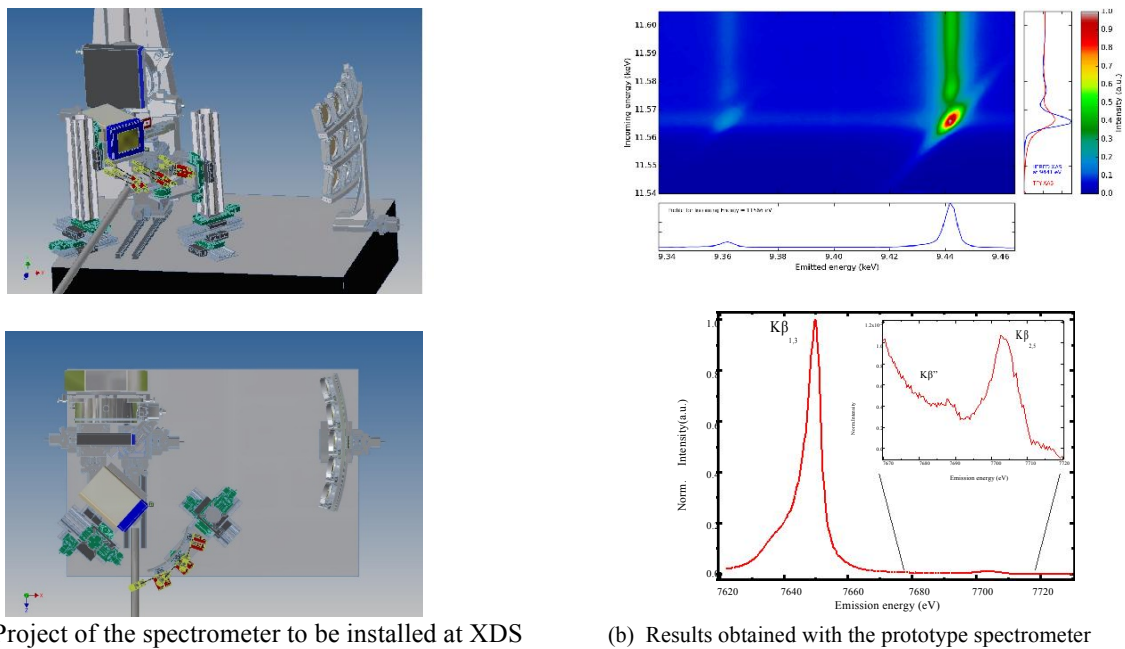
An Infrastructure for X-ray Emission Spectroscopy with High Energy Resolution at LNLS

F. Alves Lima¹, M. E. Saleta¹, R. P. Santos¹ and M. A. Eleotério¹

¹ Laboratório Nacional de Luz Síncrotron, Campinas (SP),
Brazi.frederico.lima@lnls.br

X-ray Emission Spectroscopy (XES) with improved energy resolution is an experimental technique that analyzes the details of the emitted photons after the excitation of a core level. This powerful technique is used in the study of several problems in physics, chemistry, geology, biology, and material's science, among others [1-4]. If the total experimental resolution is below that of the K- or L-lifetime broadening, an enhanced sensitivity on the measured XES (and the resonant derivations) spectral shape can be obtained [4]. Under special conditions it is possible to investigate the absorption edges of light elements (phosphor, sulfur, chlorine, potassium, calcium, etc.) without the use of vacuum and even study low-energy absorption edges using hard x-rays via the so-called X-ray Raman scattering (XRS) [3,5].

Here we describe the installation, commissioning and initial results of a dispersive-type X-ray spectrometer for high energy resolution XES (Figure 1). The current XES spectrometer can operate in the energy range between 5 keV and 15 keV, and will be installed permanently at the XDS beamline and made available to the user community starting from 2017. These experiments will also be available at Sirius.



(a) Project of the spectrometer to be installed at XDS

(b) Results obtained with the prototype spectrometer

Figure 1 – (a) X-ray spectrometers that will be installed at XDS beamline in 2017. (b) Resonant La XES spectra of a $PtCl_6$ sample and $K\beta$ XES of a Co_2O_3 sample measured with the prototype currently available at XDS for test measurements.

- [2]. Ament, L. J. P. et al., *Rev. Mod. Phys.*, 83:705–767 (2011).
 [3]. Kotani, A.; Shin, S., *Reviews of Modern Physics*, 73:203–246 (2001).
 [4]. Eisenberger, P.; Platzman, P. M.; Winick, H., *Physical Review Letters*, 36:623–626 (1976).
 [5]. Hämäläinen, K. et al., *Physical Review Letters*, 67:2850–2853 (1991).
 [6]. Tohji, K.; Udagawa, Y., *Phys. Rev. B*, 39(11):7590–7594 (1989)

Application of X-Ray Phase Contrast Microtomography Using Brazilian Synchrotron Light Laboratory to Improve the Visualization of External and Internal Structures of *Rhodnius prolixus* head

G. Sena¹, A. Almeida², L. Nogueira³, D. Braz¹, M. Gonzalez⁴, P. Azambuja⁵ and R. Barroso³

¹COPPE/Federal University of Rio de Janeiro, ²State University Centre of West Zone, ³Lab of Applied Phys to Biomed and Environmental Sci/Physics Institute/State University of Rio de Janeiro, ⁴Fluminense Federal University, ⁵Oswaldo Cruz Institute, Brazil. gabisenaa@gmail.com

Phase Contrast Microtomography (PhC- μ CT) using synchrotron radiation is a non-destructive technique that allows the microanatomical investigations of *Rhodnius prolixus* head, one of the most important insect vectors of *Trypanosoma cruzi* the etiologic agent of Chagas' disease, which accounts for about 12,000 deaths per year. The control of insect vector is the most efficient method to prevent this disease and this work is part of a series of articles [1-3] that uses PhC- μ CT for the study of *R. prolixus* morphology. This technique provides anatomical details that could not be seen with others techniques.

In this work, nymphs of *Rhodnius prolixus* were taken from the Laboratory of Biochemistry and Physiology of Insects, Oswaldo Cruz Foundation (FIOCRUZ), Brazil. The micro tomographic images were obtained using the new experimental setup which was recently made available at the Brazilian Synchrotron Light Laboratory (LNLS) with a 2 μ m resolution, and the results showed internal and external structures of *Rhodnius prolixus* head.

Understanding the behavior of internal and external structures of *Rhodnius prolixus* head can help to understand the mechanism of blood digestion by *Rhodnius prolixus* and its interaction with the agent of Chagas' disease, *Trypanosoma cruzi*, the parasite that grows within the insect's digestive system. PhC- μ CT is clearly one of the best imaging techniques for insect research and has allowed a better documentation of the detailed external and internal morphology of *Rhodnius prolixus* without dissecting.

References

- [1] - A. P. Almeida, D. Braz, Radiat Phys Chem **95** 243-246 (2014).
- [2] - A. P. Almeida, D. Braz, JINST **8** C07004 (2012).
- [3] - G. Sena, A. P. Almeida, J. Phys.: Conf. Ser. **499** 012018 (2014).
- [4] - C. B. Mello, D. Mendonça-Lopes, Mem. Inst. Oswaldo Cruz **103** 8 (2008).

Table top femtosecond x-ray source for time resolved x-ray diffraction experiments

George Nicolas Kontogiorgos¹, Carlos Manuel Giles¹, Carlos William Galdino¹

¹Instituto de Física "Gleb Wataghin"-UNICAMP
e-mail: gekontogiorgos@gmail.com

Advanced synchrotron radiation techniques are being developed to obtain refined analysis in materials science. One particular case of studies is devoted to obtain time resolved information using the sub-nanosecond x-ray pulses from bunches of the synchrotron storage ring allowing to probe picosecond dynamics of systems in multidisciplinary areas. Interesting applications within biological systems are the dynamics of the isomerized cis-trans conformation of rhodopsin found in human eyes [1], or the structural dynamics of myoglobin by the photo-excitation of carbon monoxide [2]. Unfortunately interesting phenomena is found in the sup-picosecond time scales not available for synchrotron techniques. An interesting complementary tool is the use of a table top laser based femtosecond x-ray sources being developed worldwide. At UNICAMP we have developed a prototype of this source where x-ray pulses are produced by the interaction of 1 mJ, 60 fs near infrared pulses focused at a titanium tape target at 1 kHz repetition rate. Actually, our group is working at a new control system to improve intensity of the source and the x-ray production tests were performed at the Quantum Electronics Department. The source characterization as well as its first use for time resolved x-ray diffraction studies will be presented.

Fe speciation in mine tailings using X-ray absorption spectroscopy

G. Bia, E. Nieva, M. G. García and L. Borgnino

*Centro de Investigaciones en Ciencias de la Tierra (CICTERRA), CONICET - Universidad Nacional de Córdoba,
Córdoba, Argentina.
gbia@cicterra-conicet.gov.ar*

In the last three decades, the mine wastes of La Concordia mine (NW Argentina) remained exposed to the weathering agents without a proper treatment. The main process occurring in these systems is the oxidation of the primary sulfides and the subsequent formation of secondary minerals such as sulfates, oxides, oxy(hydr)oxide sulfates, etc. The corresponding redox reactions involve the generation of acidity and the release to the water of a number of potentially toxic elements such as heavy metals and As [1]. Fe plays an important role in such systems as it may precipitate in the form of amorphous Fe (hydr)oxides or Fe sulfates, which act as sinks for these toxic elements. The aim of this work is therefore, to determine the oxidation state of iron, its local chemical coordination (to a radius of ~ 5 Å around Fe) and the relative proportion of the Fe species in mine wastes from La Concordia Mine.

To carry out this study, sediment samples were collected from the exposed walls of an oxidation profile formed in one of the mine tailing dams. XAFS spectra (including the X-ray absorption near-edge structure region or XANES, and the extended X-ray absorption fine structure region or EXAFS) of the sediments and Fe reference material such as (FeS₂, FeOOH, FeAsO₄) were collected at iron K-edge (7112 eV) at beamline XAFS1 at the Brazilian Synchrotron Light Laboratory (LNLS) in Campinas, Brazil. Five scans were collected for each sample, and then merged. Data analysis was performed with the Athena and Artemis packages based on the IFEFFIT program [2]. First derivative of XANES spectra allowed to discriminate four different Fe-bearing phases in the studied samples: Fe associated with phyllosilicates, oxides, sulfides and sulfate mineral. The proposed EXAFS models fit well with the experimental data, suggesting that the first coordinated shell around a central Fe atom is associated with Fe (III) octahedrally coordinated with oxygen in the uppermost layers. The proportion of these species decreases with depth in the profile. On the contrary, Fe associated with sulfides compounds form a structure of a central Fe associated with six neighbours of S atoms; this species is dominant in the bottom layers, while it was not determined in the uppermost layers of the tailings. The second coordinated shell is associated with K, Fe and Al in the uppermost, intermediate and bottom layers respectively.

According to the obtained results, the species Fe(III)-O is likely associated with sulfate, oxides and phyllosilicates minerals present in all layers of the profile, while Fe(II)-S is likely related to Fe atoms in pyrite or arsenopyrite.

[1] Lottermoser, B.G., *Mine Wastes: Characterization, Treatment and Environmental Impacts*. third ed. Springer, Berlin, Heidelberg, (2010) p. 400.

[2] Ravel B. and Newville M. ATHENA, ARTEMIS, HEPHAESTUS: data analysis for X-ray absorption spectroscopy using IFEFFIT. *J. Synchrotron Radiat.* 12, (2005) 537-541.

Acknowledgements: Authors wish to acknowledge the assistance of LNLS (Campinas-Brasil), CONICET and UNC for their support and the facilities used in this investigation. G. Bia acknowledges a doctoral fellowship from CONICET.

Saxs/waxs study of the kinetics of formation of metal organic frameworks

Gustavo M. Segovia¹, Agustin S. Picco², Jimena S. Tuninetti¹, Marcelo Ceolín¹, Omar Azzaroni¹ y Matias Rafti¹.

(1) Instituto de Investigaciones Fisicoquímicas Teóricas y Aplicadas (INIFTA) UNLP-CONICET. La Plata, Argentina.

(2) Laboratorio Nacional de Luz Sincrotron, Campinas, Brasil.

Metal organic frameworks are a relatively new class of hybrid crystalline materials constituted by metallic centers (nodes) and organic linkers (bridging ligands).ⁱ The field of application of these materials is continually growing, and includes heterogeneous catalysis, mixture separation, controlled release of drugs, and gas trapping among others.ⁱⁱ Despite the increasing number of new MOFs reported in the literature,ⁱⁱⁱ crystallization mechanisms involved in the formation of these materials are far from being understood. This is a key aspect to be assessed, since a profound physicochemical knowledge of the process governing the nucleation and growth of these complex structures will ultimately enable the rational design of MOFs with specific and tailored sizes and shapes.^{iv} In this context, in situ SAXS/WAXS experiments are of fundamental importance, allowing following both size/shape, and crystal order during particle/nanocrystal formation.^v

In this work we present results using SAXS and WAXS to characterize the kinetics (in several minutes time scale) of formation of various ZIFs. The MOFs belonging to this subclass, are derived from the coordination of imidazolate or substituted imidazolate organic bidentate linkers, and divalent cations (Zn^{2+} , Co^{2+}), which develops a tetrahedral framework that frequently has zeolite-like topology.^{vi} In this study Co-based ZIF-67, and Zn-based ZIF-8 were our specific targets. Synthetic methods are straightforward and include direct mixture of both water and methanolic solutions of precursors at room temperature.^{vii} In parallel, we investigated the effect of the addition of several modulating agents containing thiolate, carboxylic acid and amine groups both, to the synthesis mixture and to the end point of the reactions. We explore the potentially terminating effect on particle growth, while testing its suitability as agent for surface functionalization, pointing to self-assembly applications (e.g., via interactions of thiol surface groups on MOFs crystallites and Au conductive substrates). Increasingly higher modulating agent concentrations were tested in order to assess its effect on size, shape and crystallinity under kinetic conditions via SAXS and WAXS.

Preliminary results indicate that, using a chemical modulator featuring both thiolate and carboxylic acid moieties (3-mercaptopropionic acid) provokes different effects depending on the stage at which is introduced into the reaction mixture. When it is introduced mixed the linker and the metal centres at the beginning of the reaction a slower kinetics is observed and the final product preserves its crystallinity with higher sizes and lower PDI. In contrast, if the modulator is added to the final product (post-synthetic modification approach), although crystallinity is preserved, the final size of the particles is reduced and the PDI changes.

¹- (a) Hoskins, B.; Robson, R. *J. Am. Chem. Soc.* **1989**, *111* (15), 5962. (b) Yaghi, O. M.; Li, H.; Davis, C.; Richardson, D.; Groy, T. *L. Acc. Chem. Res.* **1998**, *31*, 474

¹- Ferey, G.; *Chem. Soc. Rev.* **2008**, *37*, 191.

¹- Long, J. R.; Yaghi, O. M. *Chem. Soc. Rev.* **2009**, *38*, 1213.

¹- (a) Zacher, D.; Schmid, R.; Wçll, C.; Fischer, R. A.; *Angew. Chem. Int. Ed.* **2011**, *50*, 176. (b) Lin, W.; Rieter, W. J.; Taylor, K. M. L.; *Angew. Chem. Int. Ed.* **2009**, *48*, 650. (c) McKinlay, A. C.; Morris, R. E.; Horcajada, P.; Ferey, G.; Gref, G. R.; Couvreur, P.; Serre, C.; *Angew. Chem. Int. Ed.* **2010**, *49*, 6260. (d) Surble, S.; Millange, F.; Serre, C.; Ferey, G.; Walton, R. I.; *Chem. Commun.* **2006**, 1518. (e) Millange, F.; El Osta, R.; Medina, M. E.; Walton, R. I.; *Cryst. Eng. Comm.* **2011**, *13*, 103.

¹- (a) Cravillon, J.; Schröder, C. A.; Nayuk, R.; Gummel, J.; Huber, K.; Wiebcke, M. *Angew. Chem. Int. Ed.* **2011**, *50*, 8067. (b) Goesten, M. G.; Stavitski, E.; Juan-Alcañiz, J.; Martínez-Joaristi, A.; Petukhov, A. V.; Kapteijn, F.; Gascon, J.; *Catal. Today* **2013**, *205*, 120.

¹- Park, K. S.; Ni, Z.; Côté, A. P.; Choi, J. Y.; Huang, R.; Uribe-Romo, F. J.; Chae, H. K.; O'Keeffe, M.; Yaghi, O. M. *Proc. Natl. Acad. Sci. U. S. A.* **2006**, *103*, 10186.

¹- Gross, A. F.; Sherman, E.; Vajo, J. J.; *Dalt. Trans.* **2012**, *41*, 5458.

Study of melting and cristalization of Bi nanoparticles in glass 72B2O3-28Na2O

Hermann F. Degenhardt^{1,2} and Guinther Kellermann²

¹ *Universidade de São Paulo, Instituto de Física, São Paulo, Brazil*

² *Universidade Federal do Paraná, Departamento de Física, Curitiba, Brazil.*

hfranz@if.usp.br

SAXS and WAXS techniques were used to study the crystal-to-liquid and liquid-to-crystal transitions of bismuth nanoparticles (NPs) embedded in a sodium-borate glass. The study aimed to determine the dependence of the melting T_f and crystallization T_c temperatures on the radius R of Bi spherical NPs. For that purpose, samples were prepared containing Bi NPs with different average radius and size dispersion. The results confirm previous experimental observations and are also in agreement with theoretical models that predict that there is a linear dependence between melting and crystallization temperatures on the inverse of NPs radius. The values of melting and crystallization temperatures determined from the extrapolation of $T_f \times 1/R$ and $T_c \times 1/R$ curves to $1/R \rightarrow 0$ are in good agreement with the experimental values reported in the literature for the bulk Bi. It was also observed that for Bi NPs having radius smaller than 18 Å the melting and crystallization temperatures coincide. This suggests that for Bi NPs with radius smaller than this value the existence of a permanent crystalline structure is not possible. This behavior confirms previous experimental results for Bi NPs in the same glass [1,2], and is in agreement with theoretical studies by molecular dynamics. The lattice parameters of Bi nanocrystals (a and c for hexagonal cell), calculated from the diffraction data for several samples, are smaller than the reported for bulk Bi, this contraction being larger for the lattice parameter c . These contractions are expected by theoretical models that predict this behavior as a result of relatively high fraction of atoms on the surface of NPs. From the dependence between the lattice parameters and the temperature the linear thermal expansion coefficients of Bi nanocrystals was determined. The results show the thermal expansion coefficients of Bi nanocrystals are larger than for bulk Bi. The same behavior was independently obtained from the dependence between the radius of gyration of Bi nanocrystals and the temperature, determined from SAXS. Moreover, as occurs in the case of bulk Bi, it was observed that the expansion of the c lattice parameter is larger than the expansion of the a lattice parameter. On the other hand, differently of nanocrystals the Bi nanodroplets have a thermal expansion coefficient about 40% lower than the value reported for bulk liquid Bi.

[1] G. Kellermann, A. F. Craievich, *Phys. Rev. B.*, vol. 65, 2002.

[2] G. Kellermann, A. F. Craievich, *Phys. Rev. B.*, vol. 78, 2008.

Acknowledgements: This work was supported by Conselho Nacional de Desenvolvimento Científico e Tecnológico (CNPq) and Laboratório Nacional de Luz Síncrotron (LNLS).

Synthesis and optical characterization of Y2O3:Eu and Y2O3:EuTi nanoparticles for use in bioimaging

Ísis F. Manali¹, Lucas C. V. Rodrigues², Douglas Galante¹ and Verônica C. Teixeira¹

¹Centro Nacional de Pesquisa em Energia e Materiais, Laboratório Nacional de Luz Síncrotron, 13083-970, Campinas, Brazil, ²Universidade de São Paulo, Instituto de Química, 05508-000, São Paulo, Brazil.
veronica.teixeira@lnls.br

The use of bioimages has allowed for great progress in diagnosis and treatment of diseases. With the development of new materials and imaging techniques, causes of diseases have been elucidated and specific treatments have been developed. Due to these new developments, materials and methods that can help to understand the physiological behavior of living organisms have been largely studied. Luminescent nanoparticles, which can be functionalized and directed to target organs, are among them because they can be used as markers during in situ biological processes, for example [1- 3]. In this work the main goal is to synthesize and study the optical behavior of nanosized Y2O3 based phosphors for use as markers in bioimaging.

Eu and EuTi-doped Y2O3 oxides were synthesized via sol-gel and a modified sol-gel based on coconut water [4] and their structural, morphological and optical properties were evaluated. Analysis carried out in powder X-rays diffraction indicated the presence of a Y2O3 single crystalline phase. Scherrer's equation was used for estimating the crystallite size. Scanning Electron Microscopy analysis revealed the synthesis method strongly influences the degree of agglomeration and the particle size. The photoluminescence studies showed that the observed emission is attributed to the dopants, mainly the Eu³⁺, and in all cases the Eu³⁺ 5D0 → 7F2 transition was the strongest, suggesting the ion is located in a site without inversion center symmetry [5]. The vacuum ultraviolet excitation and emission studies were done to explore the samples' optical behavior around their band gap. The produced samples presented emission in the optical transparency window of the biological tissue.

K.M. Davies, S. Bohic, A. Carmona, et al., *Neurobiol Aging*. 35, 858-66 (2014)
T. Maldiney, B. Viana, A. Bessiere, et al., *Opt Mater*, 35, 1852-1858 (2013)
M. Sun, Z.J. Li, C. Liu, et al., *J Lumin*, 145, 835-842 (2014)
V.C. Teixeira, P.J.R. Montes, M.E.G. Valerio, *Opt Mater*, 36, 1580-1590 (2014)
K. Binnemans, *Coord. Chem. Rev.* 295, 1-45 (2015)

Acknowledgements: The authors would like to thank to the CNPq, CNPEM PIBIC Program, the TGM/LNLS/CNPEM, LEC/LNBio/CNPEM, DRXP/LNNano/CNPEM and LME/LNNano/CNPEM and their staffs for the facilities.

Influence of Protic Ionic Liquid on Structure of Proton-conducting sPEEK-Zirconia Membranes for Anhydrous Fuel Cell Application

João Arthur Batalha¹, K. Dahmouche² and A. Gomes¹

¹ Universidade Federal do Rio de Janeiro, Instituto de Macromoléculas Professora Eloisa Mano, 21945-970, Rio de Janeiro, Brazil; ² Universidade Federal do Rio de Janeiro, Campus Xerém, 25245-390, Xerém, Brazil.
jabatalha@ima.ufrj.br

Operation in higher temperatures, under anhydrous conditions, is vital for the future of Polymer Electrolyte Fuel Cell (PEFC) technology. In this work, hybrid sPEEK / ZrO₂ membranes, comprising the protic ionic liquid (PIL) diethylmethylamine triflate in different contents were synthesized via sol-gel method. The membranes showed good thermal stability and the presence of ZrO₂ nanoparticles enabled PIL retention. Their structural features have been investigated at 70 °C by XRD and SAXS. For pure sPEEK, a SAXS broad peak is observed, attributed to spatial correlation between polymer nanodomains rich in SO₃H groups, consistent with a Guinier regime. Incorporation of ZrO₂ (4 wt.%) increases the crystallinity of sPEEK, but does not affect the correlation between SO₃H-rich nanodomains, suggesting weak interactions between ZrO₂ and SO₃H groups. PIL interacts with SO₃H domains, illustrated by the SAXS peak intensity decrease. Another interesting feature is that incorporation of 10 and 40 wt.% PIL leads to an increase in conductivity by the membranes: the former shows a decrease in spatial correlation between ZrO₂ nanoparticles. The structure of the latter exhibits small spatial correlation between ZrO₂ nanoparticles, lower polymer crystallinity and higher conductivity. A study of the evolution of structure, thermomechanical properties and proton conductivity of the membranes in temperatures up to 160 °C is in course, aiming the practical use of these materials in PEFCs.

[1] C.A Kawaguti, K. Dahmouche and A.S Gomes, *Polymer International*, 61 (2012) 82-92.

Acknowledgements: This work was supported by CAPES, CNPq and LNLS

Compact X-ray Spectrometer for the Nanofocus Beamline at SIRIUS

J. I. Robledo^{1,2}, H. J. Sánchez^{1,2}, C. A. Pérez³ and M. Honnicke⁴

¹IFEG, National Scientific and Technical Research Council (CONICET), C1033AAJ - CABA, Argentina;

²FaMAF, Universidad Nacional de Córdoba (UNC), X5000HUA - Córdoba, Argentina;

³Brazilian Synchrotron Light Source (LNLS), CNPEM, 13083-970 - Campinas, Brazil;

⁴Universidad Federal de Integración Latinoamericana (UNILA), Foz de Iguazú, Brazil.

jorobledo@unc.edu.a

Some initial studies have been carried out at the XRF-D09B Fluorescence beamline in order to improve the energy resolution of the X-ray emission lines for several elements emitted from the sample. Bent Crystal analyzers have been the key point for success in the improvement of energy resolution in x-ray spectrometers [1]. Nevertheless, this improvement comes with a high cost: large distances between sample, analyzer and detector. This limits the availability of these spectrometers in beamlines that do not have enough space or already have incorporated other experimental setups. Morishita *et al.* have come up with a way of significantly reducing the dimensions of the whole experimental setup, resulting in a distance between sample and detector of around 200mm [2].

At the laboratory of non-conventional fluorescence techniques (LTFNC, at FaMAF) we are working on new methodologies to retrieve oxidation state information, exploiting the information given by X-ray Resonant Raman Scattering spectra [3,4]. In this sense, X-ray spectrometers based on the same principle as Morishita's one-shot spectrometer are of interest to our studies, and so we are contributing to the design and construction of a spectrometer of this type. One of the main aims of this work is to adapt it for the CARNAUBA beamline at SIRIUS. The spectrometer has been designed to have an energy resolution of less than 10 eV and to cover the energy range of the L-emission lines from most Lanthanides, ranging from 4KeV to 8KeV.

In this work, we present the progress made until now, some results based on Monte Carlo simulation performed by McXtrace [5], the future planning and the perspectives on the construction of this spectrometer in the LNLS.

[1] J. Szlachetko, M. Nachtegaal, E. de Boni, et al. *Rev. Sci. Instrum.* **83**, 103105 (2012).

[2] K. Morishita, K. Hayashi and K. Nakajima. *Rev. Sci. Instrum.* **83**, 013112 (2012).

[3] J. I. Robledo, H. J. Sánchez, J. J. Leani and C. A. Pérez, *Anal. Chem.* **87**(7), 3639-3645 (2015).

[4] J. J. Leani, H. J. Sánchez, M. C. Valentinuzzi and C. A. Pérez, *J. Anal. At. Spectrom.* **26**, 378-382 (2011).

[5] E. B. Knudsen, A. Prodi, J. Baltser, M. Thomsen, et al. *Jour. of App. Cryst.* **46**(3), 679-696 (2013).

Acknowledgements: This work was supported by the LNLS and CONICET. The authors would like to thank the LNLS for allowing the development of this spectrometer.

Identification of lithium compounds in Li-enriched *Pleurotus djamor* mushrooms

J.M.R. da Luz¹, T.P.M. Machado¹, M.C.S. Da Silva¹, L. Vergutz², D. Galante³ and M.C.M. Kasuya¹

Universidade Federal de Viçosa, ¹*Departamento de Microbiologia*, ²*Departamento de Solos*, 36570-900, Viçosa, MG, Brazil, josemarodrigues@yahoo.com.br; ³*Brazilian Synchrotron Light Source (LNLS), Brazilian Center for Research in Energy and Materials (CNPEM), Campinas, SP, Brazil.*

The mushroom enrichment with lithium (Li) can be an alternative to obtain a more bioavailable form of this chemical element and less harmful to organisms that drug forms. This mineral has been used in the treatment of psychiatric disorders, such as bipolar disorder. The edible mushrooms, as example *Pleurotus djamor*, has the capacity to absorb, transform and accumulate substances from the growth substrate. Some minerals, e.g., selenium and sulfur are incorporated into amino acids, proteins and other organic compounds by these fungi. Previous studies have shown that this lithium fraction found in mushroom has high solubility and its intake by mice did not change any physiological and biological parameters analyzed. Therefore, the identification of molecules interacting with Li in fungus is essential for further description and characterization of those compounds. We have investigated the main species of Li in enriched mushrooms by X-ray absorption spectroscopy. However, the elemental properties of Li, especially its lightweight, make it very hard to analyze using only this method, requiring photons on the UV energy, not easily produced by laboratory sources. So, it was used the Toroidal Grating Monochromator beamline (TGM) beam line of LNLS, where spectra were recorded in total electron yield (TEY) and total fluorescence yield (modes). Using this technique it was possible to identify Li in inorganic standards (Li-chloride, Li-carbonate and Li-sulfate), but not in organic standards (Li-Acetate, Li-Citrate, Li-Palmitate and Li-Sterarate) and in mushrooms samples, maybe due to the low concentration of Li in the mushrooms or chemical interactions between Li and organic anions. This show us that others methodologies, such as Maldi-tof mass spectrometry and Transmission electron microscopy are necessary to speciation of organic Li compounds.

- [1] L. S. DE ASSUNÇÃO, J.M.R DA LUZ, M.C.S. DA SILVA, P.A.F VIEIRA, D.M.S. BAZZOLLI, M.C.D VANETTI & M.C.M. KASUYA. Enrichment of mushrooms: An interesting strategy for the acquisition of lithium. *Food Chemistry*, v. 134: p. 1123-1127 (2012).
- [2] M.D. Nunes, W.L. Cardoso, J.M.R. da Luz & M.C.M Kasuya. Lithium chloride affects mycelial growth of White rot fungi: Fungal screening for Li-enrichment. *African Journal of Microbiology Research*, v. 8(21), p. 2111-2123 (2014).
- [3] M.D. Nunes, W.L. Cardoso, J.M.R. da Luz & M.C.M Kasuya. Effects of lithium compounds on the growth of white-rot fungi. *African Journal of Microbiology Research*, v. 9(34), p.1954-1959 (2015).

Acknowledgements: This work was supported by CNPq, CAPES and FAPEMIG. The authors would like to thank *Brazilian Synchrotron Light Source (LNLS), Brazilian Center for Research in Energy and Materials (CNPEM)*.

“In-situ” XAFS and SAXS study of the kinetics of growth of Au nanowires

J. M. Ramallo-López¹, F. Schunder¹, C. Hoppe², L. J. Giovanetti¹, C. Huck-Iriart¹, F. G. Requejo¹

¹ INIFTA, UNLP -CONICET, Diagonal 113 y 64, CP 1900, La Plata, Argentina; ² INTEMA, UNMDP-CONICET, Av. Juan B. Justo 4302, CP 7608, Mar del Plata, Argentina.

ramallolopez@gmail.com

The slow reduction of Au-oleylamine complex by tri-isopropil-silano (TIPS) results in the formation of wires of nanometric radius[1]. In this work we studied the kinetics of growth of the Au nanowires (NWs) by means of “in situ” studies using X-ray Absorption Fine Structure (XAFS) Spectroscopy at the Au L₃ edge and Small Angle X-ray Scattering (SAXS). Samples were prepared by mixing a solution of 3 mg of HAuCl₄ in 2.5 ml of hexane with 100 l of Oleylamine and 150 l of TIPS. The reaction occurs at room temperature without stirring. XAFS experiments were performed using a liquid cell at the XDS beamline of the Laboratorio Nacional de Luz Sincrotron in Campinas, Brazil and using an R-XAS Looper spectrometer from Rigaku. SAXS experiments were performed using a XEUSS 1.0 laboratory beamline from XENOCs. SAXS curves were measured every 15 min during 10 hs. During the early stages of reaction a gold-oleylamine complex is formed with small changes in SAXS intensity. Then, Au NWs are formed and after 7 hours the appearance of correlation is observed. This correlation is evidenced by a set of peaks with the q position compatible with a 2-D hexagonal arrangement. XANES results (Fig. 1) show that the NWs formation proceeds in two steps. First Au is reduced from +3 to +1 forming linear complexes and during a second step Au is reduced from Au+1 to Au⁰. Both processes are progressive and no abrupt change is observed in the XANES spectra during the whole reaction. Preliminary results obtained by transmission electron microscopy would suggest the possible occurrence of an oriented attachment mechanism as responsible for the formation of gold NWs. Further experimental work aimed to test this hypothesis is currently under way.

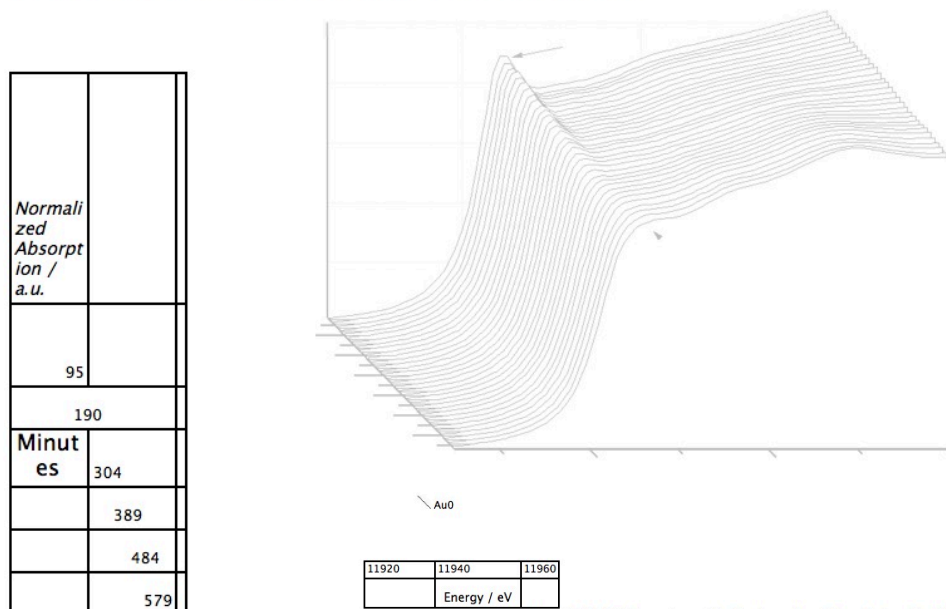


Fig. 1. XANES spectra at the L₃ Au edge taken during the NWs growth.

Au +3

[1] A. Loubat, M. Impéror-Clerc, B. Pansu, Florian Meneau, B. Raquet, G. Viau, L.-M. Lacroix, Langmuir 30, 4005 (2014).

Acknowledgements: This work was supported by CONICET, UNLP, UNMDP, ANPCyT (Argentina) and LNLS (Brazil).

Manganese Compound Mixtures Determined by Core-level RIXS Spectroscopy

Juan José Leani¹, J. Robledo¹, C. Pérez² and Héctor Jorge Sánchez^{1,3}

¹ IFEG, National Scientific and Technical Research Council (CONICET), C1033AAJ - CABA, Argentina

² Brazilian Synchrotron Light Source (LNLS), CNPEM, 13083-970 - Campinas, Brazil.

³ FaMAF, Universidad Nacional de Córdoba (UNC), X5000HUA - Córdoba, Argentina
LJ@famaf.unc.edu.ar

By way of Resonant Inelastic X-Ray Scattering (RIXS), also named X-ray Resonant Raman Scattering (RRS), the speciation of samples can be attained in a variety of experimental conditions [1-4]. Until now, this discrimination methodology had been applied only to pure oxides, achieving the speciation by two different mathematical treatments. Nevertheless, the effectiveness of this technique was not tested in samples containing mixtures of oxides of the same element. Because of this, there exists a lack in knowledge about the sensitivity of the method in discriminating the oxides in mixture compounds. In this work, the first results of quantitative speciation of mixtures of manganese compounds, using Resonant Raman Scattering Spectroscopy are presented.

The measurements were carried out at the Brazilian Synchrotron Light Source (LNLS, Campinas) in the D09B beamline in a reflection geometry and using monochromatic photons of 6450 eV, just beneath the K absorption edge of manganese. The samples under analysis were divided into two groups. The first group consisted of pellets with Mn₂O₃ and MnO₂ mixed in different proportions. The second group consisted of mixtures of Mn₂O₃ and MnO also with different amounts of each oxide. Spectra were analyzed by two independent mathematical methods: fine structure deconvolution and Principal Component Analysis.

The results show that it is possible to discriminate oxide mixtures of the same element in slightly different proportions, allowing on this way quantitative speciation of compound mixtures in a variety of experimental conditions; some of them impossible to achieve by conventional spectroscopic techniques.

[1] H.J. Sánchez, J.J. Leani, M.C. Valentinuzzi and C.A. Pérez, *Journal of Analytical Atomic Spectrometry* **26**, 378-382 (2011)

[2] H.J. Sánchez, J.J. Leani, R.D. Pérez and Carlos Pérez, *Journal of Applied Spectroscopy*, **80** 920-924 (2013)

[3] J. Robledo, H.J. Sánchez, J.J. Leani and C.A. Pérez, *Analytical Chemistry* **87** 3639–3645 (2015)

[4] J.J. Leani, H.J. Sánchez and C.A. Pérez, Volume 2015, Article ID 618279, 7 pages, *Journal of Spectroscopy* (2015)

Acknowledgements: The authors would like to thank LNLS/CNPEM for partially supported this work

RIXS combined with PCA for the Study of the $\text{Li}_4\text{Ti}_5\text{O}_{12}$ (LTO) Molecule with Different Levels of Charge

Juan José Leani¹, J. Robledo¹, F. Oliva², C. Pérez³ and H. J. Sánchez^{1,4}

¹ IFEG, National Scientific and Technical Research Council (CONICET), C1033AAJ - CABA, Argentina

² INFIQC, National Scientific and Technical Research Council (CONICET), C1033AAJ - CABA, Argentina

³ Brazilian Synchrotron Light Source (LNLS), CNPEM, 13083-970 - Campinas, Brazil.

⁴ FaMAF, Universidad Nacional de Córdoba (UNC), X5000HUA - Córdoba, Argentina

LJ@famaf.unc.edu.ar

In the last few years, the $\text{Li}_4\text{Ti}_5\text{O}_{12}$ compound (also known as LTO) has been studied as anode material of lithium ion batteries for applications as energy storage for electric and hybrid vehicles [1-3]. This LTO compound has shown exceptional features, as an extraordinary Li-ion intercalation/de-intercalation reversibility, zero-strain volume change during the cycling process and a distinguished safety performance. Additionally, LTO has a high voltage plateau in comparison with other anode material candidates, helping to avoid the formation of metallic lithium [4]. Due to both its performance and potential applications, a better knowledge of this LTO compound is of highly interest. In order to fulfill this need, different techniques and tools have to be used.

In this work, Resonant Inelastic X-ray Scattering (RIXS) has been used for studying titanium local environment changes in the LTO molecule when different levels of charge are applied. As complementary technique, XANES spectra of the Ti-K edge were also measured.

The measurements were carried out at the Brazilian Synchrotron Light Source (LNLS, Campinas) in the D09B beamline in a reflection geometry and using monochromatic photons of 4900 eV, just beneath the K absorption edge of titanium. Six samples with different charges (not charged, partially charged and fully charged) were studied. XANES measurements were obtained scanning the incident beam energy in the range 4930-5080 eV.

Principal Component Analysis (PCA) was used on both RIXS and XANES spectra in order to discriminate the changes on the titanium chemical state of the LTO molecule.

The results showed that RIXS is a very sensitive tool, allowing the detection of slight changes in the chemical environment of the LTO compound due to different levels of charge. Moreover, chemical studies similar to the ones performed with absorption techniques (XANES, EXAFS) can be performed with this novel RIXS technique, with the clear advantages of fast acquisition and the avoidance of any energy scan during the survey, being even possible to employ an X-ray tube of proper anode material or an adequate secondary target.

[1] E. Ferg, R.J. Gummow, A.d. Kock, and M.M. Thackeray, *J. Electrochem. Soc.*, 141, L147 (1994).

[2] T. Ohzuku, A. Ueda, and N. Yamamoto, *J. Electrochem. Soc.*, 142, 1431 (1995).

[3] L. Aldon, P. Kubiak, M. Womes, J.C. Jumas, J. Olivier-Fourcade, J.L. Tirado, J.J. Corredor, and C. Perez Vicente, *Chem. Mater.*, 16, 5721 (2004).

[4] J-Eui Hong, R-Gyeong Oh, and K-Sun Ryuz, *J. Electrochem. Soc.*, 162 A1978 (2015).

Acknowledgements: The authors would like to thank LNLS/CNPEM for partially supported this work

Studying the 4f electrons in the Kondo lattice antiferromagnet Ce₂RhIn₈

K. R. Pakuszewski¹, W. S. Silva², C. Giles¹, F. Rodolakis³, Julio C. Cezar², J. C. Campuzano⁴, P. G. Pagliuso¹, and C. Adriano¹

¹ Instituto de Física "Gleb Wataghin", UNICAMP, Campinas-SP, 13083-859, Brazil; ² Laboratório Nacional da Luz Síncrotron, C. P. 6192, 13083-970, Campinas-SP, Brazil; ³ Northwestern University Argonne National Laboratory Institute of Science and Engineering (NAISE), Northwestern University, Evanston, Illinois 60208, USA; ⁴ Department of Physics, University of Illinois at Chicago, Chicago, Illinois 60607, USA.
raduenz@ifi.unicamp.br

Materials which exhibit the heavy fermion behavior, such as Ce-based materials, are of great interest, as the Kondo scattering continuously grows with decreasing temperature, until it can no longer be treated as a perturbation. The electron-electron interactions can easily be tuned, leading to a variety of sometimes exotic ground states, including complex magnetic ordering and unconventional superconductivity. In some cases, it is possible to tune these ground states from antiferromagnetic to superconducting state and this tenability involves, to some extent, the control of the f-conduction electron hybridization and of the Kondo interaction [1]. Here we directly probe the temperature evolution of the 4f states of Ce₂RhIn₈ heavy fermion compound by means of Ce 4d-4f resonant angle-resolved photoemission spectroscopy (ARPES) technique. The measurements were performed at PGM beamline new ARPES chamber at the LNLS. The results show that a flat f-derived band is observed with distinct temperature dependence and a k-dependent spectral weight. At some distinct points we could also observe structures resulting from the interaction between heavy and light bands related to the Kondo-lattice formation.

[1] G. R. Stewart, Rev. Mod. Phys. 56, 755 (1984); H. V. Lohneysen et al., Rev. Mod. Phys. 79, 1015 (2007); A. C. Hewson, *The Kondo Problem to Heavy Fermions*, (Cambridge University Press, Cambridge, 1993).

Acknowledgements: This work was supported by FAPESP (grant #2015/18544-2 and #2012/04870-7) and CNPq (grant # 462368/2014-9).

Photofragmentation Study of the Acetaldehyde (CH₃CHO) at the Carbon and Oxygen K Edges.

L. C. Ribeiro¹, M. S. Arruda², F. V. Prudente¹, L. V. A. Mendes¹, A. C. F. Santos³, M. J. Santos¹, R. R. T. Marinho¹ and A. Medina¹.

¹ University Federal of Bahia, 10000-000, Salvador, Brazil; ²University Federal of Recôncavo of Bahia, 44380-000, Cruz das Almas, Brazil; ³University Federal of Rio de Janeiro, 21941-972, Rio de Janeiro, Brazil.
leonardocr2015@gmail.com

In recent decades, due to the progress of astronomical observations, a lot of more complex organic molecules have been discovered in the interstellar medium, located millions of light years from Earth. One of these molecules is the acetaldehyde (CH₃CHO), which has great importance in astrophysics. It is considered a prebiotic molecule. According to some theories, these molecules have been formed in space and brought by comets and meteorites, giving rise to life on Earth. It would be related with the formation of biomolecules necessary for the generation and maintenance of life, like the nucleic acids (DNA and RNA) and proteins. Acetaldehyde was one of the molecules observed in Hale-Bopp comet using radio spectroscopic observations [1]. Other prebiotic molecules had also been studied by our group (see, for example, reference [2, 3]). This work presents an experimental spectroscopic study of the acetaldehyde, also known as ethanal (CH₃CHO). Our main purpose was to investigate the possible ionization and dissociation routes of this molecule. Therefore, as the ionizing radiation it was used the Brazilian Synchrotron Radiation Facility (LNLS), in Campinas-SP. The experiment was performed with photons in the energy range of soft X-ray at the SGM beamline. We have used the time of flight mass spectroscopy technique to measure coincidence of electrons with one (PEPICO) or two (PEPIPICO) ions. Initially, we have obtained the Total Ion Yield (TIY) spectra to find the energy of the main electronic transitions. From the PEPICO spectra in this energy region, we identified the fragments produced according to their mass to charge ratio. We have also obtained Partial Ion Yield (PIY) spectra for each ionic fragmentation as a function of the incident radiation energy. Analyzing the PEPIPICO spectra, we have determined the relative yield of ionic fragment pairs measured in coincidence. Finally, we have found the most probable dissociation paths of the acetaldehyde for the different photon energies. We observed at the TIY spectra, both at the lower energy of the C (carbonyl) edge as at the O edge, a more intense peak assigned to the transition to a π^* antibonding orbital. The other structures were assigned to excitations to Rydberg series orbitals. With the analysis of PIY spectra, we identified the more produced fragments in each energy region. From the PEPIPICO spectra, we assigned the delayed charge separation as the main fragmentation mechanism for most of the measured pairs.

[1] J. Crovisier *et al.* A&A, 418, 1141-1157 (2004);

[2] M. S. Arruda, *et al.*, J. Phys. Chem. A, 119, 10300-10308 (2015).

[3] M. S. Arruda, *et al.*, J. Phys. Chem. A, 144,1441101 (2016).

Acknowledgements: This work is supported by CAPES, LNLS and UFBA.

Evaluation of niobia based catalysts for the esterification reaction: the effect of calcination temperatures

L.L. Rade¹, C.O.T. Lemos¹, R. M. Ribas², R. S. Monteiro^{2,3} and C. E. Hori¹

¹ Universidade Federal de Uberlândia, Faculdade de Engenharia Química, Uberlândia, Brazil; ² Companhia Brasileira de Metalurgia e Mineração - CBMM, 38183-903, Araxá, Brazil; ³ Catalysis Consultoria Ltda., 22793-081, Rio de Janeiro, Brazil
Leticia.rade@gmail.com

Biodiesel can be produced either by transesterification reaction of vegetable oils/fats and by esterification reaction of fatty acids [1]. Esterification reactions are commonly catalyzed using mineral liquid acids such as sulfuric acid, hydrochloric acid and organic acids like p-toluenesulfonic acid (p-TsOH) [2]. However, the use of heterogeneous catalysts shows an easier catalyst separation and product purification, it can be easily reused and there is no need to replace the consumed catalyst in a short time. According to studies about biodiesel production, the esterification reaction requires acid catalysts. Niobia based materials, such as niobic acid and niobium phosphate, have a great potential as catalysts in the production of biodiesel, as the acidity is maintained in aqueous reactions, they present large surface area and regular porosity. The objective of this work was to investigate the continuous production of biodiesel from oleic acid through the esterification reaction using ethanol and niobium compounds (niobic acid and niobium phosphate) as solid acid catalysts. In this work, the catalytic activities of the catalysts calcined at different temperatures were evaluated. For this purpose, the catalysts were pretreated at different calcination temperature in air for 2h and were analyzed by X-ray diffraction in-situ (XRD in-situ), nitrogen adsorption and temperature-programmed desorption of ammonia (NH₃-TPD). Results showed that, for both catalysts, the surface area, acidity and catalytic activity for the esterification reaction decrease with increasing the calcination temperature. However, the niobium phosphate presented higher thermal stability and acidity than niobic acid, as the niobium phosphate maintains its amorphous structure even when calcined at 700 ° C, maintaining its acidic properties and surface area.

[1] A. C. A. Abdala, V. A.S. Garcia, C. P. Trentini, L. Cardozo Filho, E. A. da Silva, and C. Silva. Hindawi Publishing Corporation. International Journal of Chemical Engineering. Article ID 803783 (2014).

[2] A. L. Bassan, D. R. Nascimento, R. A.S. San Gil, M. I. P. da Silva, C. R. Moreira, W. A. Gonzalez, A. C. Faro Jr., T. Onfroy, E. R. Lachter. Fuel Processing Technology 106, 619 (2013).

Acknowledgements: The authors are grateful to CBMM and FAPEMIG for the financial support and LNLS for the use of the XPD beamline.

Effect of the Exposure to Air in the morphology of water soluble Silver Nanoparticles Coated with MUA

Lisandro J. Giovanetti¹, José M. Ramallo-López, M. Cristina E. Hoppe, Félix G. Requejo

¹ *Instituto de Investigaciones Físicoquímicas, Teóricas y Aplicadas (INIFTA), Universidad Nacional de La Plata - CONICET, Sucursal 4 Casilla de Correo 16, 1900 La Plata, Buenos Aires, Argentina.*

² *Institute of Materials Science and Technology (INTEMA), University of Mar del Plata and National Research Council (CONICET), J. B. Justo 4302, 7600 Mar del Plata, Argentina
lisandro@fisica.unlp.edu.ar*

Metallic nanoparticles exhibit size and shape-dependent properties that are of interest for applications ranging from catalysts and sensing to optics, antibacterial activity and data storage [1-3]. For instance, the antibacterial activity of different metal nanoparticles such as silver colloids is closely related to their size; that is, the smaller the silver nuclei, the higher its antibacterial activity. Moreover, the catalytic activity of these nanoparticles is also dependent on their size as well as their structure, shape, size distribution, and chemical-physical environment. Thus, control over the size and size distribution is an important task. Generally, specific control of shape, size, and size distribution is often achieved by varying the synthesis methods, reducing agents and stabilizers. One important point for the use of metallic nanoparticles in technological applications is the possibility to stabilize them in non-toxic solvent (water, DMSO, etc) by surface modification using different types of capping agents.

A large variety of experimental techniques has been developed in recent years to synthesize metal NPs coated with different stabilizing thiols. Metal protected clusters (MPCs) coated with alkanethiols can be obtained and subsequently modified in their functionalization through the well-known “place exchange reaction” developed by Murray’s group[4]. Kinetic results obtained for gold NPs show that the rate of ligand exchange depends on several factors like concentration, size of the entering ligand and chain length of the protecting monolayer. As an example of the use of this procedure to incorporate thiocarboxylic acids, Simard et al.[5] developed amphiphilic gold NPs through place exchange of octanethiol with 11-mercaptoundecanoic acid (MUA). Recently Hoppe et. al. reported a new route of synthesis that gives as result Ag nanoparticles (AgNPs) of a well-controlled size and soluble in water in one step[6]. In this work the local atomic structure and chemical nature of this newly synthesized AgNPs functionalized with MUA have been probed combining TEM, UVvis, X-ray absorption fine structure spectroscopy (XAFS) and Small Angle X-ray scattering. Complementary information about chemical and electronic structure was obtained combining XAFS data obtained at the SXS beamline at the Ag-L₃ and S-K edges. Ag-K edge EXAFS data obtained at the XDS beamline was also measured in order to obtain the average Ag atoms local structure. In order to study the effect of the exposition to air all samples were measured dry and in its original solvent (water), in order to avoid modifications of the surface morphology and chemistry produced by the exposure to atmosphere. In this contribution we discuss the role of the exposure to air in the physicochemical state of the MUA molecules attached to the NP surface. The combination of all of these techniques shows that Ag atoms in the AgNP are in metallic form and also are bonded to S atoms from the capping. A discussion about the type of Sulfur species in the AgNP is also presented.

[1] K. Yoosaf, B. Ipe, C.H. Suresh, K.G. Thomas J. Phys. Chem. C, 1287 (2007), p. 111

[2] A. Vilchis-Nestor, V. Sánchez-Mendieta, M. Camacho-López, R. Gómez-Espinosa, M. Camacho-López, J. Arenas-Alatorre Mater. Lett., 62 (2008), p. 3103

[3] Y. Choi, N. Ho, C. Tung Angew. Chem. Int. Ed., 707 (2007), p. 46.

[4] Templeton, A. C.; Wuelfing, W. P.; Murray, R. W. Acc. Chem. Res. 2000, 33, 27 and references therein.

[5] Simard, J.; Briggs, C.; Boal, A. K.; Rotello, V. M. Chem. Commun. 2000, 1943.

[6] I. dell’Erba, I. E., Hoppe, C. E. & Williams, R. J. J. Langmuir 26, 2042–2049 (2010).

Acknowledgements: We thank CONICET (PIP No 1035), UNLP and LNLS (Projects XAFS1-18861 and SXS-17998) for the financial support of this research.

Advances in the design of new energy storage materials using the new TGM setup for VUV-luminescence studies

Lucas C.V. Rodrigues¹, Cassio C.S. Pedroso¹, Leonnam G. Merízio¹, José M. Carvalho²,
Ian P. Machado¹, Otávio P. Bezzan¹, Maria C.F.C. Felinto³, Hermi F. Brito¹,
Verônica C. Teixeira⁴ and Douglas Galante⁴

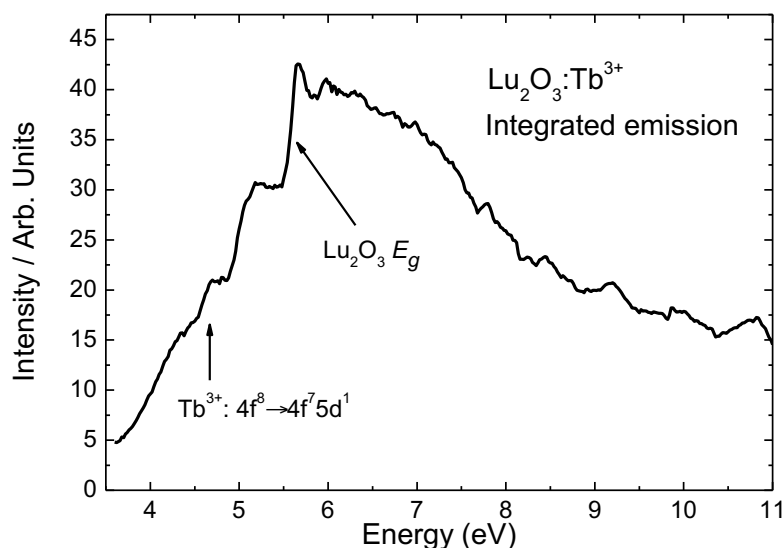
¹Universidade de São Paulo, Instituto de Química, Departamento de Química Fundamental, 05508-000, São Paulo-SP, Brazil, ²University of Turku, Department of Chemistry, FI 20014, Turku, Finland, ³Instituto Nacional de Pesquisas Energéticas e Nucleares, Centro de Química e Meio Ambiente, 05508-000, São Paulo-SP, Brazil, ⁴Laboratório Nacional de Luz Síncrotron-CNPEM, 13083-970, Campinas-SP, Brazil.
lucascvr@iq.usp.br

Research on persistent luminescence materials has increased continuously since the mid-1990s due to their versatile applications in, for example, emergency signalization, image storage and bioimaging [1, 2]. Nowadays their use has been suggested as energy storage materials since light can be stored depending on the temperature. However, the development of new materials is still mainly carried out on a trial-and-error basis.

The use of VUV-excited luminescence experiments can yield precious information on how the persistent luminescence works. For example, the determination of the dopants energy levels or the host's band gap can be done measuring the excitation spectrum of the sample (Figure).

The new setup also allowed the study of the charging and discharging phenomena of persistent luminescence at different energies, below and above the band gap, yielding valorous data to understand the mechanism of energy storing in optical materials.

In this presentation we show the advances on the elucidation of the energy storage mechanisms under the analysis of the spectroscopic behavior of several persistent luminescence materials, all studied at the new TGM setup for luminescence measurements.



- [1] T. Aitasalo, J. Hölsä, H. Jungner, M. Lastusaari and J. Niittykoski J, J. Phys. Chem. B 110, 4589 (2006).
[2] K. Van den Eeckhout, P.F. Smet and D. Poelman, Materials 3, 2536 (2010).

Acknowledgements: This work was supported by CAPES and CNPq. The authors would like to thank to all LNLS staff.

XANES study of nickel(II) coordination complexes: comparison of the electronic structure for different geometries and ligand alkylic chain length

Luciana C. Juncal and Rosana M. Romano

CEQUINOR (UNLP, CCT-CONICET La Plata). Departamento de Química, Facultad de Ciencias Exactas, Universidad Nacional de La Plata. Blvd. 120 N° 1465, CC 962, La Plata (CP 1900), Argentina
romano@quimica.unlp.edu.ar

The aim of this work is the electronic structure determination of nickel(II) coordination complexes with ligands of the general formula ROC(S)S-, motivated in their wide variety of applications, ranging from their use in the preparation of NiS nanoparticles and thin films, the applications in semiconductor materials, heterogeneous catalysis, their ability as activators in froth flotation processes, to their potential pharmacological uses. In a recent investigation, we report an experimental quantitative molecular orbital diagram of Ni(CH₃(CH₂)₂OC(S)S)₂ constructed using the information extracted from the different techniques (PES, XANES, UV-visible and resonance Raman spectroscopy combined with theoretical methods).[1]

In this work we present a comparative study of the electronic properties of a series of Ni (II) complexes with different coordination numbers and geometries, and with ligands of different sizes, synthesized in our Laboratory in La Plata. The XANES spectra in the S K-edge region were measured at the DO4A-SXS beamline at room temperature and a pressure below 5x10⁻⁸ mbar, in the 2430-2530 eV energy range. Solid samples were ground to a fine powder and placed on a double-sided sulfur free carbon tape. Energy was calibrated with the 2520 eV value of the excitation energy of the Mo 1s electrons. The DO4B-XAFS1 beamline was used to measure the Ni K-edge spectra. Uniform shaped tablets of 1 mm thickness, obtained from solid samples diluted in boron nitride, were placed in a sample holder, together with a nickel foil used for the energy calibration. Figure 1 resumes some of the obtained results, revealing clear differences between the different complexes, that were discussed in terms of their electronic structure.

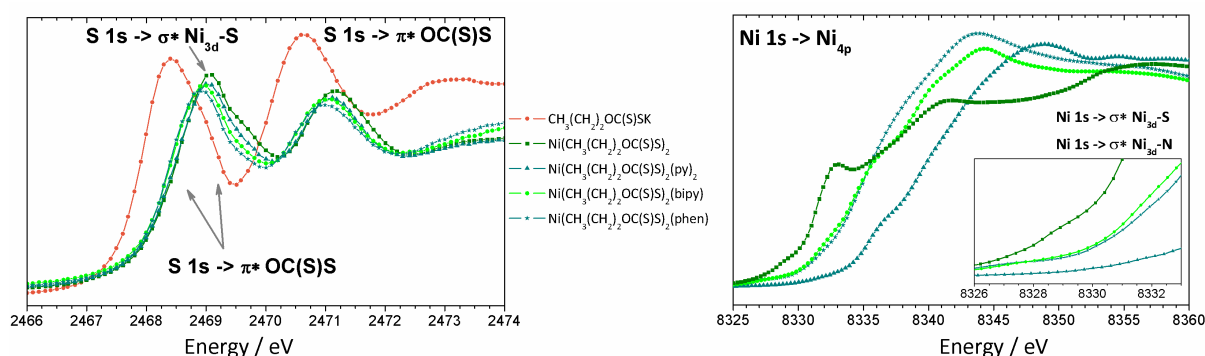


Figure 1. S 1s (left) and Ni 1s (right) XANES spectra of CH₃(CH₂)₂OC(S)S⁻K, Ni(CH₃(CH₂)₂OC(S)S)₂ and Ni(CH₃(CH₂)₂OC(S)S)₂(N-donor)_x, with N-donor = py, bipy o phen.

[1] L.C. Juncal, J. Avila, M. C. Asensio, C.O. Della Védova, R.M. Romano, submitted for publication.

Acknowledgements: This work has been largely supported by LNLS under Proposals SXS-16063 and XAFS1-17950. We thank the beamlines staff for their assistance throughout the experiments, and also Facultad de Ciencias Exactas, Universidad Nacional de La Plata, CONICET and ANPCyT for financial support.

Phase-Retrieval as a Regularization Problem

Marcelo R. Dos Anjos^{3,5}, Eduardo X. Miqueles*¹, João C. Cerqueira², Elias S. Helou⁴, Nikolay Koshev⁴ and Nathaly Archilla¹

¹Brazilian Synchrotron Light Source - CNPEM, Campinas, SP - Brazil ²Dept. of Electrical Eng. - University of Campinas, Campinas, SP - Brazil ³Federal University of Amazonas, Humaitá, AM - Brazil ⁴ICMC, University of São Paulo, São Carlos, SP – Brazil ⁵Programa de Pós Graduação em Física Ambiental, University of Mato Grosso, Cuiabá, MT - Brazil
Email: anjos@ufam.edu.br

It was recently shown that the phase retrieval imaging of a sample can be modelled as a simple convolution process. Sometimes, such a convolution depends on physical parameters of the sample which are difficult to estimate a priori. In this case, a blind choice for those parameters usually lead to wrong results, e.g., the image segmentation process. In this manuscript, we propose a simple connection between phase-retrieval algorithms and optimization strategies, which lead us to more concise ways to determine the physical parameters.

Acknowledgements: This work was supported by Conselho Nacional de Desenvolvimento Científico e Tecnológico CNPQ; Fundação de Amparo à Pesquisa do Estado de São Paulo FAPESP.

Charge transfer effects in the chemical reactivity of Pd_xCu_{1-x} nanoalloys

M.V. Castegnaro¹, A. Gorgeski¹, B. Balke², M.C.M. Alves¹ and J. Morais¹

¹ *Lab. de Espectroscopia de Elétrons – UFRGS – Porto Alegre - Brazil;* ² *Institut für Anorganische und Analytische Chemie, Johannes Gutenberg-Universität, Mainz, Germany.*
marcus_castegnaro@hotmail.com

This work reports on the synthesis and characterization of Pd_xCu_{1-x} (x = 0.7, 0.5 and 0.3) nanoalloys obtained via an eco-friendly chemical reduction method based on ascorbic acid and trisodium citrate. The average size of the quasi-spherical nanoparticles (NPs) obtained by this method was about 4 nm, as observed by TEM. The colloids containing the different NPs were then supported on carbon in order to produce powder samples (Pd_xCu_{1-x}/C) whose electronic and structural properties were probed by different techniques. XRD analysis indicated the formation of crystalline PdCu alloys with nanoscaled crystallite size. Core-level XPS results provided a fingerprint of a charge transfer process between Pd and Cu and its dependency on the nanoalloy composition. Additionally, it was verified that the alloying is able to change the NPs reactivity towards oxidation and reduction. Indeed, the higher the amount of Pd in the nanoalloy, less oxidized are both the Pd and the Cu atoms in the as-prepared samples. Also, *in situ* XANES experiments during thermal treatment under reducing atmosphere, showed that the temperature required for a complete reduction of the nanoalloys depends on their composition. These results envisage the control at the atomic level in order to tune novel catalytic properties of such nanoalloys.

Acknowledgements: This work was funded by CAPES, CNPq, FAPERGS, LNLS (SXS-15314 and XAFS1-17120 proposals) and LNNano (TEM-HR-14037 and TEM-HR 15294 proposals). The authors would like to thank the LNLS, LNNano, LII-UFRGS, LCN-UFRGS and CME-UFRGS staff for their support. M. V. Castegnaro thanks CAPES and CAPES/DAAD/PROBRAL for his PhD fellowships

Heterojunctions of Graphene and Pd and Pd/Pt Alloy Nanoparticles: H₂ Sensing and Potential Catalytic Applications

Dalfovo, M. C., Huck Iriart, C., Giovanetti, L. J., Requejo, F. G. and Francisco J. Ibañez, F. J.

*Instituto de Investigaciones Fisicoquímicas, Teóricas y Aplicadas (INIFTA), Universidad Nacional de La Plata - CONICET, Sucursal 4 Casilla de Correo 16, 1900 La Plata, Buenos Aires, Argentina
mcdalfovo@inifta.unlp.edu.ar / mcdalfovo@gmail.com*

Graphene is the first two-dimensional (2D) crystalline material with outstanding properties. This has opened new avenues towards various applications including the construction of sensitive platforms. In this particular matter, decorating graphene with transition-metal catalyst nanoparticles (NPs) seems to be quite promising platform to explore into the electronic properties of the heterojunction. There are multiple applications which include H₂ sensing, H₂ storage and heterogeneous catalysts. In this work we addressed some of the aforementioned applications by chemically synthesizing alkylamine-coated Pd and Pd/Pt NPs and assembling them as films on Graphene and aminopropyl-triethoxysilane (APTES)-modified Si substrates for H₂ sensing and potential catalytic applications. Here, we performed small-angle X-ray scattering (SAXS) and grazing incidence small-angle X-ray scattering (GISAXS) experiments in order to explore into the shape, order, and size of NPs solutions and in solid-state films, respectively. Real-time GISAXS was used to monitor interparticle distance, NPs size and film structure upon H₂ sensing. In order to explore into the Pd-H and Pt-H interaction, we performed X-ray absorption near edge structure (XANES) in an atmosphere with and without H₂. The results showed distinct film behavior depending on both; the type of NPs (Pd versus Pd/Pt alloys) and the nature of substrates. Finally, we will show some preliminary results of their catalytic reactivity.

Monitoring the redox process for cerium and aluminum-based catalysts by in situ XANES

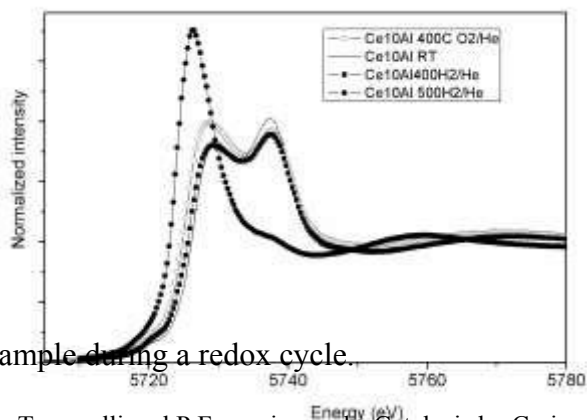
M. C. Rangel¹, J. Fonseca^{1,2}, N. Bion², C. M. Morais², Y. E. L. Fonseca³, D. Duprez² and F. Epron²

¹Instituto de Química, Universidade Federal da Bahia, Campus Universitário de Ondina, Federação, 40 170-290, Salvador, BA, Brazil; ²Université de Poitiers, CNRS, UMR7285, ³Institut de Chimie des Milieux et Matériaux de Poitiers (IC2MP), 4 rue Michel Brunet, 86073 Poitiers Cedex 9, France; ³Departamento de Engenharia-Química, Instituto de Química, Universidade do Estado do Rio de Janeiro R. São Francisco Xavier, 524. Maracanã Rio de Janeiro, RJ, Brazil

Email_M.C Rangel_mcarrov@ufba.br

In recent times, ceria has been extensively used in several reactions both as supports and catalysts [7]. These applications are mainly related to ceria storage capacity as well as to the mobility of oxygen atoms in the lattice as a consequence of $\text{Ce}^{4+}/\text{Ce}^{3+}$ redox couple, besides the basic properties of ceria. In spite of these advantages, pure ceria does not have suitable specific surface area and thermal stability comparable to industrial catalyst supports, such as alumina. Aiming to obtain improved catalysts for the preferential oxidation of carbon monoxide (CO-PROX), a detailed study of structural and redox properties of aluminum and cerium oxide was performed in this work. As pointed out early, cerium is effective in improving the thermal stabilization of alumina but few studies have addressed the cerium state in the lattice. Some XPS studies showed the presence of Ce^{3+} species but it was not shown if they are atomic species on the surface or whether they lie in the tetra, penta- and octahedral vacancies of alumina. The samples (cerium-containing ordered mesoporous alumina, CeXAl (X (molar ratio)= 2, 5, 10, 15 and 20 and a commercial nanosized ceria) were prepared by Evaporation Induced Self Assembly (EISA) method and characterized by several methods. The X-ray absorption spectra at Ce L3-edge energy range, widely used to characterize the cerium oxidation state and the nanoparticle structure, was used in the experiments.

[8]. The spectra were acquired in transmission mode at the XAFS2 beamline at the Brazilian Synchrotron Light Laboratory (LNLS) in the 5665-6150 eV energy range. The sample pellets were placed into a tubular (cylindrical) furnace and heated ($10\text{ }^\circ\text{C min}^{-1}$) up to $1000\text{ }^\circ\text{C}$, under reducing flow ($5\%\text{H}_2/\text{He}$, 40 mL min^{-1}) by steps of $100\text{ }^\circ\text{C}$, keeping the sample for 30 min at each step. Then the reducing flow was replaced by pure helium and then by oxidizing atmosphere ($5\%\text{O}_2/\text{He}$, 10 mL min^{-1}). The XANES spectra were taken at each step during heating and cooling. The XANES



results evidenced that the reduction of cerium atoms for nanosized commercial ceria occurred at temperatures higher than $400\text{ }^\circ\text{C}$, while the complete cerium reduction occurred at temperature between 400 and $500\text{ }^\circ\text{C}$ for CeXAl samples. The reversibility of this process (reoxidation of cerium atoms after reduction) was confirmed for the redox cycle. The EXAFS spectra showed that cerium cations are highly dispersed since the Ce-Ce interaction shell is practically absent in the CeXAl samples.

Figure 1. Selected XANES spectra of Ce10Al

A. Trovarelli and P Fornasiero, eds, Catalysis by Ceria and Related Materials, 2nd ed., Imperial College Press, London, (2012) pp. 1-879.

R. B. Duarte, O.V. Safonova, F. Krume, M. Makosch and J. A., van Bokhoven, ACS Catal. 3, 1956-1964. (2013).

Acknowledgements: This work was supported by CNPq and LNLS. The authors would like to thank...

Application of SR μ XRF to evaluate the efficacy of Pb soil extraction of hyperaccumulator plant species versus fastgrowing plants used for phytoextraction of soil contaminants

Mera M. F.¹, Rubio, M.^{1,2,3}, Pérez C. A.⁴, Carranza L.¹, Cazón S.¹, Ravera M.¹

¹CEPROCOR. Álvarez de Arenales 180 B° Junios (5000), Córdoba, Argentina; ²FAMAF. Ciudad Universitaria (5000).

Córdoba, Argentina; ³CONICET, Rivadavia 1917 (1033), Buenos Aires, Argentina. ⁴LNLS, Laboratório Nacional de Luz Síncrotron, Caixa Postal 6192, CEP 13083-970, Campinas, SP, Brazil.

Phytoextraction, also called phyto-accumulation, refers to the uptake and translocation of toxic metals from contaminated soils by plant roots into the harvestable parts of the plants which can then be removed from site.

Synchrotron-based X-ray fluorescence techniques enables substantial advances in several disciplines of plant science since it allows in situ examination of elements within vegetable tissues in order to understand the mechanisms involved in metal(loid) uptake and metabolism in plants⁽¹⁻³⁾

The aim of this work was to evaluate the phytoextraction capacity of two kind of vegetable species: hyperaccumulator plant species such as *Brassica napus* and fast-growing non-hyperaccumulator plants such as *Festuca arundinacea*. The goal was to develop an efficient phytoextraction technology for the remediation of Pb contaminated soils.

The measurements were carried out at the D09B XRF Fluorescence beamline of the LNLS. The experiments were conducted in *Brassica napus* and *Festuca arundinacea* plants, grown in Pb soil contaminated and in crops in hydroponics conditions exposed to lead at residential and basal levels, in controlled environment, cultivated in greenhouses at CEPROCOR.

The results revealed that *Brassica napus* extracted Pb from the ground and translocated it to the leaves more effectively than *Festuca arundinacea* plants grown in contaminated soil, where lead remained at the root. Furthermore, a co-distribution was observed between Pb and Zn, P, S and Fe.

The conclusions of this study suggest that *Brassica napus* is a potential plant to be used for phytoextraction of Pb from soil.

Outcomes are intended to be used to evaluate the experimental design of phytoextraction in laboratory aiming at scaling the right information to actual industrial waste problems in order to develop an efficient technology to recover the soil quality.

[9]. Donner E. and col, Mapping Element Distributions in Plant Tissues Using Synchrotron XRF Techniques. Chapter 9, 2012.

[10]. Lombi E. and col, In situ analysis of metal(loid)s in plants: State of the art and artefacts. Environmental and Experimental Botany, 72, 2011, 3-17.

[11]. Sarret G and col., Use of Synchrotron-Based Techniques to Elucidate Metal Uptake and Metabolism in Plants, Chapter 1, Advances in Agronomy, 119, 2013, 1-82.

Acknowledgements: this work was developed at Brazilian National Synchrotron Light Laboratory under the proposal XRF-18934. The authors would like to thank the LNLS staff for its technical support.

Adsorption of Alkanethiols on Well Defined and Nanoparticle Pd Surfaces

M. H. Fonticelli¹, A. A. Rubert¹, J. C. Azcárate¹ and A. de Siervo²

¹ *The Research Institute of Theoretical and Applied Physical Chemistry (INIFTA), National University of La Plata - CONICET, Sucursal 4 Casilla de Correo 16, 1900 La Plata, Argentina.*

² *Dep. de Física Aplicada - Instituto de Física Gleb Wataghin Universidade Estadual de Campinas - UNICAMP
Rua Sérgio Buarque de Holanda, 777, Cid. Universitária "Zeferino Vaz"
13083-859, Campinas, SP, Brasil
mfonti@inifta.unlp.edu.ar*

It is known that, opposite to the model system -Au(111) surfaces-, the adsorption of thiols on Pd surfaces lead to mixed sulfide/thiolate interfaces. Furthermore, it was proposed that: (a) the ability of the metal surface to induce the S-C bond cleavage is related with changes in the surface density of states (DOS),[1] and (b) the disorder in ~ 3 nm thiolate-protected nanoparticles is promoted by the strong S-Pd bond in the sulfide layer that surrounds the NPs.[2]

Nowadays, the needing of a deeper understanding of the thiol/Pd interfaces is evident because of the interest that thiolate Self-Assembled Monolayers (SAMs) have on catalysis. Medlin et al. have recently demonstrated that alkanethiol SAMs improve the selectivity of Pd surfaces (both planar and nanoparticles) towards a variety of reactions.[3,4] However, the SAMs' role on the catalytic activity is not analyzed in close correlation with their actual composition. Furthermore, two recent works renewed the interest of thiol SAMs' on platinum group metals (PGMs). Esaulov et al. recently claimed that the component at ~ 162 eV belongs to thiolates, while that at 163eV to atomic sulfur[5], which is contrary to previous assignments and the predictions based on the electronegativity of sulphur species. This is, for itself, an interesting puzzling problem to resolve. On the other hand, recent high resolution XPS measurements of thiol SAMs on Ni(111) showed that sulfide is also a coadsorbate for this metal.[6]

We have studied Pd(111) and (100) surfaces modified by dodecanethiol and by mercaptobenzene in the PGM beamline at LNLS. We were able to resolve the component at BE Sp3/2 ~ 162.6 - 162.8 eV, which could not be separated from that assigned to molecular species (BE Sp3/2 ~ 163.4 eV) in previous studies. The data support our previous assignment (*i.e.* the component at ~ 162 eV belongs to atomic sulfur, while that at 163eV to thiolates), and shows that the thermal treatment increases the relative sulfide contribution to the S2p signal. Also, we used laboratory XPS and standard characterization techniques (UV-visible spectroscopy and transmission electron microscopy (TEM) –for nanoparticles- and LEED -for single crystals-) to characterize thiol modified surfaces.

Our study of Self-Assembled Monolayers of thiols on Pd surfaces (polycrystalline, Pd(111), Pd(100) and 3nm in diameter nanoparticles), which were built-up in liquid media, demonstrate that sulfide species are present irrespective of the chemical nature of the thiol (aliphatic or aromatic), or the atomic arrangement of the metal surface. Furthermore, we demonstrate that the surface composition under the in operando conditions (T=463 K [4]) of a relevant catalytic processes correspond to mixed thiolate-palladium(II) sulfide layer.

[1] P. Carro, G. Corthey, A. A. Rubert, G. Benitez, M. H. Fonticelli, R. C. Salvarezza, *Langmuir* 26, 14655 (2010).

[2] G. Corthey, et. Al. *J Phys Chem C* 118, 24641 (2014).

[3] Schoenbaum, C. A.; Schwartz, D. K.; Medlin, J. W., *Acc. Chem. Res.* 47, 1438 (2014).

[4] S. H. Pang, C. A. Schoenbaum, D. K. Schwartz, J. W. Medlin, J. W. *ACS Catalysis* 4, 3123 (2014).

[5] J. Jia, A. Bendounan, K. Chaouchi, S. Kubsy, F. Sirotti, L. Pasquali, V. Esaulov, *J Phys Chem C* 118, 24983 (2014)

[6] F. Blobner, et. Al. *J Phys Chem C* 119, 15455 (2015)

Acknowledgements: This work was supported by LNLS (Proposal SGM - 17848), CONICET and UNLP.

Short-term bonding of freshly added cadmium in Brazilian Oxisols

Marina Colzato^{1,2}, M.Y. Kamogawa¹, H.W.P. Carvalho², L.R.F. Alleoni¹ and D.L. Hesterberg³

¹ Universidade de São Paulo, Centro de Energia Nuclear na Agricultura, 13400-970, Piracicaba, Brazil; ² Universidade de São Paulo, Escola Superior de Agricultura Luiz de Queiroz, 13418-900, Piracicaba, Brazil; ³ North Carolina State University, Soil Science Department, 27607, Raleigh, USA.
mcolzato@usp.br

Cadmium is one of the most toxic elements for all animals and plants [1]. The chemical speciation of soil Cd should dictate its bioavailability and potential toxicity to plants and animals, and its transfer pathways through the food web to humans. Our research evaluated short-term conversion of freshly added cadmium in Brazilian Oxisols with high Cd sorption capacities. Oxisols found in humid tropical regions, including in extended areas under agriculture in developing countries and Brazil, have pH-dependent charge due to abundant organic matter, oxide minerals, and kaolinite, [2]. The objective of this research was to utilize Cd L_{III}-edge XANES analysis to determine short-term changes in Cd speciation in Oxisols reacted with soluble Cd(II). Six soil samples, comprising three Oxisols (Anionic Acrudox, Rhodic Hapludox and Typic Hapludox), one Mollisol (Mollic Epiaquent), and two Entisols (Typic Argiudolls and Typic Quartzipsamments), were incubated for 0.5 and 6 hours with cadmium chloride solution to obtain a final concentration of 4.45 mmol Cd kg⁻¹. Complementary incubation for 4 months were submitted to chemical fractionation. Adsorbed Cd standards for XANES analyses were prepared for pure materials of leonardite, kaolinite, montmorillonite, goethite, gibbsite and hematite. Standards of CdS, CdCl₂ and Cd₃(PO₄)₂ were diluted with saccharose to 4.45 mmol Cd kg⁻¹. The samples were dried, homogenized and placed as thin film onto a double-sided carbon tape on a sample holder. Cadmium L_{III}-edge (3538 eV) XANES data were collected under vacuum at the Soft X-Ray Spectroscopy (D04A-SXS) beamline of the Brazilian Synchrotron Light Laboratory – LNLS. For each sample, three to ten spectra were collected in fluorescence mode within energy range between 3500 and 3620 eV. Data were baseline corrected, normalized, and fit using the Athena data analysis software [3]. Scans were merged to improve the signal-to-noise ratio and E₀ was set to the maximum in the first derivative spectrum. A unique normalization was needed for samples and some standards due to interference by the K absorption edge of naturally occurring potassium at 3608 eV. Standards of pure (K-free) salts and saccharose normalized using a linear fit to the post edge region served as a guide for normalizing other samples at the point of maximum absorption. Linear Combination Fitting (LCF) was used to fit samples, with CdCl₂ selected as an obligatory standard because it was the source of Cd added to the samples. Cadmium-leonardite, a surrogate for Cd on organic matter, was represented in fits for all soil samples; ranging from 18-19% in the Typic Quartzipsamments, 36% in Typic Argiudolls, and up to 77% in Rhodic Hapludox samples. The Typic Quartzipsamments data could be fit with up to 31% of the CdCl₂ standard, indicating a lack of adsorption and ultimately precipitation of this salt upon drying. The proportions of the standards giving best fits for each soil sample had only minor variations between 0.5 and 6 hours of reaction time, and showed no definite trend across soil classes. In conjunction with longer-term incubation studies involving chemical fractionation, our results suggest that Cd(II) discharged into Oxisols would bind rapidly with soil organic matter or remain in soluble forms with little change in speciation and bioavailability following up to 4 months of residence time in the soils.

[1] A. Kabata. Trace elements in soil and plants (CRC Press, 2011)

[2] Z.L. He, H.P. Xu, Y.M. Zhu, X.E. Yang, X.E. Chen. G.C. J. Environ. Sci. Health. 805 (2005).

[3] B. Ravel and M. Newville, J. Synch. Rad. 12, 537 (2005).

Acknowledgements: This work was supported by University of São Paulo.

Characterization and low-resolution structure of an extremely-thermostable esterase of potential biotechnological interest from *Pyrococcus furiosus*

Mario de Oliveira Neto¹, César Augusto Gandin¹, Fernanda Mandelli², Thiago A. Gonçalves^{2,3} and Fabio Marcio Squina².

¹ Universidade Estadual Paulista (UNESP), Departamento de Física e Biofísica, Instituto de Biociências de Botucatu, Botucatu, SP, Brasil; ² Laboratório Nacional de Ciência e Tecnologia do Bioetanol (CTBE), Centro Nacional de Pesquisa em Energia e Materiais (CNPEM), Campinas, SP, Brasil, ³ Universidade Estadual de Campinas (UNICAMP), Departamento de Bioquímica, Instituto de Biologia (IB), Campinas, SP, Brasil
cesargandin@gmail.com

Enzymes isolated from extremophiles often exhibit superior performance and potential industrial applications. There are several advantages to performing biocatalysis at elevated temperatures, including enhanced reaction rates, increased substrate solubility and decreased risks of contamination. Furthermore, thermophilic enzymes usually exhibit high resistance against many organic solvents and detergents, and are also more resistant to proteolytic attack. In this study, we cloned and characterized an esterase from the hyperthermophilic archaeon *Pyrococcus furiosus* (Pf_Est) that exhibits optimal activity around 80 °C and pH 6.5. According to the circular dichroism spectra data, the secondary structure of *P. furiosus* esterase, which is predominantly formed by a β -sheet structure, is very stable, even after incubation at 120 °C. We performed SAXS to determine the low-resolution structure of Pf_Est, which is monomeric in solution at 80 °C and has a molecular weight of 28 kDa. SAXS also revealed an oligomerization tendency at room temperature, related to the enzyme activity. The K_m and V_{max} values for this esterase acting on p-nitrophenyl palmitate (pNPP) were 0.53 mM and 6.5×10^{-3} U, respectively. Pf_Est possesses transesterification capacity, presenting better results when isobutanol is used as an acyl acceptor ($2.69 \pm 0.14 \times 10^{-2}$ $\mu\text{mol} \cdot \text{min}^{-1} \cdot \text{mg}^{-1}$). Collectively, these biophysical and catalytic properties are of interest for several biotechnological applications that require harsh conditions, including high temperature and the presence of organic solvents.

Acknowledgements: This work was supported by CNPq and FAPESP. The authors would like to thank LNLS and staff of SAXS beamline.

Photoluminescence studies under UV and VUV excitation of undoped and rare-earth doped CaYAl_3O_7

Mário E. G. Valerio¹, Giordano F. C. Bispo¹, Adriano B. Andrade¹ and Verônica C. Teixeira²

¹ Physics Department, Federal University of Sergipe, 49100-000 São Cristóvão, SE, Brazil; ² Brazilian Synchrotron Light Laboratory, National Center for Research in Energy and Material, 13083-970, Campinas – SPE
gfredericoc@gmail.com.br, mvalerio@ufs.br

The CaYAl_3O_7 (CYAM) has been studied due to its luminescence properties when doped with rare earth (RE) ions [1-3]. Several potential applications have been pointed, i.e., sensing structural damage[1], solid-state light source for white LED's[2] and temperature sensors[3]. In this work the Pechini method was used to produce CYAM undoped and doped with Eu^{3+} , Tb^{3+} , Ce^{3+} and Sm^{3+} . Thermal analysis and XRD measurements showed that $1000^\circ\text{C}/4\text{h}$ was the best condition for the CYAM synthesis. Scanning electron microscopy (SEM) showed that submicrometric particles with irregular shape were obtained. Photoluminescence (PL) studies were carried out by exciting samples in the range from 4.2 up to 10.9 eV using the facilities of the Toroidal Grating Monochromator (TGM) beamline [4] (proposals TGM-17892, TGM-18991 and TGM-20150122) at LCLS (Brazilian Synchrotron Light Laboratory). The emission spectra were registered from 1.6 to 6.2eV and 3D plot of the PL as functions of both excitation and emission energies were built to detail the electronic transitions under several excitations. This plot allowed a study of the changes in band structure caused by doping with different rare earth ions. Undoped CYAM sample showed complex emission spectra related with the presence of F and F^+ centres besides self-trapped exciton (STE). The relative intensity of three mains emissions were found to depend on the excitation energy. The fundamental interband transition was found to be around 7 - 7.5eV. The $\text{CYAM}:\text{Ce}^{3+}$ sample showed a broad emission band peaking at 2.88eV(430nm) related to the $^5\text{d}_1 \rightarrow ^2\text{F}_{7/2;5/2}$ transitions. This band changed its intensity as a function of the excitation energy but the position of the is always the same. This feature was also observed for $\text{CYAM}:\text{Sm}^{3+}$, where the typical $^4\text{G}_j \rightarrow ^6\text{H}_j$ transitions of the Sm^{3+} ions were observed, and for $\text{CYAM}:\text{Tb}^{3+}$, where the Tb^{3+} $^5\text{D}_4 \rightarrow ^7\text{F}_6$, $^5\text{D}_4 \rightarrow ^7\text{F}_4$ and $^5\text{D}_4 \rightarrow ^7\text{F}_2$ emissions were observed. In $\text{CYAM}:\text{Eu}^{3+}$ the $^5\text{D}_0 \rightarrow ^7\text{F}_2$ emission was found to have higher intensity than the $^5\text{D}_0 \rightarrow ^7\text{F}_1$ emission. This happened because of the low local symmetry of the Ca/Y site. The 3D PL plots showed that for the Ce^{3+} and Tb^{3+} -doped samples besides the the RE typical transitions, the interband fundamental transitions that was also obtained for the undoped material. Charge transfer band (CTB) localized around 5.32eV and 4.04eV were observed for Sm^{3+} and Eu^{3+} -doped samples, respectively. All these information allowed the proposal of a model including the positions of the energy levels of the dopants as well as the F, F^+ and STE transitions.

[1] H. Zhang, H. Yamada, N. Terasaki, C.-N. Xu, Blue Light, J. Electrochem. Soc. 155, J128. (2008).

[2] S. Unithrattil, K.H. Lee, W.J. Chung, W. Bin Im, J. Lumin. 152, 176, (2014).

[3] V. Singh, V.K. Rai, K. Al-Shamery, J. Nordmann, M. Haase, J. Lumin. 131, 2679, (2011).

[4] R.L. Cavasso Filho, A.F. Lago, M.G.P. Homem, S. Pilling, A. N. de Brito, J. Electron Spectros. Relat. Phenomena. 156, (2007).

Acknowledgements: This work was supported by CNPq, INAMI, CAPES, FINEP and FAPITEC-SE. The authors would like to thank Brazilian Synchrotron Laboratory, the Multiuser Center for Nanotechnology of the Federal University of Sergipe and its staff for the use of the laboratory facilities.

Study of the profile of layer formed in plasma nitrided ASTM F138 stainless steel

D.Olzon-Dionysio^(1,a), S. D. de Souza⁽¹⁾, L. G. Martinez⁽²⁾, E. H. da Silva⁽³⁾ and M. Olzon-Dionysio⁽¹⁾

UFVJM- Diamantina, MG, Brazil, (2) IPEN- São Paulo, SP, Brazil, (3) Belgian Nuclear Research Centre (SCK-CEN)/Vrije Universiteit Brussel (VUB), LABO and BEFY, Brussels, Belgium

(a) Corresponding author: dolzon@gmail.com

The ASTM F138 and AISI 316L stainless steels are used as biomaterials and for industrial applications. Studies related to the application of plasma nitriding to such materials have been given much attention and it has been the subject of a systematic study in our research [1-5]. If temperatures up to 400^o C is used in the process, a nitrided layer of some micrometers is produced, which improves important properties in this context as high hardness, wear resistance and also corrosion resistance. The nitrided layer is formed by the **composite layer** which consists of iron and chromium nitrides, and concentrates on the surface, as well as the nitrogen **diffusion layer** which is located in the inner region, known as expanded austenite γ_N . Compared to matrix γ -phase reflections, γ_N -phase diffraction peaks are broader and shifted to lower angles. The $\gamma_N(200)$ peak positions are more deviated relatively to $\gamma(200)$ than other planes, demonstrating a distortion from the cubic fcc unit cell. Up to now, the crystalline structure of this phase is still a matter of debate and it has not been completely clarified. We have developed some measurements using synchrotron radiation, which allows for both a higher intensity and a better resolution, in order to elucidate this important phase formed in the nitriding process [4,5]. With the aim of investigate the depth distribution of composite layer of some ASTM F138 samples, which were nitrided at 400^o C at different conditions of AC voltage frequency, synchrotron radiation diffraction was carried out using 7.0 keV energy. The XRD patterns were measured using different grazing angles. Measurements revealed that the iron and chromium nitrides, from the composite layer, decrease rapidly with depth. The results will be presented and discussed, contributing to better elucidate this important phase formed in the nitriding process.

[1] S. D. de Souza, M. Olzon-Dionysio, E. J. Miola and C. O. Paiva-Santos. *Plasma Nitriding of sintered AISI 316L at Several Temperatures*- Surf. Coat. Technol. 184/2-3 (2004) 176.

[2] M. Olzon-Dionysio, S.D. de Souza, R.L.O. Basso, S. de Souza. *Application of Mössbauer spectroscopy to the study of corrosion resistance in NaCl solution of plasma nitrided AISI 316L stainless steel*-Surf. Coat. Technol. 202 (2008) 3607.

[3] S.D.de Souza, M.Olzon-Dionysio, R.L.O.Basso, S.de Souza *Mössbauer spectroscopy study on the corrosion resistance of plasma nitrided ASTM F138 stainless steel in chloride solution*-Mater.Character. (2010) 992 DOI 10.1016/j.matchar.2010.06.015

[4] M. Campos, S. D.de Souza, L. G. Martinez; M.Olzon- Dionysio *Study of expanded austenite formed in plasma nitrided AISI 316L samples using synchrotron radiation diffraction*--Mater.Res.(2014) 17(5): 1302-1308 DOI:10.1590/1516-1439.285914

[5] M. Campos, *Investigação das fases formadas na superfície do aço inoxidável AISI 316L nitretado a plasma*-São Carlos. PhD thesis-DF- UFSCar, Advisor : M.Olzon- Dionysio, finished in abril/2013.)

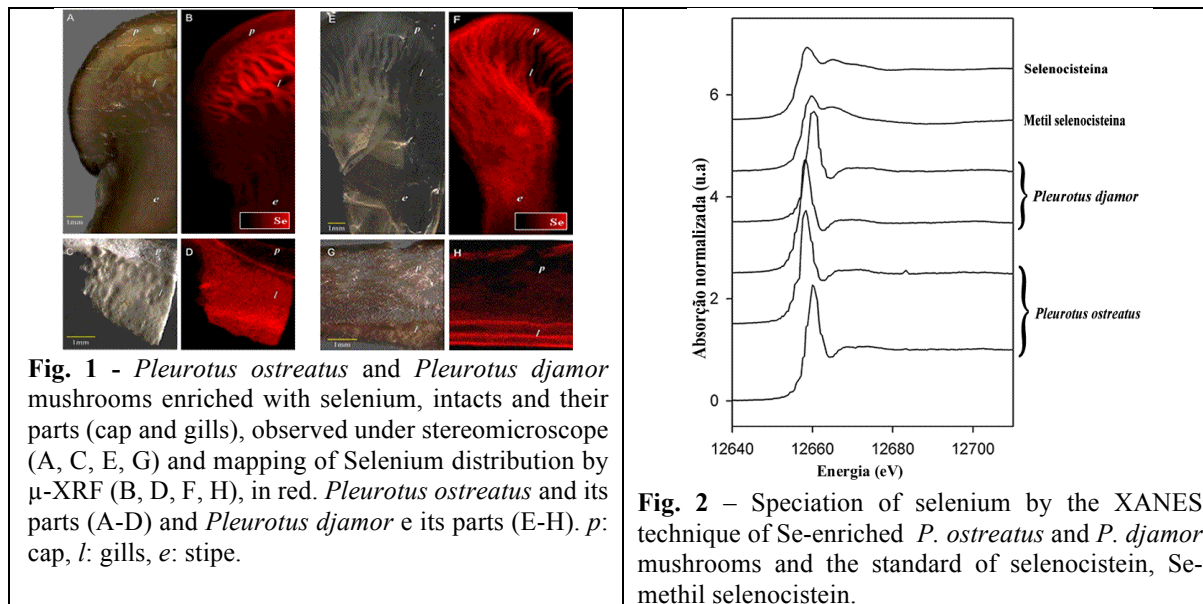
Acknowledgements: This work was supported by FAPESP, CAPES and FAPEMIG. The authors would like to thank M. Campos for valuable discussions.

Selenium distribution and speciation in biofortified mushroom

M.C.S. Da Silva¹, P.A.Z. Sereño¹, M.D. Nunes¹, L.F.S. Souza Filho², L. Vergutz³, C.A. Perez⁴, D. B. Abdala⁴ and M.C.M. Kasuya¹

Universidade Federal de Viçosa, ¹Departamento de Microbiologia, ³Departamento de Solos, 36570-900, Viçosa, MG, Brazil; ²Universidade Federal do Oeste da Bahia, Barra, BA, Brazil; ⁴Brazilian Synchrotron Light Source (LNLS), Brazilian Center for Research in Energy and Materials (CNPEM), Campinas, SP, Brazil
mcassiabio@yahoo.com.br

Mushrooms enrichment with different minerals can be an effective way to combat food deficiency in some micronutrients [1]. Among them we have selenium (Se) which is essential for the functioning of various selenoproteins which perform important functions in the body [2]. The aim of this study was to evaluate the distribution and speciation of Se in mushrooms of *Pleurotus* spp. enriched with this micronutrient. Thus, *Pleurotus ostreatus* and *Pleurotus djamor* mushrooms enriched with selenium were analyzed using synchrotron-based μ -XRF and μ -XANES. Through the mapping done, it was observed that there was a greater accumulation of Se in the gills than in other mushroom structures, such as cap and stipe (Figure 1). μ -XANES analysis at the selenium K-edge showed that the Se was accumulated mainly in reduced forms. μ -XRF analysis proved to be an efficient and practical technique for detection of Se in different parts of the mushroom. However, further work should be done regarding chemical speciation via XANES spectroscopy to allow a more accurate distinction of the different forms of reduced Se present in the plant material.



[1] L. ASSUNÇÃO, M. C.S. DA SILVA, M., FERNANDEZ, M., GARCÍA-BARRERA, T., GOMÉZ-ARIZA, J. L., BAUTISTA, J., & KASUYA, Speciation of selenium in *Pleurotus ostreatus* and *Lentinula edodes* mushrooms. *Journal of Biotechnology Letters*, v. 5, p. 079-086 (2014).

[2] M. P. RAYMAN. Selenium and human health. *The Lancet*, v. 379, p. 1256-1268, (2012).

Acknowledgements: This work was supported by CNPq, CAPES and FAPEMIG. The authors would like to thank the *Brazilian Synchrotron Light Laboratory (LNLS)* for granting access to the XRF beamline under the research proposal N° D09B XRF 19011.

PDF Studies on Quasi-Amorphous Materials: Magnetic Nanoparticles and Low Z Materials

M. E. Saleta¹, B. Pianciola², E. Lima Jr.² and F. Alves Lima¹

¹ *Laboratório Nacional de Luz Sincrotrón, Campinas (SP), Brazil;* ² *CONICET and Centro Atómico Bariloche, CNEA, S.C. de Bariloche (RN), Argentina.*
martin.saleta@lnls.br – martin.saleta@cab.cnea.gov.ar

The analysis of X-ray total scattering data by atomic pair distribution function (PDF) technique is an attractive characterization tool in material science, alternative to conventional X-ray diffraction (XRD) [1]. Contrary to XRD that only reflects information about the average structure, PDF analysis allows the detection of small local distortions [1], bringing information of the local and medium-range order. This method has been used to study amorphous phases of materials, i.e., those presenting XRD patterns containing broad and low-intensity Bragg peaks. Additionally, it has been useful in structural studies of nanomaterials in which their characteristic sizes limit the proper study by conventional XRD analysis [1]. Here we describe the basic experimental protocol to obtain X-ray total scattering data with good quality to be analyzed by PDF and illustrate the capabilities and limitations currently available at LNLS to perform these experiments. Finally, we present two scientific cases in which conventional XRD analysis fail to provide structural information.

In the following we present some directions that should be followed during the total scattering experiments aiming to be interpreted by PDF: (i) reaching high momentum transfer (Q), preferably higher than 20 \AA^{-1} ; (ii) obtaining high resolution in Q and good statistics (high signal-to noise ratio) for high Q -values; and finally, (iii) using instruments with low background noise, since the data need to have a better signal-to-noise ratio than for Rietveld refinement [1]. All of these experimental recommendations can be easily obtained at the XDS beamline at LNLS [2]. In this work we present the PDF analysis of two systems: CoFe₂O₄ nanoparticles and microcrystalline cellulose (low Z material). The magnetic properties of CoFe₂O₄ NPs are usually dominated by their size. For example, the NPs with $d=8 \text{ nm}$ have almost single-domain behavior occupying approximately the whole NP. In the sample with $d=6 \text{ nm}$, the surface anisotropy is large enough to alter the ferrimagnetic order in the NP shell. Larger particles ($d > 8 \text{ nm}$) showed some reduction of MS with respect to the bulk, pointing to the existence of partial inversion [3]. Our PDF investigation of these NPs focus on determining the structural arrangement of the smallest NPs, which cannot be performed properly by Rietveld analysis, and finally correlating the local range order of the NPs with their magnetic properties.

Microcrystalline cellulose (MCC) is a compound commonly used in industry. Since several decades, MCC has been widely used as an additive to pharmaceuticals, foods, cosmetics, etc. From a structural point of view, the cellulose has several crystalline polymorphs and amorphous phases (polyamorphous) and it is speculated that the use of different phases can alter the properties of the final material (drugs or cosmetics). We expect to study the structure of different MCC and quantify the amorphous phase applying PDF technique. In the three different samples investigated the C-C distances, characteristic of the glucose molecule, could be unambiguously identified due to their distinctive features in the PDF curve. We found this to be independent of the crystalline polymorph or amorphous phase.

T. Egami & S. Billinge, “Underneath the Bragg peaks: structural analysis of complex materials. Pergamon, (2003).
F.A. Lima, et al. submitted to J. Synchr. Rad. (2016).
B, Pianciola et al. J. Magn. Mater. 377, 44-51 (2015).

Acknowledgements: The author thanks Prof. S. Cuffini (UNIFESP) for the cellulose samples and XDS staff for their technical support during the experiment.

EXAFS characterization of confined gold nanoparticles for the detection of small molecules in label-free impedance aptasensors

Martín Mizrahi³, Ana Sol Peinetti¹, Helena Ceretti², Graciela González¹, Silvana Ramírez², Félix Requejo³, Javier Montserrat^{2,4} and Fernando Battaglini¹

¹INQUIMAE (CONICET) – Depto. de Química Inorgánica, Analítica y Química Física, Fac. Cs. Ex. y Nat., Universidad de Buenos Aires, Ciudad Universitaria, Pabellón 2, C1428EHA Buenos Aires, Argentina.

²Universidad Nacional de Gral. Sarmiento, J. M. Gutierrez 1150, B1613GSX, Prov. de Bs. As., Argentina.

³Instituto de Investigaciones Fisicoquímicas Teóricas y Aplicadas – INIFTA (CONICET y Dto. Química, Fac. Cs. Ex., UNLP), 1900 La Plata, Argentina.

⁴INGEBI (CONICET), Vuelta de Obligado 2490, 1428 Buenos Aires, Argentina.
mizrahi@fisica.unlp.edu.ar

Nanotechnology has expanded the applications of previously known molecules, like DNA and RNA oligonucleotides, developing uses as diverse as image guided cancer therapy to nanostructures for biosensing. In this last field, small molecules are an interesting analytical target because their important roles in many fields such as serving as cell signaling molecules, as drugs in medicine, as pesticides in farming, and many others. In this work, a controlled architecture of nanoelectrodes, with a similar size to small molecule-binding aptamers, is synthesized inside nanoporous alumina. Au nanoparticles are electrogenerated in the alumina cavities showing a fast electron transfer process toward ferrocyanide. These capped-free nanoparticles (Al/Al₂O₃/AuNP) are easily modified with a thiol-containing aptamer (Al/Al₂O₃/AuNP/S-APT) for the label-free detection of adenosine monophosphate (Al/Al₂O₃/AuNP/S-APT-AMP) by electrochemical impedance spectroscopy (EIS). When the AMP is recognized, the aptamer configuration change in this small confined surface dramatically modifies the ability of the probe to access the AuNP (Figure 1). For the sample Al/Al₂O₃/AuNP/S-APT, a nanoparticle size of 2.2 nm and a sulfur coverage of *ca.* 60% were estimated by Extended X-Ray Absorption Fine Structure (EXAFS) at Au L₃-edge (Figure 2). EIS and EXAFS results show that the use of a small electrical conducting surface inside an insulating environment can be very sensitive to conformational changes, introducing a new approach to the detection of small molecules exemplified here by the direct and selective detection of adenosine monophosphate (AMP) in the nanomolar scale.

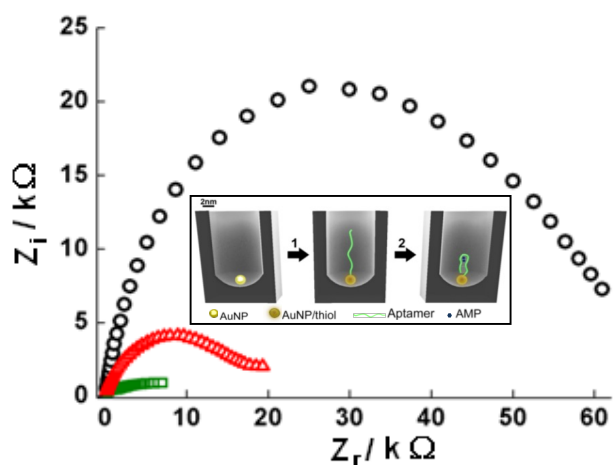


Figure 1: Nyquist plot. Al/Al₂O₃/AuNP (squares); Al/Al₂O₃/AuNP/S-APT (triangles); Al/Al₂O₃/AuNP/S-APT-AMP (circles). Inset: representation of the system. Step 1: Co-adsorption of the aptamer. Step 2: AMP recognition (conformational change in the aptamer).

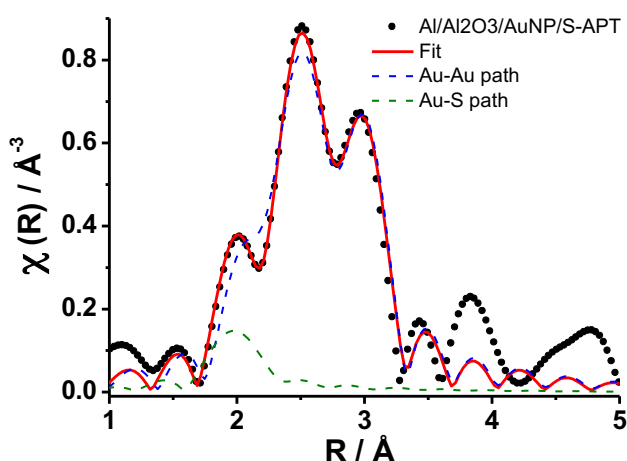


Figure 2: Fourier transform of the EXAFS oscillation (circles) and fit (red line) of the Al/Al₂O₃/AuNP/S-APT sample. Dashed blue line and green line indicate the Au-Au and Au-S contributions, respectively.

Acknowledgements: This work was supported by: XAFS1 beamline (LNLS, Brasil) proposal 17189, PIP 01035 (CONICET, Argentina), ANPCyT PICT-2011-0406 and PICT-2011-0367.

Local structure of Er³⁺ and Yb³⁺ in oxyfluoride borate glasses studied by EXAFS

M. Rodriguez^{1,2}, R. Keuchkerian², Santiago Figueroa³ and L. Fornaro¹

¹ Centro Universitario Regional del Este, Universidad de la República, Rocha, Uruguay.

² Facultad de Química, Universidad de la República, Montevideo, Uruguay.

³ Laboratório Nacional de Luz Síncrotron (LNLS), Centro Nacional de Pesquisa em Energia e Materiais (CNPEM),
Campinas, Brasil;

mrodriguez@cure.edu.uy

Up to now there was a great effort in the search for new materials with improved up-conversion properties as a way of improvement solar cells efficiency. Transparent glass ceramics are promising materials for that purpose. Generally, these materials are doped with rare earth elements to produce the up conversion process. Silica glass ceramics are well studied systems; on the other hand few reports exist about the use of borate glasses. Here, we report the erbium and ytterbium environments using x-ray-absorption fine-structure spectroscopy (EXAFS) on the Er and Yb LIII edge in borate glasses, with nominal composition 28,5 MO-57,0B₂O₃-9,5NaF-3,75YbF₃-1.25ErF₃ and 29,7 BaO-59,4B₂O₃-9,9NaF-0,75YbF₃-0.25ErF₃ (% in mol) where M: Ca, Sr, Ba. Crystallized samples were also investigated. The average Er-F bond separation was found to vary slightly near 2.27 Å meanwhile the Yb-F separation vary near 2.3 Å. Similar results were found for glass ceramics. The implications of these results in understanding structure-property relationships in borate glass and glass ceramics will be discussed.

Acknowledgements: This work was supported by Agencia Nacional de Innovación e Investigación (ANII-FSE-1_2013_1_10575) and Programa de Desarrollo Ciencias Básicas (PEDECIBA). The authors would like to thank L. Suescun, R. Faccio and S. Vazquez (DETEMA-FQ) for XRD measurements.

Effect of matrix composition in the kinetic of grow of Pb nanodroplets in lead-borate glass

Maximilia F. de Souza^{1,2} and Guinther Kellermann²

¹ *Universidade de São Paulo, Instituto de Física, São Paulo, Brazil*

² *Universidade Federal do Paraná, Departamento de Física, Curitiba, Brazil.
mfs@if.usp.br*

We studied the effect of matrix composition on the formation and growth of Pb nanodroplets embedded in $(x-2)\text{PbO}-(100-x)\text{B}_2\text{O}_3-2\text{SnO}_2-2\text{Pb}$ glasses during isothermal treatments at several temperatures. Glasses with different concentrations of PbO ($x = 40, 45, 50, 55$ and 60 in mol %) were produced using the melt-quenching method. The mixture of fine grained PbO, B_2O_3 and SnO powders was melted in vacuum at 780°C during 1 hour to improve homogeneity. SnO was used to partially reduce the PbO leading to the formation of Pb and SnO_2 homogeneously diluted in the glasses. After melting the material was fast quenched down to room temperature using the splat-cooling technique. As a result thin glass platelets transparent to visible light and having thickness ranging between 60 and 110 micrometers were obtained. Samples of the different glasses were studied by small-angle x-ray scattering (SAXS), transmission electron microscopy (TEM) and differential scanning calorimetry (DSC). Studies by DSC showed that the glass transition temperature T_g decreases with increasing concentration of PbO. TEM images of glasses previously treated at temperatures favorable to the formation and growth of Pb nanodroplets showed that nanoparticles have nearly spherical shape and some dispersion in their size. The analysis of SAXS intensity curves, measured *in situ* at several times during the thermal treatments, allowed the determination of the dependence on time of the average radius, size dispersion, number density and total volume occupied by the nanodroplets. The results showed that a substantial number of small nanoparticles are already formed during the production of the glass platelets. Three different successive stages were observed during the growth of Pb droplets: i) an initial period in which occurs the dissolution of nanodroplets with subcritical size, ii) a classical nucleating and growth stage, in which droplets grow at the expense of the Pb atoms initially dissolved in the glass, and iii) a final stage where the formed Pb droplets continue to grow at a progressively smaller rate. The results showed that during the stage of nucleation and growth the diffusion of Pb atoms in glasses follows an Arrhenius-type law. This behavior allowed us to determine the activation energy of growth of Pb nanodroplets for the here studied compositions of lead-borate glasses. The results of SAXS also allowed us to determine the conditions (composition, temperature and time of thermal treatment) that minimize the dispersion in size of Pb nanoparticles.

[1] A. Gorgesky. Cinética de formação e crescimento de nanopartículas de Pb no vidro $52\text{PbO}-45\text{B}_2\text{O}_3-3\text{SnO}_2-3\text{Pb}$. *Master thesis* (2013)

Acknowledgements: This work was supported by Coordenação de Aperfeiçoamento de Pessoal de Nível Superior (CAPES) and Laboratório Nacional de Luz Síncrotron (LNLS).

Identification of arsenic solid species in sulfide mine tailings from the Concordia Mine Argentina using X-ray absorption spectroscopy

N.E Nieva, L. Borgnino and M.G Garcia.

*Earth Sciences Research Center (CICTERRA), CONICET - National University of Cordoba, Argentina.
nancynieva@outlook.com*

When mine waste rich in sulfides are exposed to the weathering agents and to the action of microorganisms, a highly acidic drainage, rich in dissolved metal(oid)s and sulfate is generated. The main process involves the oxidation of the parent sulfide and the subsequent precipitation of secondary minerals. During such process, elevated concentrations of arsenic are released to the water and then incorporated into a cycle that includes the precipitation/dissolution of As-bearing minerals as well as adsorption/desorption from Fe or Al (hydr)oxide sites.

The aim of this work is to analyze the As solid speciation in sediments accumulated in the tailing dams of La Concordia mine, Argentina Puna.

Samples were collected from different layers observed in the exposed walls of an oxidation profile formed in one of the tailing dams. Mineralogy was characterized by XRD and SEM/EDS. Arsenic K-edge spectra (11867 eV) were collected at beamline XAFS1 at the Brazilian Synchrotron Light Laboratory (LNLS) in Campinas, Brazil along with some As reference material such as scorodite, $\text{Na}_2\text{HAsO}_4 \cdot 7\text{H}_2\text{O}$, As_2S_3 , and $\text{NaAsO}_2 \cdot 4\text{H}_2\text{O}$. The X-ray absorption near edge structure (XANES) spectra were analyzed using the Athena program [1].

The main primary minerals determined by XRD and SEM/EDS are quartz, K-feldspar, zircon, and illite, as well as sulfides such as arsenical pyrite, arsenopyrite, some scarce grains of galena and polymetallic sulfides. The main secondary As minerals are As-jarosite and Fe (hydr)oxysulfates, which are more abundant in the uppermost layers [2].

According to the obtained results the As XANES spectra, all samples show characteristic edge features that correspond to As^{5+} compounds. However, samples from the bottom layers show pre-edge shoulders in the range of As^{3+} species. The results indicate that As^{5+} -O compounds are dominant in all layers, but their percentages decrease with depth. In contrast, the proportion of the As^{3+} species, As^{3+} -S and As^{3+} -O, increases in depth. Considering the samples mineralogy, As(V) species likely correspond to As-jarosite, and arsenate ions sorbed onto ferric oxyhydroxides. On the other hand, As^{3+} -S species likely correspond to polymetallic sulfides while As^{3+} -O could be assigned to arsenite ions sorbed onto ferric oxyhydroxides.

The obtained results indicate that As^{5+} compounds predominate all along the tailing profile, with minor contributions of As^{3+} species. The latter are more abundant in the bottom layers. The results suggest that after 30 years of exposure, oxidation has affected almost the entire profile. This has important environmental implications, because As is mostly associated with the more labile phases identified in the sediments.

[1] B Ravel. and M Newville 2005. ATHENA, ARTEMIS, HEPHAESTUS: Synchrotron Radiat. 12, 537-541.

[2] N.E Nieva, L Borgnino, F Locati and M.G García 2016. Science of the Total Environment. 550, 1141–1151

Acknowledgements: Authors wish to acknowledge the assistance of CONICET and UNC whose support facilities and funds were used in this investigation. The Brazilian Synchrotron Light Laboratory (LNLS, Brazil) facilities were used in this investigation.

Aluminum Titanate (Al_2TiO_5) ceramics: complementary Al and Ti K-XAS studies

N.M. Rendtorff²³, L. Andrini¹, R. Moreira Toja², M.A. Violini²³, M.R. Gauna², M.S. Conconi² and F. Requejo¹⁴

¹ Instituto de Físicoquímica Teórica y Aplicada (INIFTA) (UNLP-CONICET La Plata), 64 y Diagonal 113, La Plata Argentina. ² Centro de Tecnología de Recursos Minerales y Cerámica (CETMIC): (CIC-CONICET-CCT La Plata), Camino Centenario y 506, C.C.49 (B1897ZCA) M.B. Gonnet, Argentina. ³ Dpto. De Química, Facultad de Ciencias Exactas, Universidad Nacional de La Plata, UNLP, 47 y 115, La Plata, Argentina. ⁴ Dpto. de Física, Facultad de Ciencias Exactas, Universidad Nacional de La Plata, 47 y 115, La Plata, Argentina.
rendtorff@cetmic.unlp.edu.ar

Aluminum titanate (Al_2TiO_5) ceramics are excellent thermal shock-resistant materials due to their unique combination of low thermal expansion and low Young's modulus. These are adequate for insulating and severe thermomechanical applications [1]. Based in X-Ray and neutron diffraction studies, Al_2TiO_5 was found to be one of several materials, which are isomorphous with the mineral pseudobrookite (Fe_2TiO_5) [2]. In this structure, each Al^{3+} or Ti^{4+} cations are surrounded by six oxygen ions forming distorted oxygen octahedral. Apparently, these AlO_6 or TiO_6 octahedra form (0 0 1) oriented double chains weakly bonded by shared edges. This structural feature might be responsible for the strong thermal expansion anisotropy, which generates localized internal stresses to cause severe micro-cracking.

In this study we present an Al-K XANES and a Ti-K XANES/EXAFS study of two different aluminum titanates: one obtained from the calcination (1500 °C) of Alumina and Anatase [1], and another from commercial powder (industrial grade). Complementary XRD - Rietveld analysis was also performed for long-range order studies.

Spectra features obtained for the two different samples were described and compared. No important differences were observed between both studied powders. In agreement with the mentioned experimental evidence, the detected local structure consists in distorted octahedral sites in both cases.

[1] N.M. Rendtorff, G. Suárez, and E.F. Aglietti, *Cerâmica*, 60 (355), 411-416 (2014).

[2] R.D. Skala, D. Li, and I.M. Low, *J. of the Eur. Ceram. Soc.* 29(1), 67-75 (2009).

Microstructural characterization of a natural/synthetic hybrid material by means of PALS and SAXS

Pablo S. Anbinder¹, Carlos Macchi¹, Javier Amalvy² and Alberto Somoza¹

¹ *CIFICEN (UNCPBA-CICPBA-CONICET) and IFIMAT (UNCPBA), Pinto 399, B7000GHG Tandil, Argentina;*

² *Instituto de Investigaciones Fisicoquímicas Teóricas y Aplicadas (INIFTA), CCT La Plata CONICET-UNLP, Diag. 113 y 64, La Plata, Argentina.
anbinder@exa.unicen.edu.ar*

Chitosan is a biopolymer which offer great potentiality as packaging material, due to its inherent antimicrobial activity, non-toxicity and biodegradability [1,2]. Chemical modification of chitosan, specially grafting with different polymers is an important topic in the production of bio-based materials with enhanced properties. In the present study, two chitosan with different deacetylation degree (DD%) and molecular weight were grafted with different proportions of *n*-butyl acrylate, in a surfactant-free emulsion system. Stable dispersions with high grafting efficiency were obtained and the microstructure of the dispersions and casted films was analyzed by small angle x-ray scattering (SAXS) and positron annihilation lifetime spectroscopy (PALS). Results were studied and compared taking into account the DD%, molecular weight and grafting ratio.

A core-shell structure was obtained on grafted samples dispersions and, on the other hand, a rupture of the typical rigid rod-structure of the polysaccharides was evidenced in hybrid films. Grafted polybutylacrylate chains break specific interactions in chitosan matrix, increasing the free nanohole volume and their fraction.

Differences in DD% and molecular weight in pristine chitosan play an important role in grafted samples microstructure because of the number and distribution of graft sites.

[1] M. Rinaudo. Chitin and chitosan: properties and applications. *Prog Polym Sci* 31, 603-632, (2006).

[2] L.L. Lloyd, J.F. Kennedy, P. Methacanon, M. Paterson, C.J. Knill. Carbohydrate polymers as wound management aids, *Carbohydr. Polym.* 37, 315-322, (1998).

Acknowledgements: This work has been supported by the Brazilian Synchrotron Light Laboratory (LNLS) under proposal 17764 – SAXS2. The authors would like also to acknowledge to CONICET, CICPBA and ANPCYT for financial support.

Study of structural features and aggregation of S-layer proteins from lactobacilli

Patricia Bolla¹, P. Peruzzo², M. Casella¹ and M. de los A. Serradell³

¹ Centro de Investigación y Desarrollo en Ciencias Aplicadas »Dr. J. Ronco« CINDECA. ² Instituto de Investigaciones Físicoquímicas Teóricas y Aplicadas INIFTA. ³ Cátedra de Microbiología, Facultad de Ciencias Exactas, UNLP. Universidad Nacional de La Plata, Departamento de Química, La Plata, Buenos Aires, Argentina
pbolla@quimica.unlp.edu.ar

Crystalline S-layers are the outermost cell envelope components of many bacteria and archaea. S-layers are monomolecular arrays composed of identical protein or glycoprotein subunits with molecular weights ranging from 40 to 200 kDa. Isolated S-layer proteins (SLP) show an intrinsic tendency to reassemble into regular arrays after removal of the disrupting agent used in the extraction procedure. The self-assembly products generated in suspension may have the form of flatsheets, open-ended cylinders or closed vesicles [1]. In this work, SAXS measurements on SLP isolated from three different strains of *Lactobacillus kefir* were performed using the SAXS1 beamline at the LNLS (Campinas, Brazil) wavelength 1.55°Å; exposure time of 200 sec.; sample detector distance of 1 m). In the first step the SLP in PBS was studied. In a second step the dynamic of protein aggregation in presence of Ca⁺² was performed. The scattering patterns of SLP were significantly different in absence or presence of Ca⁺². Moreover, the pair distribution function P(R) of SLP SAXS data showed substantial variations as analyzed using the program GNOM, such as changes in Dmax of SLP upon addition of Ca⁺². Particularly, Dmax of SLP from *Lb. kefir* 8348 increased (from 20,35nm to 42,27nm) and Dmax of SLP from *Lb. kefir* 5818 decreased (from 36,45nm to 15,07nm), meanwhile the SLP from *Lb. kefir* 83111 did not show significant changes.

[1] M. Sára and U.B. Sleytr. J. Bact 182, 859–868 (2000).

Acknowledgements: The authors would like to acknowledge Brazilian Synchrotron Light Laboratory (LNLS), Campinas, Brazil. CONICET and ANPCYT are thanked by financial assistance. The authors are member of CONICET

Hydrogen production by steam reforming of acetic acid using hydrotalcite precursors

R. P. Borges¹, R. A. R. Ferreira¹, R. C. Rabelo-Neto², F. B. Noronha², C. E. Hori¹

¹ Universidade Federal de Uberlândia, School of Chemical Engineering, Av. João Naves de Ávila, 2121, Bloco 1K, 38408-144, Uberlândia – MG, Brazil.

² National Institute of Technology, Division of Catalysis and Chemical Processes, Av. Venezuela, 82, Centro, 20081-312, Rio de Janeiro – RJ, Brazil.
cehori@ufu.br

Four hydrotalcite-like precursors Ni-Mg-Al were prepared through co-precipitation method in constant pH varying the molar ratio of bivalent metals Ni²⁺/Mg²⁺ into 0.3, 0.4, 0.5 and 0.6. Molar ratio M³⁺/(M³⁺ + M²⁺) was maintained constant on 0.25. The samples were characterized using *in situ* X-ray diffraction (XRD) and X-ray Absorption Near Edge Structure Spectroscopy (XANES) which was performed on K absorption border of Ni ($E_0 = 8333$ eV). Temperature Programmed Surface Reactions (TPSR) were performed at a heating rate of 10 K/min from room temperature to 873 K, during 1 hour, using a reaction solution of 1% acetic acid:3% water:96% helium with a flow rate of 200 mL/min. Through *in situ* XRD patterns it is possible to infer that all samples were reduced over time, although no reduction was detected below 873 K. These results are in agreement with the literature [1] and can be attributed to the different Ni²⁺/Mg²⁺ molar ratio and to a possible formation of a metallic solution Ni-Mg-Al-O in the precursors with a lower Ni²⁺/Mg²⁺ ratio. XANES analysis during the steam reforming of acetic acid (SRAA) showed that samples kept practically the same degree of reduction throughout the catalytic test, indicating that feed did not oxidize the samples. For all samples, the catalytic activity begin at temperatures above 673 K. Ketonization and decomposition reactions of acetic acid may happen around 673 K, as their characteristic products (CH₄, CO₂ e H₂) start to rise considerably at this temperature. It is noticed through CO₂ e CO signal increase that decomposition and steam reforming reactions occur in parallel. SRAA itself start to occur between 823 and 873 K for all samples, except for 05NiMg that had ketonization, decomposition and SRAA reactions occurring at really close temperatures. H₂ and CO intensity remained high for all catalysts (except 06NiMg), that presented some decrease in H₂ signal at the end of the reaction period. This drop could be attributed to the deactivation due to carbon deposition.

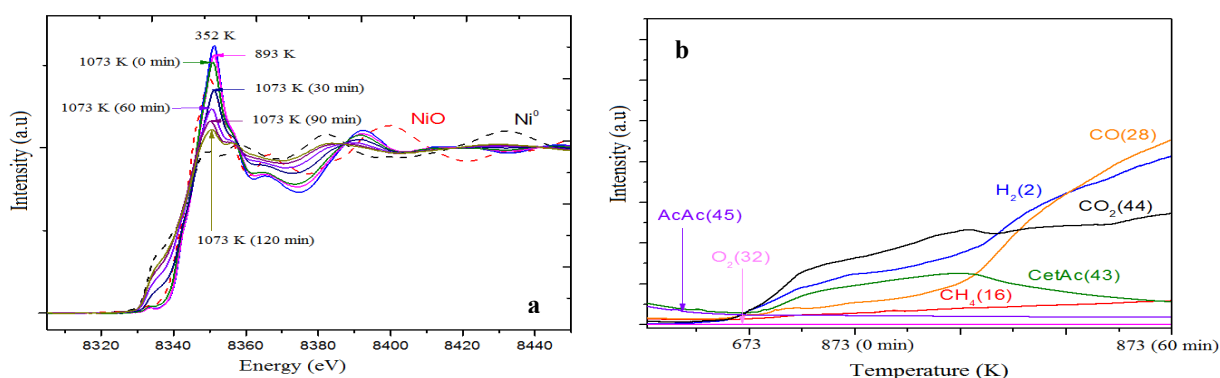


Figure 1: TPR-XANES (a) and TPSR (b) using precursor Ni²⁺/Mg²⁺ = 0.3.

[1] R. Guil-Lopez, R. M. Navarro, A.A Ismail, S.A Al-Sayari, J. L. G Fierro, International Journal of Hydrogen Energy 40 (2015) 5289-5296.

Acknowledgements: The authors wish to acknowledge the financial support of CAPES, FAPEMIG and CNPq. We also thank LNLS for the use of XPD and XAFS1 beamlines

Morphology and size study of (Gd,Er,Yb)-doped NaYF₄ nanoparticles through the X-ray Line Profile Analysis.

R. Lora-Serrano¹, W Iwamoto¹, E. Estevez-Rams², Jeann C. Rodrigues¹, and B. Aragón-Fernandez².

¹ Instituto de Física, Universidade Federal de Uberlândia, 38400-902, Uberlândia, MG, Brazil

² Facultad de Física, Universidad de la Habana, San Lázaro y L, CP 10400 La Habana, Cuba
rloraserrano@ufu.br

X-ray line profile analysis (XLPA), i.e. the analysis of the broadening, shifting and asymmetries of the Bragg reflections due to microstructure, enables the thorough characterization of the properties of materials, especially those of nanostructured materials. XLPA makes a quantitative analysis of the microstructure in terms of grain and subgrain size, dislocation structure and dislocation densities and planar defects, especially stacking faults and twin boundaries [1]. In this work, we use the XLPA to determine the shape and size of the system of nanoparticles (NPs) Gd-, Er- and Yb-doped NaYF₄. For Yb/Er and Yb/Tm co-doped NaYF₄ samples, the up converting fluorescence effect has been observed [2]. It is known that in nanosystems both size and shape of the particles can change the physical properties. In particular, the title samples crystallize in both hexagonal (*h*) and cubic (*c*) symmetries depending on the dopant and heat treatment [2,3].

The powder diffraction data were collected at the XPD beamline of the Brazilian synchrotron lightsource. For the deconvolution of the instrumental contribution, standard samples of LaB₆-NIST were used. The analysis was carried out by using the convolutional multiple whole profile (CMWP) fitting procedures [1]. To obtain the mean size of crystallites and/or their size-distributions, specific functional form of size-distribution has to be assumed. The log-normal size distribution function has been used to describe the size profile of our samples. For *h* NPs, size distribution of about 400 nm were obtained, while less than 100 nm were observed for *c* Nps, depending on the heat treatment. This is in agreement with TEM and HRTEM results [3]. Our results are correlated with the optical and magnetic properties observed.

[1] T. Ungár. J. Mater. Sci. 42:1584–1593 (2007).

[2] Holanda *et al.* Phys. Rev. Lett. 107, 026402 (2011)

[3] W. Iwamoto *et al.* J. Nanosci. Techn. 10, 5708 - 5714 (2010).

Acknowledgements: This work was supported by FAPEMIG and CAPES.

Biochemical and structural characterization of 1-Cys Peroxiredoxin from the human opportunistic pathogen *Aspergillus fumigatus*

R. Bannitz-Fernandes¹; K. F. Godoy²; C. A. Tairum³; I. Malavazi²; M. A. Oliveira³ and L. E. S. Netto¹

² Universidade Federal de São Carlos – São Carlos, Brazil; ¹ Instituto de Biociências, Universidade de São Paulo – São Paulo, Brazil; ³ Universidade Estadual Paulista, Campus do Litoral Paulista – São Vicente, Brazil.
bannitzfernandes@ib.usp.br

Peroxiredoxin (Prx) are Cys-based, thiol-dependent peroxidases that contain one or two conserved Cys residues. To date, all characterized Prx display the universal motif Pro-X-X-X-Thr/Ser-X-X-Cys. Here, we aim to structurally and biochemically characterize AfPrxA, a 1-Cys Prx (Prx6 subfamily) from the human opportunistic pathogen *Aspergillus fumigatus*. Initially, the reactivity of AfPrxA towards H₂O₂ was determined through a HRP competitive assay as $3.7 \times 10^7 \text{ M}^{-1} \text{ s}^{-1}$. Remarkably, AfPrxA presents a unique motif among Prx enzymes (Ser-X-X-X-His-X-X-Cys) and in spite of it still displays an extraordinary reactivity towards H₂O₂. Therefore, we are attempting to obtain the crystal structure of AfPrxA. Several crystals were obtained and to date, the best result was obtained with AfPrxA pre-reduced, alkylated with iodoacetamide and treated with trypsin (resolution 3 Å). Additionally, we are investigating the reducing system of AfPrxA, which is still an elusive issue for enzymes belonging to the Prx6 subfamily. Therefore, we produced recombinant enzymes of the thioredoxin (Trx) system from *Aspergillus fumigatus* and none of them could reduce AfPrxA. In contrast, ascorbate and dihydrolipoic acid were able to support the peroxidase activity of AfPrxA. Once ascorbate could reduce this protein *in vitro* (10^3 order constant), we quantify the erythroascorbate concentration inside the fungus as approximately 200 μM. Therefore, erythroascorbate might act as a reducing agent of AfPrxA *in vivo*. The unique characteristics of this protein might be important to the development of new therapeutical approaches for diseases caused by *A. fumigatus* as AfPrxA shares low identity with the human Prx (41%).

Acknowledgements: CEPID/Redoxoma; FAPESP; Capes-CNPq.

Chromobacterium violaceum OhrA and OhrB: New Considerations on the Enzymatic Mechanism Steps

Domingos, RM¹; Meireles, DA¹; da Silva Neto, JF²; Alegria, TGP¹; Teixeira, RD³; Netto, LES¹

¹Instituto de Biociências, Universidade de São Paulo, Brasil ²Faculdade de Medicina de Ribeirão Preto, Universidade de São Paulo, Brasil ³Instituto de Química, Universidade de São Paulo, Brasil

Chromobacterium violaceum (Cv) are opportunistic pathogenic bacteria that have developed complex strategies to cope with oxidative insults generated from the host. Among them, Ohr (Organic Hydroperoxide Resistance proteins) are Cys-based, lipoil-dependent peroxidases with extraordinary reactivity towards organic hydroperoxides (10^6 – 10^8 M⁻¹.s⁻¹), but not hydrogen peroxide. Ohr proteins belong to the Ohr/OsmC protein family and exist mostly in bacteria. Here, we describe the crystal structures of CvOhrA (2.06Å of resolution) and its paralogue CvOhrB (2.10Å of resolution) both in the oxidized form. The crystal X-ray diffraction data were processed by the software interface, XDSgui. The space groups identified were P3221 and P61 for CvOhrA and CvOhrB respectively. The data set was processed taking into account the CC1/2>50% and the $i/\sigma > 0.8$ as thresholds for the higher resolution data, in order to obtain the best-quality refined model. The phases and respective electron densities were obtained by molecular replacement, by using the previously solved crystal structure of Pseudomonas aeruginosa Ohr (PDB:1N2F) (67% and 65% of identity to CvOhrA and CvOhrB respectively) as search model. The electron density of both, OhrA and OhrB clearly reveals an intact catalytic disulfide bond in each of the two monomers, which are intertwined into a canonical dimer. Furthermore, the loop containing a fully conserved arginine is found in the open configuration. By means of a lipoamide/lipoamide dehydrogenase-coupled assay, we performed structure/activity relationships, for the first time comparing two paralogue Ohr enzymes. CvOhrA was twice as more active than CvOhrB. Site-directed mutations and co-crystallization ligand trials will be performed in order to validate hypothesis related to specific roles of new residues implied in catalysis.

Acknowledgements: Fapesp, INCT Redoxoma, CNPq, CAPES.

Analysis of the crystal electric field ground state of intermetallic TbRhIn₅ by using soft X-ray absorption spectroscopy

R. P. Amaral¹, D. J. Garcia², D. Betancourth³, P. G. Pagliuso³, J. G. S. Duque³ and R. Lora-Serrano¹

¹ Universidade Federal de Uberlândia, Instituto de Física, 38408-100, Uberlândia, Brazil; ² Consejo Nacional de Investigaciones Científicas y Técnicas (CONICET) and Centro Atómico Bariloche, S. C. De Bariloche, Río Negro, Argentina; ³ Centro Atómico Bariloche and Instituto Balseiro (U. N. Cuyo), 8400 Bariloche, Río Negro, Argentina; ⁴ Instituto de Física “Gleb Wataghin”, UNICAMP, 13083-970, Campinas, São Paulo, Brazil.
bertprd@gmail.com

Magnetic properties of rare earth ions are due to localized 4f electrons. The Crystal Electric Field (CEF, the static electric potential due to surrounding ions) acts as a perturbation potential and is responsible for breaking the degeneracy of the $2J+1$ multiplet in the ground state of those ions. In this work we present the results and discussion of the linear-polarization soft X-ray spectroscopy (LPXAS) data collected at the Tb M_4 and M_5 edges of the intermetallic compound TbRhIn₅. TbRhIn₅ is an antiferromagnetic (AFM) compound with Néel temperature $T_N \sim 46$ K and CEF influence in its magnetic properties (T_N and microscopic magnetic structure) were studied by means of a mean field model[1]. The data were taken at the PGM and SXS beamlines of the Brazilian synchrotron lightsource (LNLS). By comparing to the theoretical spectra calculated within the multiple scattering approximation of the MultiX[2] platform, we aim to study the influence of the perturbing electric potential on TbRhIn₅ ground state. Figure 1 shows a comparison between experimental and theoretical XAS spectra at the Tb M_4 and M_5 edges with light polarized perpendicular (E_{\perp}) and parallel (E_{\parallel}) to the crystallographic c-axis. This work is the first attempt to use LPXAS in the experimental study of the CEF influence on the ground state symmetry of rare earth ions in intermetallic compounds using the Brazilian lightsource.

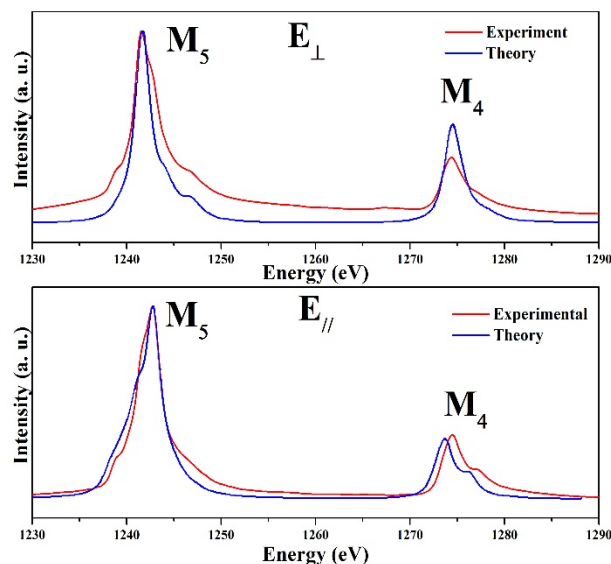


Figure 1 - Comparison between experimental and theoretical XAS spectra at Tb M_4 and M_5 edges with light polarized perpendicular (E_{\perp}) and parallel (E_{\parallel}) to the crystallographic c-axis.

[1] R. Lora-Serrano *et al.*, Phys. Rev B 74, 214404 (2006).

[2] A. Uldry, F. Vernay and B. Delley, Phys. Rev B 85, 125133 (2012).

Acknowledgements: This work was supported by CNPEM. The authors would like to thank Laboratório Nacional de Luz Síncrotron.

Study of the synthesis method and barium substitution on nickel catalysts for dry reforming of methane using XPD line

R. S. Gomes¹, C. B. Rodella², R. S. Batista¹, M. S. Santos¹, D. S. Costa¹ and S. T. Brandão¹

¹ Universidade Federal da Bahia, Departamento de Química Geral e Inorgânica, 40170-115, Salvador, Brazil

² Centro Nacional de Pesquisa em Energia e Materiais, Laboratório Nacional de Luz Síncrotron, 13084-971,

Campinas, SP – Brazil

ruansilveira3@hotmail.com

In the present work was studied the dry reforming of methane over nickel based catalyst and the influence of barium on the reaction. The objective was to investigate the difference between Ni/La₂O₃ catalysts obtained from different preparation routes (wetness impregnation or citrate method) in the catalytic performance. The catalysts NiP (derived from LaNiO₃), NiS (derived from NiO/La₂O₃) and Ba20 (derived from La_{0.8}Ba_{0.2}NiO₃) were characterized by experiments XRD in situ performed at XPD line (LNLS) at high temperatures. It was observed that for all catalysts under in situ reaction there was the formation of NiC_x specie. This is in agreement with the mechanism proposed by Verykios et al [1], where CH₄ is decomposed by Ni sites forming C-Ni_{ads} specie and H_{2ads}. The NiC_x specie can lead to decreasing in CH₄ and CO₂ conversion. However, with increasing the temperature it was observed that NiC_x specie was consumed probably by La₂O₂CO₃ specie. Therefore, this specie is crucial in the catalyst regeneration. As depicted in Figure 1, the catalyst Ba20 initially showed more resistant in carbon deposition even having similar conversion of reactants. However, the highest capacity of Ba20 in adsorb CO₂ molecules can lead the Ni sites to be more restricted, blocking the access of methane molecules to the active sites, and this way decreasing the catalyst activity in the range of 500-900 °C (data not detailed in this abstract). The catalyst NiP (d= 9 nm) and Ba20 (d = 17 nm) showed high activity than NiS (d = 19 nm). This behavior is in agreement with the average crystallite sizes calculated by Debye-Scherrer. These results demonstrate that the catalysts obtained from the perovskite structure are able to produce nickel particles more active and stabilize smaller particles compared to the catalyst derived from NiO/La₂O₃ synthesized by wetness impregnation.

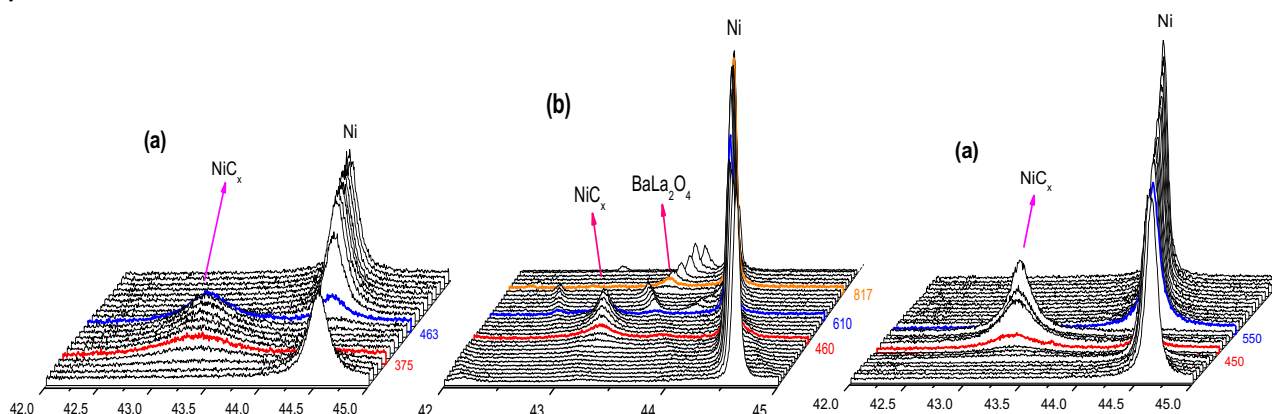


Figure 1. X-ray diffraction patterns: a) NiP, b) Ba20, c) NiP under in situ conditions; CH₄/CO₂ = 1.

[1] E. Verykios et al. Journal of Catalysis 158, 51-63 (1996).

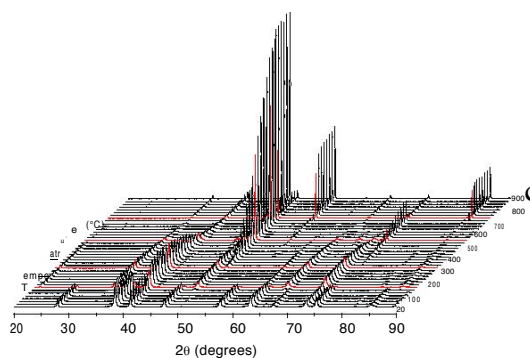
Acknowledgements: This work was supported by CNPq. The authors acknowledge the support of the LNLS/CNPEM for beamline time.

A reduction behavior study of aluminum and copper-doped iron oxides by XRD

Sarah Maria Santana Borges¹, Maria do Carmo Rangel¹, Cristiane Barbieri Rodella²

¹Instituto de Química, Universidade Federal da Bahia, Campus Universitário de Ondina, Federação, 40 170-290, Salvador, BA, Brazil; Laboratório Nacional de Luz Síncrotron (LNLS), Rua Giuseppe Máximo Scolfaro, 10000 - Bairro Guarará, 13083-970 - Campinas – SP, Brazil
Email_MCRangel_mcarrov@ufba.br

The water gas shift reaction is by far the most used route to purify hydrogen-rich streams obtained from natural gas steam reforming, during the industrial production of hydrogen. For commercial purposes, the reaction is performed in two steps, the first one carried out at high temperatures (HTS, *high temperature shift*) in favorable kinetic conditions. The commercial catalysts for the HTS step is a chromium and copper-doped iron oxide, mostly available as hematite ($\alpha\text{-Fe}_2\text{O}_3$) which is reduced *in situ* to produce magnetite (Fe_3O_4), the active phase. The reaction should be controlled in order to avoid the over reduction of magnetite to metallic iron, which can catalyze the hydrocarbon production. In spite of the high activity and selectivity and low cost, there is a need for searching chromium-free solids, avoiding damages to the environment and to the humans, during the handling and discarding of these catalysts. In previous works [1,2], we have shown that chromium can be replaced by aluminum in HTS catalysts. However, there is a lack of information about the solid transformations during the reduction and operation steps, being a barrier for the optimization and commercialization. In the present work, the phase changes during the reduction step were studied, by *in situ* X-ray diffraction experiments using synchrotron light at LNLS. Samples were prepared from iron nitrate, aluminum nitrate and ammonium hydroxide, followed by impregnation with copper nitrate. Solids with (i) Fe/Al (molar)= 10; (Fe/Cu= 10 and (iii) Fe/(Al, Cu)= 10 were obtained besides pure iron oxide. The X-ray diffractograms were obtained *in situ* under flow (100 ml min^{-1}) of 5% H_2/He mixture. The solid was heated (5°C min^{-1}) from room temperature up to the 900°C and a spectrum was collected each 6 min. For all samples hematite was found at room temperature and changed to magnetite, except for pure hematite which changed to wustite at temperatures as low as 197°C . All phase changes was strongly dependent on solid composition. For copper and iron-based sample, cupric oxide (CuO) was found while cuprous oxide (Cu_2O) was detected for aluminum and copper-doped catalyst. For all samples, the temperature of phase changes was strongly dependent on catalyst composition. It was noted that both aluminum and copper alone inhibited wustite production at low temperatures whereas the simultaneous presence of



these dopants avoids this transformation in the whole temperature range. However, the presence of wustite delayed the iron metallic production, which was found for all samples at different temperatures depending on the catalyst composition. Figure 1 illustrates the phase changes in aluminum and copper-doped samples. These results provide useful information for the industrial applications, since that they showed that aluminum and copper can prevent wustite formation at temperatures higher (587°C) than the reaction temperature (370°C).

Figure 1. X-ray diffractograms as a function of temperature for aluminum and copper-doped hematite.

[12]. M. C. Rangel and C. G. Araújo, *Stud. Surf. Sci. Catal.* 130, 1601 (2000).

[13]. M. C. Rangel and C. G. Araújo, *Catal. Today* 62, 201 (2000).

Acknowledgements: This work was supported by CNPq and LNLS. SMSB would like to thank CNPq for her scholarship.

Synthesis and characterization for XRD with synchrotron light of a PtNb CO tolerant electrocatalyst for polymeric membrane fuel cells

Thairo A. Rocha and Ernesto R. Gonzalez¹

¹ Instituto de Química de São Carlos, Universidade de São Paulo, São Carlos, SP, Brazil.
thairo41@gmail.com

This abstract presents the results of a bimetallic PtNb/C electrocatalyst prepared by thermal treatment in dilute reductive atmosphere (5% H₂ in Helium) to obtain a CO-tolerant electrocatalyst [1]. The studies show that materials prepared by impregnating Pt and Nb salts onto high surface area carbon, followed by heat treatment in a reducing atmosphere consisting of a gas mixture of 5 % v/v H₂/He, leads to the formation of nanoparticles with an intermetallic PtNb phase and to the formation of different non-stoichiometric Nb_yO_x. This was observed by X-Ray Diffraction analysis performed in XPD beam line at LNLS. Figure 1 shows the diffractograms collected with samples exposed in different temperatures, with the furnace's atmosphere varying from an inert to reducing atmosphere. Thus, was possible to detect an almost "online" formation of nanoparticles and determine precisely in which temperature occurs the formation of intermetallic phases PtNb and in which temperature occurs the reduction of Nb₂O₅ species to Nb_xO_y.

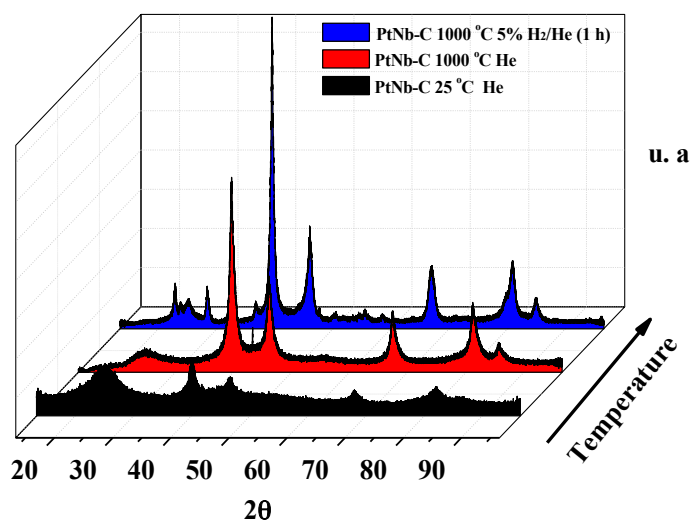


Figure 1- X-ray diffractograms of the thermal-treated PtNb/C electrocatalyst. In black and red, inert atmosphere at 25 °C and 100 °C respectively. In blue, dilute reductive atmosphere at 1000 °C after 1 hour.

[1] Rocha, T. A et al., ECS Transactions, 69 (17) 57-66 (2015).

Acknowledgements: The authors thank the Fundação de Amparo à Pesquisa do Estado de São Paulo (FAPESP). In particular, Thairo A. Rocha thanks CNPq (Proc. 142146/2012-9) for a PhD scholarship.

Structure and Photoluminescence properties of europium-doped hydroxyapatite 3-D scaffolds.

Thiago A.R.M. Lima¹ and Mário E.G. Valerio²

¹ *Federal Institute of Sergipe, Department of Engineering, Estância, Brazil;* ² *Laboratory of Advanced Ceramics Materials, Physics Department, Federal University of Sergipe, São Cristóvão, Brazil.*
thiago.remacre@gmail.com

Studies of calcium phosphates produce significant technological advances in non-invasive cancer and infection treatment. The applicability of hydroxyapatite (HAP) scaffolds is increasingly used to smart drug delivery systems due their biocompatible and ability to fluorescence probe incorporation [1]. The luminescence probe inclusion, such as Eu^{3+} , able a development on traceable biodegradable scaffolds. The literature reports challenges are the europium ion replacement site into hydroxyapatite scaffolds. The present study provides a Eu^{3+} site incorporation analysis and their relation with europium luminescence, as well as, an important new knowledge about three-dimensional HAP scaffolds design by a novel dual-template (corn starch/ C_{16}TAB). X-ray absorption spectroscopy techniques (XANES and EXAFS) were used to investigate the valence and the location of the dopant and the results showed that Eu^{3+} ions are incorporated preferentially at the Ca(1) site in the HAP structure with local charge compensating via oxygen interstitial ion and Photoluminescence results suggest that Ca sites symmetry getting even more distorted in samples synthesized with C_{16}TAB as template. Scanning Electron Microscopy (SEM) combined with Ultra-Small Angle X-ray Scattering (USAXS) techniques showed that the porous arrangement is promoted by needle-like shape HAP nanoparticles and that the pore size distributions depend on the order of addition of the calcium and the phosphate ion source solutions during the template preparation stage. The role of the corn starch and the surfactant on the general properties of the three-dimensional (3-D) scaffold formation is discussed comparing structure, photoluminescence, USAXS and SEM results obtained for samples prepared without any of the organic templates and samples with just the C_{16}TAB surfactant.

[1] F. Chen, Y.J Zhu, K.H Zhang, J. Wu, K. Wang, Q. Tang, X. Mo, Europium-doped amorphous calcium phosphate porous nanospheres: preparation and application as luminescent drug carriers, *Nanoscale Res Lett.* 6 (1) (2011).

[2] J. Ilavsky, F. Zhang, A.J. Allen, L.E. Levine, P.R. Jemian, G.G. Long, Ultra-Small-Angle X-ray Scattering Instrument at the Advanced Photon Source: History, Recent Development, and Current Status, *Metall Mater Trans A.* 44 (2013) 68-76.

Acknowledgements: This work was financial supported by National Council for Scientific and Technological Development (CNPq) (No. 149437/2010-2). The authors would like acknowledge the LNNano and CMNano-UFS infrastructure, additionally the collaboration of Brazilian Synchrotron Light Laboratory (LNLS) staff during the SAXS (D11A-10980), XAFS (14456) and SEM-FEG (13187) experiments, as well as ChemMatCARS Sector 15 is principally supported by the National Science Foundation/Department of Energy under grant number NSF/CHE-0822838.

Use of synchrotron radiation on the investigation of Gd₂O₃: Eu³⁺ structural and optical properties

Valdivânia A. Nascimento¹, Ísis F. Manali², Cristiane B. Rodella², Lucas C. V. Rodrigues³, Douglas Galante² and Verônica C. Teixeira²

¹Universidade Federal do Piauí, Centro de Tecnologia, 64049-550, Teresina, Brazil; ²Centro Nacional de Pesquisa em Energia e Materiais, Laboratório Nacional de Luz Síncrotron, 13083-970, Campinas, Brazil, ³Universidade de São Paulo, Instituto de Química, 05508-000, São Paulo, Brazil.
veronica.teixeira@lnls.br

Luminescent materials are that one able to absorb some kind of energy and reemit it in the visible range at the electromagnetic spectrum. They can be used in several application such as primary sensors of radiation detection systems, lighting, bioimaging, etc. [1]. In this work, undoped and Eu-doped gadolinium oxides were synthesized via sol-gel based on polyvinyl alcohol and their structural, morphological and optical properties were evaluated. Analysis carried out in powder X-rays diffraction indicated that samples calcined at 800, 900 and 1000°C exhibited the Gd₂O₃ single crystalline phase. Rietveld refinement indicated a small distortion on the lattice parameters for doped sample when compared to the undoped ones. The crystallite size was estimated using the Scherrer's equation and nanometric crystallites where found. Scanning Electron Microscopy showed the particles are nanosized. The X-ray absorption near edge spectra indicated Eu is mainly in the 3+ oxidizing state, in all Eu-doped samples. The X-ray excited optical luminescence showed the optical channel in Gd₂O₃: Eu³⁺ is the dopant and the main emission line corresponds to the transition ⁵D₀ ← ⁷F₂ that indicates that Eu³⁺ is located in a site without inversion center symmetry [1,2]. The excitation spectra in the ultraviolet, with visible monitoring of the transition ⁵D₀ ← ⁷F₂, indicated four broad bands, which corresponded to the Eu³⁺ charge transference and excitations of Gd³⁺ and Eu³⁺. The vacuum ultraviolet excitation showed that the Gd₂O₃ optical band gap is at ~5,3 eV (234 nm) [3] and the emission is similar before and after the band gap. The chromatic coordinate revealed a red emitting phosphor that can be used for detecting radiation or as a phosphor for building devices active in the ultraviolet.

- [14]. G. Blasse, B.C. Grabmaier, Luminescent Materials, (Spring-Verlag, 1994) p. 1
- [15]. K. Binnemans, Coord. Chem. Rev. 295, 1–45 (2015)
- [16]. P. Dorenbos, J Lumin, 111, 89–104 (2005)

Acknowledgements: The authors would like to thank to the CNPq, CNPEM Summer Program, CNPEM PIBIC Program and to the XAFS2, TGM, XRD1 and XPD/LNLS/CNPEM beamline staffs for helping during the experiments and also to the LME/LNNano for SEM measurements.

In-situ XAS and XRD study of CuO/SrTiO₃ and NiO/SrTiO₃ catalysts

Vitor C. Coletta¹, Francielle C. F. Marcos², Francisco G. E. Nogueira³, Maria I. B. Bernardi¹,
Elisabete M. Assaf² and Valmor R. Mastelaro¹

¹ Universidade de São Paulo, Instituto de Física de São Carlos, 13566-590, São Carlos, Brazil; ² Universidade de São Paulo, Instituto de Química de São Carlos, 13566-590, São Carlos, Brazil; ³ Universidade Federal de São Carlos, Departamento de Engenharia Química, 13565-905, São Carlos, Brazil.
vitor.coletta@usp.br

Recently, strontium titanate (SrTiO₃) has been studied for application in catalysis of different reactions with a partial substitution of titanium by Cu or Ni and as a support for metallic particles. [1,2] Copper and nickel are considered as low-cost metals with high activity for the water-gas shift reaction. [3] Looking for this application, we synthesized SrTiO₃ nanoparticles by a sol-precipitation method [4] to use as a support for Cu and Ni by wet-impregnation. Since the oxidation state plays an important role in the catalysis of the water-gas shift reaction, we studied these samples in ambient and reducing conditions in XPD and XAFS1 beamlines of LNLS. To exemplify the results, Figure 1 shows XANES spectra of reduced samples. The results are a basis for the reduction pretreatment to activate the catalysts and study them *in situ* under reaction conditions.

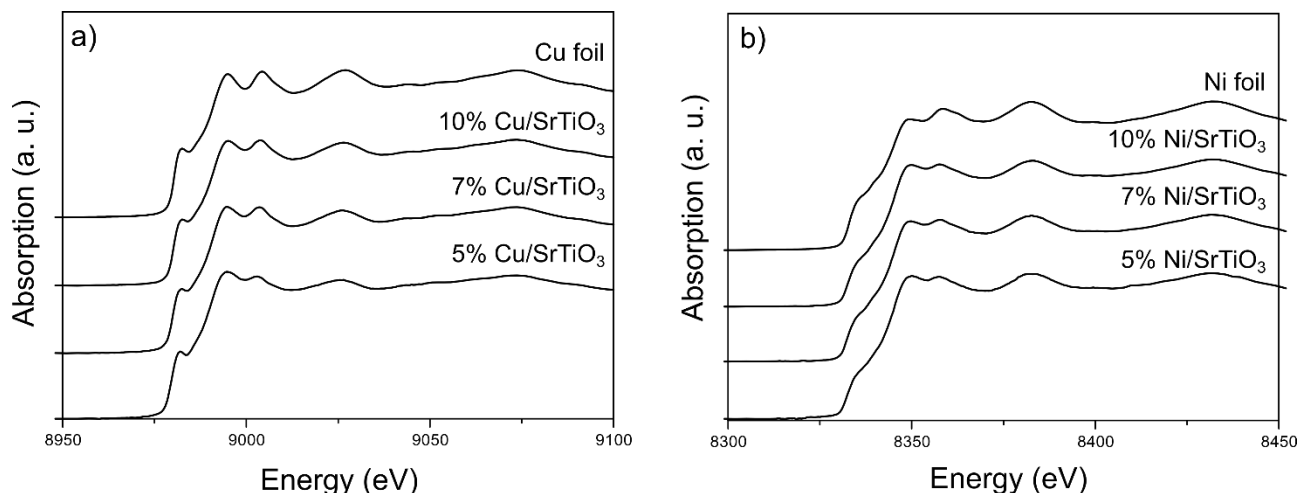


Figure 1: XANES spectra (a) at Cu K-edge of reduced Cu/SrTiO₃ samples at 300°C and (b) at Ni K-edge of reduced Ni/SrTiO₃ samples at 550°C. The samples were reduced with 5% H₂/He at 60 mL/min for 30 min. Spectra for metallic Cu and Ni standards are shown for comparison.

- [1] F. E. López-Suárez, M. J. Illán-Gómez, A. Bueno-López, J. A. Anderson, Appl. Catal. B 104, 261 (2011).
- [2] J. A. Enterkin, W. Setthapun, J. W. Elan, S. T. Christensen, F. A. Rabuffetti, L. D. Marks, P. C. Stair, K. R. Poppelmeier and C. L. Marshall, ACS Catal. 1, 629 (2011).
- [3] T. L. LeValley, A. R. Richard, M. Fan, Int. J. Hydrogen Energy 39, 16983 (2014).
- [4] Y. Hao, X. Wang and L. Li, Nanoscale 6, 7940 (2014).

Acknowledgements: This work was supported by São Paulo Research Foundation – FAPESP (grant 2013/09573-3) and the National Council for Scientific and Technological Development – CNPq (grants 304498/2013-0 and 140631/2013-5). The authors also thank the Brazilian Synchrotron Light Laboratory (LNLS) for the use of its beam line experimental facilities XPD and XAFS1 (proposal numbers 17734 and 18857).

Simulated entrapment of microorganisms in halites under Martian conditions and interplanetary transfer of life

X.C. Abrevaya¹, D. Galante^{2,3}, P. Tribelli⁴, F. Nóbrega⁵; G. Araujo^{3,6}; M.E. Varela⁷; F. Rodler^{8,9}; F. Rodrigues¹⁰; T. Gallo³ and J. E. Horvath²

¹ Instituto de Astronomía y Física del Espacio (IAFE), UBA – CONICET, Ciudad Autónoma de Buenos Aires, Argentina. Email: abrevaya @iafe.uba.ar; ² Research Unit in Astrobiology, IAG – USP, São Paulo, Brazil; ³ Brazilian Synchrotron Light Laboratory (LNLS/CNPEM), Campinas – SP, Brazil; ⁴ Depto de Química Biológica, FCEyN – UBA, IQUBICEN – CONICET, Ciudad Autónoma de Buenos Aires, Argentina; ⁵ Instituto Oceanográfico, USP, São Paulo, Brazil; ⁶ Instituto de Química, USP, São Paulo, Brazil; ⁷ Programa de Pós-Graduação em Biotecnologia, ICB/USP, São Paulo, Brazil; ⁸ ICATE - CONICET, San Juan, Argentina; ⁹ Max Planck Institut für Astronomie, Heidelberg, Germany; ¹⁰ Harvard-Smithsonian Center for Astrophysics, Cambridge, USA.

The presence of evaporitic environments on Mars was evidenced during the last years through the data obtained from measurements on this planet [1-7]. Additionally, as part of these environments, there are several evidences that support the existence halites on Mars (NaCl evaporitic minerals). The evaporation of brine pockets is one of the hypothesis to explain the formation of halites on this planetary body and halite inclusions in the SNC meteorite Nakhla are a mineralogical evidence of the presence of halites on Mars, because of its pre-terrestrial origin [8,9]. On Earth, extremophilic microorganisms that live at very high salt concentrations known as halophilic archaea were found entrapped inside ancient halites in evaporitic deposits from 250 Mya [10,11]. These microorganisms were proposed as possible life forms on Mars and possible candidates for the interplanetary transfer of life [12]. All this evidences open the possibility of an extraterrestrial origin of life on the Earth, considering the Lithopanspermia hypothesis (interplanetary transfer of life through meteorites). In fact, in previous works performed at the TGM beamline (LNLS, Brazil), we showed that some species of microorganisms are capable to survive to several doses of VUV radiation (57.5–124 nm) and vacuum as those related to the conditions of the interplanetary space [13,14]. We expanded these experiments in this work, analyzing the survival of microorganisms entrapped in halites under simulated Martian (-80°C, 8 mbar, 95%CO₂:5%N₂) conditions in a Martian simulation chamber. The entrapped microorganisms were then exposed to VUV radiation up to 40000 Jm⁻² and vacuum (10⁻⁴ Pa) (TGM beamline, LNLS, Brazil) as those found during an interplanetary travel. The results are in agreement with our previous works that show that the survival of the microorganisms is dependent on the specie. This is the first experiment on the survival of microorganisms subjected to a simulated entrapment in halites under Martian simulated conditions, and therefore, the first time that a simulated interplanetary travel test these conditions.

[1] Clark B.C. and Van Hart D.C., *Icarus* 45, 370 (1981).

[2] Rieder R. et al., *Science* 306, 1746 (2004).

[3] Tosca N. J. and McLennan S. M., *Earth Planet. Sci. Lett.* 241, 21 (2006).

[4] Osterloo M. et al., *Science* 319, 1651 (2008).

[5] Osterloo M. et al., *JGR* 115 E10012 (2010).

[6] Glotch T. D. et al., 44th LPSC Abstract #1549 (2013).

[7] Jensen H. and Glotch T. D., *JGR* 116 E00J03 (2011).

[8] Gooding J. L. et al., *Meteoritics* 26, 135 (1991).

[9] Bridges J.C. and Grady M.M., *Meteoritics & Planetary Science* 34, 407 (1999).

[10] Grant W.D. et al., *Extremophiles* 2, 279 (1998).

[11] McGenity et al., *Environmental Microbiology* 2, 243 (2000).

[12] Stan Lotter H. et al., In : *Halophilic microorganisms*. Springer Verlag; Berlin, Heidelberg, N.Y. (2004) pp. 89–102.

[13] Abrevaya X.C. et al., *Astrobiology* 11, 1034 (2011).

[14] Abrevaya X.C. et al., 25th RAU 18pp (2015).

Acknowledgements: The authors thank to FAPESP for financial support and CNPEM-LNLS, for provide the facilities and beamtime.

Unusual photofragmentation mechanisms of chlorinated species elucidated by a combination of double and triple ionic coincidences spectra

Yanina B. Bava,¹ Y. B. Martinez,¹ R. L. Cavasso Filho² and R. M. Romano¹

¹ CEQUINOR (UNLP, CCT-CONICET La Plata). Departamento de Química, Facultad de Ciencias Exactas, Universidad Nacional de La Plata. Blvd. 120 N° 1465, CC 962, La Plata (CP 1900), Argentina.

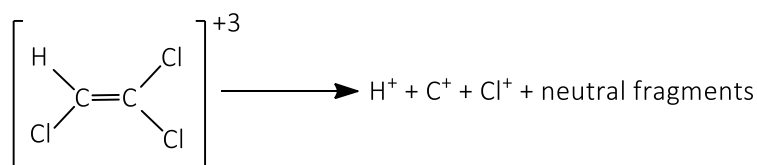
² Universidade Federal do ABC. Av. dos Estados, 5001. CEP 09210-580 Santo André, São Paulo, Brazil. romano@quimica.unlp.edu.ar

Photofragmentation mechanisms of small molecular compounds after shallow- or core-electron ionization can be determined by using coincidence techniques (Photoelectron-Photoion-Photoion-Coincidences, PE2PICO), as presented for example in reference 1 and references cited therein. In this work we discuss the importance of the combined study of the PE2PICO and PE3PICO spectra to understand some unusual photofragmentation mechanisms of chlorinated species, trichloroethylene (HCIC=CCl₂, 3CE), deuterotrachloroethylene (DCIC=CCl₂, D3CE) and tetrachloroethylene (Cl₂C=CCl₂, 4CE), after ionization of Cl 2p and C 1s electron.

The studies were performed in the TGM and SGM beamlines at LNLs, with the experimental station for gaseous samples and coincidence techniques (PEPICO, PE2PICO and PE3PICO) using a Wiley-Mac Laren time-of-flight mass spectrometer. The pressure of the sample inside the chamber was maintained below 5.10⁻⁶ mbar, which guarantees the study of only unimolecular fragmentation mechanisms.

Different fragmentation mechanisms were proposed by the analysis of the bidimensional PE2PICO spectra, being the most important Cl⁺/C₂Cl₂⁺/Cl and CCl₂⁺/CCl₂⁺ for 4CE, and Cl⁺/XC₂Cl₂⁺ and XC₂Cl⁺/Cl₂⁺ (with X = H or D) for 3CE and D3CE. However, some of the islands with positive slopes, as for example the H⁺/C⁺ coincidence presented in Figure 1, could not be interpreted in terms of any fragmentation mechanisms of M²⁺. In these cases, the analysis of the PE3PICO projections, also shown in Figure 1 for the selected example, are needed for the correct evaluation of the PE2PICO spectra. Clearly, the fragments were produce after a triple ionization, giving

H⁺, C⁺, Cl⁺ and neutral fragments. This behaviour was also observed for the deuterated sample, corroborating the proposed fragmentation channel.



[1] Y. B. Bava, Y. Berrueta Martínez, A. Moreno Betancourt, M. F. Erben, R. L. Cavasso Filho, C. O. Della Védova and R. M. Romano, *ChemPhysChem*, 16, 322–330 (2015).

Acknowledgements: This work has been supported by LNLs under Proposals TGM-17872 and SGM-17920. We thank Arnaldo Naves de Brito and SGM beamline staff for their assistance throughout the experiments. The authors thank Facultad de Ciencias Exactas, Universidad Nacional de La Plata, CONICET and ANPCyT

Comparative study of photoionization and photofragmentation mechanisms of sulfur VOCs

Yanina B. Bava,¹ Yanina Berrueta Martínez,¹ Reinaldo L. Cavasso Filho,² Yeny A. Tobón Correa,³ Sophie Sobanska³ and Rosana M. Romano¹

¹ *CEQUINOR (UNLP, CCT-CONICET La Plata). Departamento de Química, Facultad de Ciencias Exactas, Universidad Nacional de La Plata. Blvd. 120 N° 1465, CC 962, La Plata (CP 1900), Argentina.*; ² *Universidade Federal do ABC. Av. dos Estados, 5001. CEP 09210-580 Santo André, São Paulo, Brazil.*; ³ *Laboratoire de Spectrochimie Infrarouge et Raman, UMR CNRS 8516, Université Lille 1 Sciences et Technologies, Bât, C5, 59655 Villeneuve d'Ascq Cedex, France.*
romano@quimica.unlp.edu.ar

Photochemical studies of volatile organic compounds are relevant for the understanding of atmospheric chemistry. In this work, and as part of a general project dedicated to the elucidation of photofragmentation mechanisms generated from the interaction between the synchrotron radiation and compounds with atmospheric interest (see for example references 1 and 2, and references cited therein), we present the comparative study of photoionization and photofragmentation mechanisms of sulfur VOCs. We selected three model species: methyl thioglycolate (MTG), $\text{CH}_3\text{OC}(\text{O})\text{CH}_2\text{SH}$, allyl methyl sulfide (AMS), $\text{CH}_2=\text{CHCH}_2\text{SCH}_3$, and S-allyl thiopropionate (SATP), $\text{CH}_2=\text{CHCH}_2\text{SC}(\text{O})\text{CH}_2\text{CH}_3$. These compounds were studied in the TGM and SGM beamlines at LNLS using synchrotron radiation in two energy regions, 7.3-300 eV and 100-1000 eV, respectively, using the chamber for gaseous samples and coincidence techniques.

Total Ion Yield (TIY) spectra in the energy region corresponding to the S 2p, C 1s and O 1s core electrons were obtained. The TIY spectra around the S 2p threshold, ~ 173 eV, show two intense peaks corresponding to the spin-orbit coupling resonances, from S 2p_{1/2} and S 2p_{3/2} towards $\sigma^*(\text{C}-\text{S})$. In the O 1s energy region only one peak was observed, corresponding to the transition from O 1s to $\pi^*(\text{C}-\text{O})$, for the MTG and SATP molecules. Instead, the C 1s TIY spectra present different peaks assigned to resonances $\text{C}1\text{s} \rightarrow \pi^*(\text{C}=\text{O})$, $\text{C}1\text{s} \rightarrow \pi^*(\text{C}=\text{C})$ and $\text{C}1\text{s} \rightarrow \sigma^*(\text{C}-\text{S})$. "Site specific excitation" was detected, allowing the identification of different kind of carbon atoms in each of the studied molecules.

Photoelectron-Photoion-Coincidence (PEPICO) spectra were taken in the valence energy region at different irradiation energies starting from the ionization potential, while in the core electron energy regions the spectra were measured at each resonance and below and above every resonance. PE2PICO spectra were also obtained, and the fragmentation mechanisms were elucidated from the shape and the slope of the coincidence islands in these bidimensional spectra. In all the cases, HCS^+ and H_3^+ (both interstellar ions) were detected as products of molecular ion fragmentation. The most abundant ions are CO^+ (for MTG and SATP), C_3H_3^+ (generated from the allyl groups), and HCS^+ (for the three molecules). The PE2PICO spectra of MTG are dominated by the coincidence islands with the H^+ ion and by other two islands, $\text{CH}_3^+/\text{HCS}^+$ and $\text{COH}^+/\text{HCS}^+$. In the PE2PICO spectra of AMS the most important coincidence is $\text{C}_3\text{H}_3^+/\text{HCS}^+$ and for the SATP $\text{C}_2\text{H}_3^+/\text{C}_3\text{H}_3^+$. Three- and four-body dissociation channels were observed for each molecule and the comparison between them were proposed.

[1] Y. B. Bava, Y. Berrueta Martínez, A. Moreno Betancourt, M. F. Erben, R. L. Cavasso Filho, C. O. Della Védova and R. M. Romano, *ChemPhysChem*, 16, 322–330 (2015).

[2] A. Moreno Betancourt, Y. B. Bava, M. F. Erben, R. Cavasso-Filho, S. Tong, M. Ge, C. O. Della Védova and R. M. Romano, *J. Photochem & Photobiol A*, 324, 184–191 (2016).

Acknowledgements: This work has been supported by LNLS under Proposals TGM-17872 and SGM-17920. We thank Arnaldo Naves de Brito and SGM beamline staff for their assistance throughout the experiments. The authors thank Facultad de Ciencias Exactas, Universidad Nacional de La Plata, CONICET, ANPCyT and MinCyT-ECOS for financial support

